This is to certify that the

dissertation entitled

Probing Interface Organization and Optical Nonlinearities in Asymmetric Layered Interfaces Using Surface Second Harmonic Generation

presented by

Stephen Bakwanamoh Bakiamoh

has been accepted towards fulfillment of the requirements for

Ph.D. degree in Chemistry

Major professor

Date 4/24/02

DATE DUE	DATE DUE	DATE DUE

PROBING INTERFACE ORGANIZATION AND OPTICAL NONLINEARITIES IN ASYMMETRIC LAYERED INTERFACES USING SURFACE SECOND HARMONIC GENERATION

By

Stephen Bakwanamoh Bakiamoh

A DISSERTATION

Submitted to
Michigan State University
In partial fulfillment of the requirements
for the degree of

DOCTOR OF PHILOSOPHY

Department of Chemistry

2002

ABSTRACT

PROBING INTERFACE ORGANIZATION AND OPTICAL NONLINEARITIES IN ASYMMETRIC LAYERED INTERFACES USING SURFACE SECOND HARMONIC GENERATION

By

Stephen Bakwanamoh Bakiamoh

The ability to control interfacial structure and composition thereby imparting in them unique chemical, physical, and optical properties make them interesting systems to study for both fundamental and technological reasons. Such interfacial assemblies have potential utility in surface-dependent technologies such as chemical sensing, nonlinear optics, separation science, information storage, microelectronics, and corrosion protection. Layer-by-layer deposition, as in self-assembled mono- and multilayer assemblies, can provide spatial resolution normal to the substrate over composition and molecular organization that is critical to the macroscopic properties of the resulting interface. However, the extent of organization required within the material to achieve the desired properties remains to be fully resolved.

This work reports on the use of asymmetric metal ion coordination chemistry in conjunction with surface second harmonic generation (SHG) and linear optical spectroscopy (FTIR, ellipsometry, UV-visible) to understand molecular organization intrinsic to layered assemblies. Asymmetric multilayer assemblies are assembled using structurally simple bifunctional alkanes incorporating $\chi^{(2)}$-activity within the coordinating metal centers. Surface preparation was carried out by direct phosphorylation of surface

silanol groups with $POCl_3$ in collidine resulting in a reduction in sample preparation time from about 24 hours to less than an hour. Linear optical characterization (FTIR and ellipsometry) suggests moderately well organized multilayers that are chemically and thermally robust.

The $\chi^{(2)}$ response intrinsic to the inorganic interlayer of ionically-bound multilayer systems such zirconium phosphonate monolayers was also investigated for the first time using surface second harmonic generation intensity measurements on asymmetric bifunctional alkanes multilayer systems. Studies on ionically-bound interfaces usually focus on the chemical and/or optical properties of the organic constituents, R, in $Zr(PO_3R)_2$ sheets because of the structural diversity in organic moieties. Surface second harmonic generation data revealed a small nonlinear response from this part of the assembly relative to that attainable from a rigid chromophore with a large hyperpolarizability. In addition, angle-dependent surface second harmonic generation was used to investigate surface organization and structure under potentially heterogeneous conditions as a function of surface chromophore loading density. The SHG data are consistent with complex surface structure formation characterized by two domains; a dominant well-ordered domain with an average chromophore tilt angle coincident with the surface normal, and a second, more random domain characterized by an average chromophore angle of ~39°. The relative contribution of the disordered domain was found to decrease with increasing chromophore loading density. This finding suggests disorder inherent in most layered materials resulting from either non-uniformity of surface active sites or adsorbate aggregation.

DEDICATION

Dedicated to my Family, and

In Everlasting Memory of my Beloved Mother,

KUBATU BAKIAMOH

ACKNOWLEDGEMENTS

My sincerest thanks go first and foremost to Prof. Gary Blanchard for his patience, support, encouragement, and guidance throughout my graduate career in Michigan State University. Gary has always been there whenever I needed him and he has always shown interest in my professional and personal development. His genuine interest in the welfare and development of his students has made graduate school a less stressful experience and for this, I will always be grateful. Gary is simply a great guy to work with and I am very privileged to have had that opportunity to work closely with him. I will also like to thank Gary's family for the numerous times they agreed to have us over for the annual "game dinner"

My thanks also go to my committee members: Prof. Simon Garrett, Prof. Thomas Pinnavaia, and Prof. Marcos Dantus for their time and advice. It has been a pleasure to have each of you on my committee. In particular, I have always enjoyed talking to Simon about both my work and real life issues and I thank him very much for his time, patience, and advice that he freely offered when I needed them.

My thanks go to all the members of the Blanchard group who have helped in diverse ways to make graduate school a little more bearable. They have listened to my ideas, problems, frustrations, and presentations and offered very valuable suggestions that made a difference in my research. In particular, Punit, Joe, and Lee, and Jay have been very good company to me in and out of the lab and I will never forget how much less stressful graduate school has been with your support and company.

My special thanks to Dr. Albert Schlueter, my guardian in the United States, whose efforts made it possible for me to get my education in this country and whose inspiration saw me through graduate school. I am also very thankful to my very special friend Elizabeth Wayumba who has always listened to my numerous frustrations in the lab. Your support, love, and encouragement have helped maintain my sanity throughout this work for which I am very grateful. To my very good friend and brother Charles Ngoweh, my thanks for your support and encouragement as we both struggled through graduate school.

Most importantly, I want to thank my family, in Ghana, from the bottom of my heart for the sacrifices they have made to enable me to be educated to this level and for their "never-ending" prayers that have given me the courage and strength to make through school. I love you all.

Finally, I my thanks to all who have contributed in one way or another in making my stay in MSU a memorable one.

God bless you all!

TABLE OF CONTENTS

LIST OF TABLES

LIST OF FIGURES

Chapter 1

Introduction

The design of molecule-based interfacial materials with useful physical and chemical properties including their function in electronic, optical, magnetic, and catalytic applications is the focus of intense research in interfacial chemistry and materials science. In particular, research and development of self-assembled mono- and multilayer structures (SAMs) through chemical modification of surfaces, and organic self-assembly at interfaces are areas that have received a great deal of attention for both fundamental and practical reasons. The study of surface properties such as wetting and adhesion,[1,2] friction,[3-5] corrosion prevention,[6-8] and electron transfer reactions[9,10] is possible through the use of SAMs. In addition, structurally and chemically well-defined SAMs have potential utility in a number of technologies spanning chemical sensing,[11,12] electronic, electro-optic, and photonic devices,[13-18] optical information storage, and second-order nonlinear optics.[19-22] For these applications, it is important to obtain thermally stable and uniform films with a high degree of ordering and dense packing of the constituent chromophores.

Common techniques available for the development of organized molecular assemblies at interfaces are Langmuir-Blodgett deposition, alkyltrichlorosilane growth on silicon, disulfides and alkanethiol growth on gold, and metal-phosphonate layer growth as schematized in Figure 1.1.

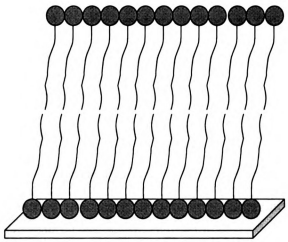

LB films

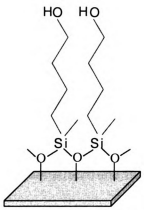

alkyltrichlorosilanes
on silicon

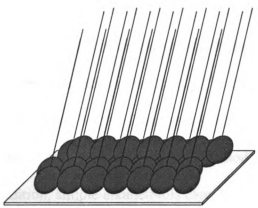

Alkanethiols
on gold

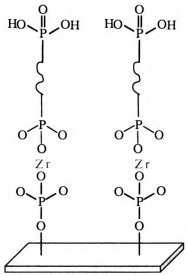

Metal phosphonate
monolayers

Figure 1.1. Selected stages in the development of self-assembled mono- and multilayer structures.

Molecular self-assembly started with Langmuir-Blodgett (LB)[23,24] films prepared by the transfer of monolayers preassembled at the air-water interface onto planar substrates. The LB self-assembly technique is based on spontaneous adsorption of thermodynamically stable surface monolayers from solution, resulting in the formation of well-organized structures with control over the constituents. LB films are metastable due to the weak van der Waals' forces holding them together. These layered assemblies are sensitive to contaminants and are limited in the number of layers that can be assembled. To circumvent these shortcomings, Sagiv and coworkers[25,26] demonstrated the formation of thermodynamically stable multilayers by sequential surface chemical activation and adsorption of alkyltrichlorosilanes from solution. These interfaces were relatively well ordered and durable, but they were highly water sensitive, forming incomplete monolayers in the absence of water, and polymerizing in the presence of excess water. This approach to layered assembly formation did not permit the growth of more than 2 or 3 layers before structural defects became significant.

Perhaps the most widely studied and best-characterized self-assembling systems are the alkanethiols on gold.[27-33] Though alkanethiol monolayers are highly ordered, recent work by the Blanchard group[34,35] has shown that these interfacial structures are formed with relatively modest thermodynamic driving forces and are therefore labile. In addition, simple alkanethiols cannot be used to form regular multilayer structures. While the above ways of forming layered interfacial assemblies are limited to the formation of a few layers that may not be sufficiently robust for long-term applications, the Mallouk, Katz, and Thompson groups[36-43] have pioneered a durable and versatile means of fabricating highly organized and robust multilayer assemblies with molecular control

over interface identity and, in some cases, orientation. This family of materials is based on metal-phosphonate chemistry, where transition metal ions such as zirconium are bonded with organophosphonates via ionic coordination chemistry. There was no orientational control within the initial layers assembled using symmetrical (α,ω)-organobisphosphonates, due to lack of selectivity in bonding.[39,40] However, with the use of asymmetric ω-hydroxyorganophosphonates, Katz and coworkers[44] incorporated orientational selectivity in bonding by ensuring that only the phosphonate functionality bonds to the metal ions. Directional multilayers are obtained by sequentially reacting the terminal hydroxyl groups with $POCl_3$ in 2,4,6-collidine, then with H_2O to yield a reactive surface, followed by zirconation and adsorption of ω-hydroxyorganophosphonate ligands from solution. Recently, novel hybrid multilayer assemblies that exhibit both lateral and vertical stability have been demonstrated using ionic and/or covalent linking chemistry within a given multilayer assembly.[45-49]

The driving force behind the advances that have led to molecular-level control of interface structures is the need to develop organized interfaces suitable for practical applications. Of particular importance to interface chemistry is the question of intralayer organization of molecules and its effect on macroscopic interface properties. The degree of molecular order or crystallinity within photoactive or electroactive polymer thin films, for example, is crucial in determining their luminescent[50] and conducting[51] efficiencies and therefore their efficacy as materials for light-emitting diodes (LEDs) and light-emitting electrochemical cells (LECs). For most applications of organic materials, including electron transfer reactions, pattern definition, optoelectronic device fabrication, and nonlinear optical applications, the organization within the material is critical.[52-57]

However, there is a fundamental question of the extent of organization (orientation, coverage, and distribution) required within the material to achieve the desired physical and chemical properties. Uncertainty in the nature and extent of interface organization arises largely from the complex nature of many surfaces and interfaces, and the inability of many experimental techniques to distinguish the molecular properties of the thin surface region from contributions by the bulk. Electron scattering and diffraction, photoemission, Auger, and mass spectroscopy can be operated only in vacuum, while most optical techniques do not possess the requisite surface specificity or sensitivity, and can be used only if the signal contributed from the bulk can be suppressed.[58] Of the techniques used for the study of surfaces, optical second harmonic generation (SHG) is one of a few inherently surface-sensitive techniques that meet the challenge of bulk and surface signal separation.[59,60] The second harmonic generation process is the conversion of two photons of light of frequency ω to a single photon of frequency 2ω which, in the dipole approximation requires a noncentrosymmetric medium. In this approximation, randomly oriented media with inversion symmetry such as bulk liquids, gases, and amorphous and centrosymmetric crystalline solids do not generate second harmonic signals. At interfaces and phase boundaries, inversion symmetry is necessarily broken and, as a result, SHG is generated selectively from the interfaces. Surface SHG is a surface-sensitive technique that is used frequently to probe surfaces and interfaces under ambient conditions, largely free from signal contributions from the bulk. SHG has been used to investigate a variety of surface phenomena including surface structure and organization[16,61-75] at various interfaces such as solid/air,[73,76,77] solid/liquid,[59,76,77] liquid/liquid,[67,75-80] and liquid/air[63,72,77,81-83] interfaces.

The magnitude of the second harmonic response generated at an interface is a measure of the surface susceptibility, $\chi^{(2)}$, determined by the number of molecules on the surface, their molecular hyperpolarizability, and their orientational distribution. To obtain an efficient nonlinear optical material, it is necessary to use molecules with large first hyperpolarizabilities that organize into suitable noncentrosymmetric lattices. In studies on zirconium phosphonate multilayers and other interfacial assemblies, the focus has been on the chemical and/or optical properties of the organic gallery constituents, R, positioned between the $Zr(PO_3R)_2$ sheets, because of the greater structural diversity available with organic moieties. Significant effort has gone into the design and synthesis of complex second order nonlinear organic chromophores,[21,84-89] but little work has been reported on the role of the coordinated metal ion layers in determining the overall properties of the films. Chapter 2 of this dissertation describes the synthesis and characterization of oriented multilayer interfaces made of structurally simple (α,ω)-bifunctional alkanes, [R-O-PO_3^{2-}-M^{4+}-$^{-}O_3$S-R] and [R-O-PO_3^{2-}-M^{4+}-$^{-}O_2$C-R], where the orientation and optical properties of the layered assemblies are imparted through asymmetric inorganic association chemistry. Our approach to creating oriented multilayer assemblies is based on the three-step synthetic strategy pioneered by Katz and coworkers.[44] The resulting interfaces are robust and resistant to chemical attack, but Fourier Transform IR data reveal only limited order within the aliphatic portions of the layers. For these multilayers, the dominant nonlinear optical response arises from the inorganic portion of the layers. This route to creating nonlinear optical materials in multilayer structural motifs relies on the intrinsic directionality[16] and the comparatively high density attainable with layered, coordinated systems.[36,42]

Chapter 3 details the next step in this work, were we use surface Second Harmonic Generation (SHG) measurements to probe microscopic organization in asymmetrically bound (α,ω)-bifunctional alkane multilayer assemblies that were synthesized and characterized in Chapter 2. Second harmonic generation intensity measurements were also used to estimate the overall contribution of the inorganic interlayer to the overall $\chi^{(2)}$ response of ionically bound bifunctional alkane multilayer assemblies where the nonlinear response is generated from the asymmetrically coordinated metal ion center between layers. The use of bifunctional alkanes precludes any $\chi^{(2)}$ response from the purely aliphatic moiety due to the negligible hyperpolarizability of σ bonds, and allows the interrogation of systems with structures that are likely not too different from the metal bisphosphonates. Optical null ellipsometry and FTIR data point to regular growth in terms of thickness and layer density, though an overall decrease in the order of the aliphatic chains as a function of number of asymmetric adlayers was suggested by the FTIR data. The SHG data point to increasing disorder with layer growth after about eight layers, and a relatively small nonlinear activity for the inorganic interlayer constituents within the layers. We interpret the deviation from linearity of $\sqrt{I_{2\omega}}$ vs. number of layers to be consistent with an increase in distribution of the nonlinear chromophore tilt angles with layer growth.

Chapter 4 discusses the use of surface second harmonic generation measurements to understand the molecular details of potentially heterogeneous surface coverage as it relates to surface distribution of adsorbate molecules and microscopic organization within the layers. Predetermined amounts of a rigid chromophore with a large first hyperpolarizability (β) were deposited on quartz surfaces from solutions containing

specific concentrations of the chromophore and a spacer molecule with comparable length and negligible nonlinear response. UV-visible absorption spectroscopy showed a linear increase in surface chromophore loading density and SHG intensity measurements were used to probe the surface structure. This chapter discusses the complex structural issues associated with the construction of layered interfaces and presents theories and models to support the experimental data that point to the formation of two domain structures.

Finally, Chapter 5 summarizes the findings reported in Chapters 2-4 and provides a discussion of future directions for this project. In this work, surface second harmonic generation intensity measurements together with asymmetric layer synthesis have been shown to be a powerful means for probing surface and interface organization. This chapter discusses how second harmonic intensity measurements can be combined with second harmonic microscopy measurements to give a more complete picture of surface and interface structure.

1.1 Literature Cited

(1) Abbott, N. L.; Whitesides, G. M. *Langmuir* **1994**, *10*, 1493-1497.

(2) Laibinis, P. E.; Whitesides, G. M. *J. Am. Chem. Soc.* **1992**, *114*, 1990-1995.

(3) Kim, H. I.; Graupe, M.; Oloba, O.; Koini, T.; Imaduddin, S.; Lee, T. R.; Perry, S. S. *Langmuir* **1999**, *15*, 3179-3185.

(4) Lee, S.; Shon, Y.-S.; Colorado, R., Jr.; Guenard, R. L.; Lee, T. R.; Perry, S. S. *Langmuir* **2000**, *16*, 2220-2224.

(5) Xiao, X.; Hu, J.; Charych, D. H.; Salmeron, M. *Langmuir* **1996**, *12*, 235-237.

(6) Zamborini, F. P.; Crooks, R. M. *Langmuir* **1998**, *14*, 3279-3286.

(7) Zamborini, F. P.; Campbell, J. K.; Crooks, R. M. *Langmuir* **1998**, *14*, 640-647.

(8) Jennings, G. K.; Munro, J. C.; Yong, T.-H.; Laibinis, P. E. *Langmuir* **1998**, *14*, 6130-6139.

(9) Guo, L.-H.; Facci, J. S.; McLendon, G. *J. Phys. Chem.* **1995**, *99*, 8458-8461.

(10) Hockett, L. A.; Creager, S. E. *Langmuir* **1995**, *11*, 2318-2321.

(11) Crooks, R. M.; Ricco, A. J. *Acc. Chem. Res.* **1998**, *31*, 219-227.

(12) Ishihara, T.; Higuchi, M.; Takagi, T.; Ito, M.; Nishiguchi, H.; Takita, Y. *J. Mater. Chem.* **1998**, *8*, 2037-2042.

(13) Hickman, J. J.; Ofer, D.; Laibinis, P. E.; Whitesides, G. M.; Wrighton, M. S. *Science* **1991**, *252*, 688-691.

(14) Gardner, T. J.; Frisbie, C. D.; Wrighton, M. S. *J. Am. Chem. Soc.* **1995**, *117*, 6927-6933.

(15) Batchelder, D. N.; Evans, S. D.; Freeman, T. L.; Haeussling, L.; Ringsdorf, H.; Wolf, H. *J. Am. Chem. Soc.* **1994**, *116*, 1050-1053.

(16) Katz, H. E.; Wilson, W. L.; Scheller, G. *J. Am. Chem. Soc.* **1994**, *116*, 6636-6640.

(17) Wollman, E. W.; Kang, D.; Frisbie, C. D.; Lorkovic, I. M.; Wrighton, M. S. *J. Am. Chem. Soc.* **1994**, *116*, 4395-4404.

(18) Abbott, N. L.; Rolison, D. R.; Whitesides, G. M. *Langmuir* **1994**, *10*, 2672-2682.

(19) Kanis, D. R.; Ratner, M. A.; Marks, T. J. *Chem. Rev.* **1994**, *94*, 195-242.

(20) Nie, W. *Adv. Mater.* **1993**, *5*, 520-545.

(21) Marder, S. R.; Sohn, J. E.; Stucky, G. D. Editors. *Materials for Nonlinear Optics: Chemical Perspective. ACS Symposium Series,* **1991**, 455.

(22) Prasad, P.; Williams, D. J. *Introduction to Nonlinear Optical Effects in Molecules and Polymers, Wiley, New York* **1991**.

(23) Blodgett, K. B. *J. Am. Chem. Soc.* **1935**, *57*, 1007-1022.

(24) Langmuir, I. *J. Am. Chem. Soc.* **1917**, *39*, 1848-1906.

(25) Netzer, L.; Sagiv, J. *J. Am. Chem. Soc.* **1983**, *105*, 674-676.

(26) Sagiv, J. *J. Am. Chem. Soc.* **1980**, *102*, 92-98.

(27) Bain, C. D.; Whitesides, G. M. *J. Am. Chem. Soc.* **1988**, *110*, 3665-3666.

(28) Bain, C. D.; Biebuyck, H. A.; Whitesides, G. M. *Langmuir* **1989**, *5*, 723-727.

(29) Nuzzo, R. G.; Allara, D. L. *J. Am. Chem. Soc.* **1983**, *105*, 4481-4483.

(30) Nuzzo, R. G.; Fusco, F. A.; Allara, D. L. *J. Am. Chem. Soc.* **1987**, *109*, 2358-2368.

(31) Nuzzo, R. G.; Dubois, L. H.; Allara, D. L. *J. Am. Chem. Soc.* **1990**, *112*, 558-569.

(32) Xia, Y.; Whitesides, G. M. *Angew. Chem., Int. Ed.* **1998**, *37*, 550-575.

(33) Troughton, E. B.; Bain, C. D.; Whitesides, G. M.; Nuzzo, R. G.; Allara, D. L.; Porter, M. D. *Langmuir* **1988**, *4*, 365-385.

(34) Karpovich, D. S.; Blanchard, G. J. *Langmuir* **1994**, *10*, 3315-3322.

(35) Schessler, H. M.; Karpovich, D. S.; Blanchard, G. J. *J.Am.Chem.Soc.***1996**, *118*, 9645-9651.

(36) Cao, G.; Hong, H. G.; Mallouk, T. E. *Acc. Chem. Res.* **1992**, *25*, 420-427.

(37) Akhter, S.; Lee, H.; Hong, H. G.; Mallouk, T. E.; White, J. M. *J. Vac. Sci. Technol., A* **1989**, *7*, 1608-1613.

(38) Katz, H. E.; Scheller, G.; Putvinski, T. M.; Schilling, M. L.; Wilson, W. L.; Chidsey, C. E. D. *Science* **1991**, *254*, 1485-1487.

(39) Lee, H.; Kepley, L. J.; Hong, H. G.; Akhter, S.; Mallouk, T. E. *J. Phys. Chem.* **1988**, *92*, 2597-2601.

(40) Lee, H.; Kepley, L. J.; Hong, H. G.; Mallouk, T. E. *J. Am. Chem. Soc.* **1988**, *110*, 618-620.

(41) Snover, J. L.; Thompson, M. E. *J. Am. Chem. Soc.* **1994**, *116*, 765-766.

(42) Thompson, M. E. *Chem. Mater.* **1994**, *6*, 1168-1175.

(43) Yang, H. C.; Aoki, K.; Hong, H. G.; Sackett, D. D.; Arendt, M. F.; Yau, S. L.; Bell, C. M.; Mallouk, T. E. *J. Am. Chem. Soc.* **1993**, *115*, 11855-11862.

(44) Putvinski, T. M.; Schilling, M. L.; Katz, H. E.; Chidsey, C. E. D.; Mujsce, A. M.; Emerson, A. B. *Langmuir* **1990**, *6*, 1567-1571.

(45) Kohli, P.; Taylor, K. K.; Harris, J. J.; Blanchard, G. J. *J.Am.Chem.Soc.***1998**, *120*, 11962-11968.

(46) Kohli, P.; Blanchard, G. J. *Langmuir* **1999**, *15*, 1418-1422.

(47) Kohli, P.; Blanchard, G. J. *Langmuir* **2000**, *16*, 4655-4661.

(48) Major, J. S.; Blanchard, G. J. *J. Am. Chem. Soc.* **in review**.

(49) Major, J. S.; Blanchard, G. J. *J. Am. Chem. Soc.* **in review**.

(50) Xu, B.; Holdcroft, S. *Macromolecules* **1993**, *26*, 4457-4460.

(51) Nalwa, H. S. E. *Conducting Polymers: Transport, Photophysics and Applications; John Wiley & Sons, New York* **1997**, *4*.

(52) Ledoux, I.; Zyss, J.; *Novel Optical Materials and Applications* Edited by I.C. Khoo, F. S., C. Umeton *Wiley, New York* **1997**.

(53) Becka, A. M.; Miller, C. J. *J. Phys. Chem.* **1992**, *96*, 2657-2668.

(54) Corbitt, T. S.; Crooks, R. M.; Ross, C. B.; Hampden-Smith, M. J.; Schoer, J. K. *Adv. Mater.* **1993**, *5*, 935-938.

(55) Miller, C.; Graetzel, M. *J. Phys. Chem.* **1991**, *95*, 5225-5233.

(56) Miller, C.; Cuendet, P.; Graetzel, M. *J. Phys. Chem.* **1991**, *95*, 877-886.

(57) Xia, Y.; Mrksich, M.; Kim, E.; Whitesides, G. M. *J. Am. Chem. Soc.* **1995**, *117*, 9576-9577.

(58) Aspnes, D. E.; Studna, A. A. *Phys. Rev. Lett.* **1985**, *54*, 1956-1959.

(59) Shen, Y. R. *Annu. Rev. Phys. Chem.* **1989**, *40*, 327-350.

(60) Shen, Y. R. *The Principles of Nonlinear Optics*; *Wiley, New York* **1984**.

(61) Yan, E. C. Y.; Eisenthal, K. B. *J. Phys. Chem. B* **2000**, *104*, 6686-6689.

(62) Yan, E. C. Y.; Eisenthal, K. B. *J. Phys. Chem. B* **1999**, *103*, 6056-6060.

(63) Zimdars, D.; Dadap, J. I.; Eisenthal, K. B.; Heinz, T. F. *J. Phys. Chem. B* **1999**, *103*, 3425-3433.

(64) Simpson, G. J.; Rowlen, K. L. *Anal. Chem.* **2000**, *72*, 3399-3406.

(65) Simpson, G. J.; Westerbuhr, S. G.; Rowlen, K. L. *Anal. Chem.* **2000**, *72*, 887-898.

(66) Simpson, G. J. *Appl. Spectrosc.* **2001**, *55*, 16A-32A.

(67) Grubb, S. G.; Kim, M. W.; Rasing, T.; Shen, Y. R. *Langmuir* **1988**, *4*, 452-454.

(68) Shen, Y. R.; Chen, W.; Feller, M. B.; Huang, J. Y.; Superfine, R. *Mol. Cryst. Liq. Cryst.* **1991**, *207*, 77-85.

(69) Shen, Y. R. *Nature* **1989**, *337*, 519-525.

(70) Oh-e, M.; Hong, S.-C.; Shen, Y. R. *J. Phys. Chem. B* **2000**, *104*, 7455-7461.

(71) Shen, Y. R. *Surf. Sci.* **1994**, *299-300*, 551-562.

(72) Vogel, V.; Shen, Y. R. *Annu. Rev. Mater. Sci.* **1991**, *21*, 515-534.

(73) Corn, R. M.; Higgins, D. A. *Chem. Rev.* **1994**, *94*, 107-125.

(74) Corn, R. M.; Higgins, D. A. *Handb. Surf. Imaging Visualization* **1995**, 479-492.

(75) Higgins, D. A.; Naujok, R. R.; Corn, R. M. *Chem. Phys. Lett.* **1993**, *213*, 485-490.

(76) Higgins, D. A.; Byerly, S. K.; Abrams, M. B.; Corn, R. M. *J. Phys. Chem.* **1991**, *95*, 6984-6990.

(77) Higgins, D. A.; Abrams, M. B.; Byerly, S. K.; Corn, R. M. *Langmuir* **1992**, *8*, 1994-2000.

(78) Kott, K. L.; Higgins, D. A.; McMahon, R. J.; Corn, R. M. *J. Am. Chem. Soc.* **1993**, *115*, 5342-5343.

(79) Higgins, D. A.; Corn, R. M. *J. Phys. Chem.* **1993**, *97*, 489-493.

(80) Conboy, J. C.; Daschbach, J. L.; Richmond, G. L. *J. Phys. Chem.* **1994**, 9688-9692.

(81) Rasing, T.; Shen, Y. R.; Kim, M. W.; Grubb, S.; Bock, J. *Springer Ser. Opt. Sci.* **1985**, *49*, 307-310.

(82) Rasing, T.; Shen, Y. R.; Kim, M. W.; Valint, P., Jr.; Bock, J. *Phys. Rev. A* **1985**, *31*, 537-539.

(83) Kemnitz, K.; Bhattacharyya, K.; Hicks, J. M.; Pinto, G. R.; Eisenthal, K. B.; Heinz, T. F. *Chem. Phys. Lett.* **1986**, *131*, 285-290.

(84) Marder, S. R.; Beratan, D. N.; Cheng, L. T. *Science* **1991**, *252*, 103-106.

(85) Marder, S. R.; Perry, J. W.; Bourhill, G.; Gorman, C. B.; Tiemann, B. G.; Mansour, K. *Science* **1993**, *261*, 186-189.

(86) Marder, S. R.; Gorman, C. B.; Tiemann, B. G.; Cheng, L. T. *J. Am. Chem. Soc.* **1993**, *115*, 3006-3007.

(87) Meyers, F.; Marder, S. R.; Pierce, B. M.; Bredas, J. L. *J. Am. Chem. Soc.* **1994**, *116*, 10703-10714.

(88) Meyers, F.; Marder, S. R.; Pierce, B. M.; Bredas, J. L. *Chem. Phys. Lett.* **1994**, *228*, 171-176.

(89) Risser, S. M.; Beratan, D. N.; Marder, S. R. *J. Am. Chem. Soc.* **1993**, *115*, 7719-7728.

Chapter 2

Demonstration of Oriented Multilayers through Asymmetric Metal Coordination Chemistry

Summary

We report on the growth of oriented multilayer assemblies where the layers are connected through coordination to Zr^{4+} and Hf^{4+} ions. Layer orientation is achieved by asymmetric coordination at each layer. We demonstrate R-O-PO_3^{2-} -M^{4+}-$^{-}O_3S$-R and R-O-PO_3^{2-} -M^{4+} -$^{-}O_2C$-R directional coordination in multilayer assemblies. The synthetic approach to the formation of oriented multilayers is to use a ω-hydroxyalkanoic acid or a ω-hydroxyalkane sulfonic acid in combination with phosphorylation chemistry at the hydroxyl group to activate the interface at each step, allowing for the growth of additional, oriented layers. The resulting interface is resistant to chemical attack and Fourier Transform IR data reveal only limited order of the aliphatic portions of the layers.

2.1 Introduction

Self-assembling thin films and the chemical modification of surfaces are important areas in materials chemistry for both fundamental and application-oriented reasons. Fundamental interest in this class of materials stems from the desire to understand and control interfacial structure. The practical consequences of achieving such control include the recent development of several surface-dependent technologies including chemical sensing,[1-3] synthetic light harvesting,[4] electronic, electro-optic or photonic devices,[5-7] and nonlinear optics.[8,9]

The development of organized molecular assemblies at interfaces first started with Langmuir-Blodgett films and proceeded through alkyltrichlorosilane multilayers to the alkanethiol/gold monolayers and metal-bisphosphonate multilayers. This structural evolution has been driven by the need for substantial molecular-scale organization combined with physical robustness. At the present time, the most durable and versatile means for fabricating highly organized interfacial multilayer assemblies has been through the zirconium-phosphonate (ZP) chemistry pioneered by the Mallouk, Katz and Thompson groups.[9-12] Metal-bisphosphonate multilayers are bonded via ionic coordination chemistry and are thus thermally robust and reasonably well ordered, as evidenced by the fact that interfaces more than 30 layers thick can be grown easily[9,13] and their synthesis allows automatically for layer-by-layer structural control. Initially, ZP multilayers were synthesized using (α,ω)-alkanebisphosphonates, and such symmetric ligands preclude orientational control within the layers.[10,11] Katz and coworkers[8] demonstrated orientational control within a layer by applying hydroxyl-terminated phosphonates to zirconated surfaces. In that work, the identity of the ω-

hydroxyorganophosphonate was used to enforce the macroscopic orientation of the layers and the inorganic interlayer connection chemistry was locally symmetric about the metal center. Katz' use of an asymmetric ligand is a prerequisite for orientational selectivity in bonding. To form multilayer assemblies, the terminal hydroxyl groups of the layer must be reacted with $POCl_3$ and H_2O to yield a reactive surface before a subsequent layer can be added. Our approach accomplishes molecular orientation using the same three-step synthetic strategy. The unique aspect of the work we report here is that we achieve directionality within the layers using asymmetric association chemistry.

Monolayers of carboxylic acids adsorbed on various metal and metal oxide surfaces, including oxidized aluminum[14-19] and silver[20-23] have been reported. In all these cases, only monolayers have been prepared by direct adsorption of the carboxylate to the metal or metal oxide surface. Bernasek and Schwartz[24-26] have prepared layers of alkanoic acids by "priming" partially or fully hydrolyzed alumina surfaces with vapor phase zirconium *tert*-butoxide ($(t\text{-BuO})_4Zr$) at reduced pressure, followed by adsorption of alkanoic acids from solution. In that work, asymmetric and symmetric C=O stretching modes were observed between 1400 cm^{-1} and 1600 cm^{-1} and the absence of the free carboxylate (CO_2H) band at ~1740 cm^{-1} demonstrated the presence of extensive carboxylate coordination to the metal sites within the monolayers.[26]

While phosphonates and carboxylates have been used as functional groups in layered interface synthesis, we are not aware of reports where sulfonic acids have been used in the analogous formation of layers. We are also not aware of other efforts to create oriented layers through asymmetric coordination chemistry. In this paper we describe the synthesis of oriented multilayers containing carboxylic, phosphonic and sulfonic acid

functionalities on oxidized silicon and silica surfaces. We initiate layer growth by phosphorylating the hydrolyzed substrate surface in either of two ways (*vide infra*), followed by sequential adsorption of Zr^{4+} or Hf^{4+} and 10-hydroxydecanoic acid (HDA) or 3-hydroxypropanesulfonic acid (PSA). Reaction of the resulting terminal hydroxyl functionality with $POCl_3$/collidine/H_2O produces a surface that is again amenable to treatment with the metal ion. We have characterized these assemblies using optical null ellipsometry, external reflection FTIR, UV-visible spectroscopy, ^{13}C NMR, X-ray photoelectron spectroscopy (XPS), and by wet chemical means to determine their resistance to solvent attack. The formation of multiple layers is facile and the resulting oriented layers are robust. The XPS data show that for both HDA and PSA multilayers, the Zr/P ratio is ~ 1, demonstrating 1:1 trans-layer ligand stoichiometry, consistent with our linear optical response and ellipsometry data.

2.2 Experimental Section

Reagents and Materials. 10-Hydroxydecanoic acid (HDA, 85 %), 3-hydroxy-1-propanesulfonic acid (PSA), sodium salt (80 %), potassium chloride, zirconyl chloride octahydrate (98 %), hafnium oxychloride hydrate (99.99+ %), 1,16-hexadecanedioic acid (96 %), bis(3-sulfopropyl)itaconate dipotassium salt, phosphorusoxychloride (99 %), 11-mercaptoundecanoic acid (95 %), 3-mercapto-1-propanesulfonic acid (90 %), stearic-1-^{13}C acid (99 atom % ^{13}C) were all obtained from Aldrich. Other reagents used were 2,4,6-collidine (Lancaster), 3-aminopropyl-dimethylethoxysilane (United Chemical Technologies, Inc), hydrogen peroxide (J. T. Baker), ammonium hydroxide, sulfuric acid, hydrochloric acid (Columbus Chemical Industries, Inc), and chloroform-*d* (99.8 % with 1% TMS), D_2O (99.9 %) (Cambridge Isotope Laboratories). Anhydrous acetonitrile (99+ %), reagent grade acetonitrile, hexanes, dichloromethane, toluene, and ethanol were obtained from Aldrich, and tetrahydofuran was obtained from E. M. Science. All reagents were used as received, without further purification.

Multilayer Syntheses. The growth of layered structures is accomplished using a procedure similar to that we have reported before for ZP layers.[27] Si(100) wafers (Multi Crystal Optics, Inc) precut to 15 x 15 x 1 mm, were cleaned by immersion in piranha solution (3 H_2SO_4:1 H_2O_2) for 15 minutes, rinsed with flowing distilled water, hydrolyzed in 2 M HCl for 5 minutes, rinsed with distilled water, dried under a stream of N_2 and primed by immersion in a 1 % v/v solution of 3-animopropylethoxydimethylsilane in toluene under an argon atmosphere for 24 hours, followed by thorough rinsing with reagent grade hexane. The aminated Si(100) substrate was phosphorylated by reaction with 0.2 M $POCl_3$ and 0.2 M 2,4,6-collidine in anhydrous acetonitrile under argon for 15

minutes and rinsed with reagent grade acetonitrile. The phosphorylated surface was zirconated for 10 min. with a 5-m<u>M</u> solution of $ZrOCl_2$ in 60 % EtOH(*aq*). The resulting surface, schematized in Figure 2.1, could then be used for multilayer growth. Subsequent layer deposition was accomplished by immersion of substrates in solutions of HDA (1.54 m<u>M</u> in 95 % EtOH) or the sodium salt of PSA (1.54 m<u>M</u> in 70 % EtOH(*aq*)) overnight at room temperature. Subsequent layers were added by reaction of the terminal hydroxyl functionality with $POCl_3$/collidine under the same reaction conditions as indicated above, followed by zirconation and reaction with either HDA or PSA, with extensive water rinsing between each step. We also investigated the efficacy of direct phosphorylation of the silanol groups present on the substrate. For direct phosphorylation, the cleaned, hydrolyzed silicon substrate was exposed to $POCl_3$, hydrolyzed, and zirconated. Additional layers were then deposited as described above. For multilayers assembled using Hf^{4+}, the identical procedure was used save for the use of $HfOCl_2$ in place of $ZrOCl_2$. Optical null ellipsometry and FTIR, ^{13}C NMR, and UV-Visible absorption spectroscopies were used to characterize the systems as described below.

Surface Characterization. The thickness of the multilayers as synthesized was determined using a commercial optical null ellipsometer (Rudolf AutoEl-II) operating at 632.8 nm with a 70° angle of incidence. The data were acquired and reduced using Rudolf software. The refractive index of the primer and oxide layers was taken to be $\mathbf{n} = 1.462 + 0i$ and $\mathbf{n} = 1.540 + 0i$ was used for the ZP layers. Each data point reported here is the average of at least five measurements from different locations on each substrate. External reflection FTIR spectra of the multilayers were obtained using a Nicolet Magna-IR™ 550 spectrometer equipped with a $N_2(l)$ cooled MCT type A detector.

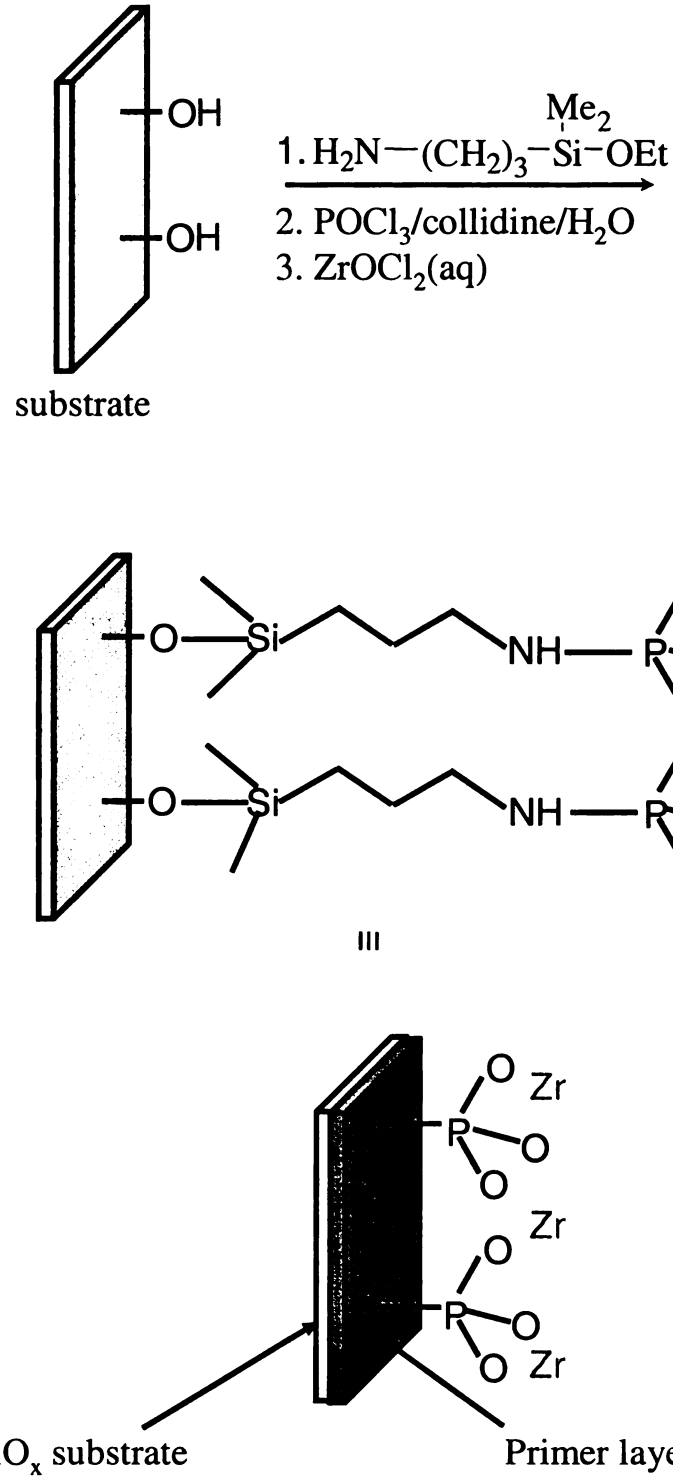

Figure 2.1 Schematic of the priming chemistry used in the formation of some of the interfaces described here. We have demonstrated that reaction of the silanol-containing surface directly with $POCl_3$/collidine then with $ZrOCl_2(aq)$ yields the surfaces with the same properties as those formed with the silane-based priming chemistry. This schematic is not intended to indicate the precise stoichiometry of the layered interface.

Spectra were acquired for the IR beam incident at angles of incidence between 70° and 80° with respect to the surface normal and spectra were averaged over at least 10,000 scans at 2 cm^{-1} resolution against a background of bare, oxidized substrate. ^{13}C NMR spectra of the multilayers grown on silica gel (60 –200 mesh, Mallinckrodt) and dispersed in $CDCl_3$ were taken with a 500 MHz Varian VXR 500 NMR spectrometer. UV-visible spectra of the carboxylate multilayers were taken using Unicam model UV-2 spectrometer. XPS measurements were made on multilayer samples using a PHI Model 5400 X-ray spectrometer. The X-ray source is the AlKα line and all values reported are referenced to the C1s line at 285.0 eV binding energy.

2.3 Results and Discussion

The work we report here focuses on the synthesis and characterization two new families of oriented multilayers. These systems contain two potentially useful functional groups, carboxylates and sulfonates. The synthetic route we employ allows molecular control over layer growth and orientation. This work is a step toward the larger goal of investigating the nonlinear optical properties of structurally simple (α,ω)-bifunctional alkanes, where asymmetric coordination at the metal centers is used to achieve the desired macroscopic orientation and $\chi^{(2)}$ nonlinear optical response of the multilayers. We report here asymmetric systems with R-OPO_3^{2-} - Zr - ^-O_2C-R and R-OPO_3^{2-} - Zr - ^-O_3S-R (Figure 2.2).

Before discussing the details of the multilayer structures we report here, it is important to consider the preparation of the substrate surface. In metal phosphonate multilayer syntheses, the oxidized silicon or silica substrate is typically primed by treatment of the surface silanol groups with an aminosilane reagent such as 3-aminopropyldimethylethoxysilane or 3-aminopropyltriethoxysilane, to give an amino-terminated surface. The amino functionalities are then reacted with $POCl_3$ in dry acetonitrile, hydrolyzed in water and zirconated in an aqueous ~ 1 m<u>M</u> $ZrOCl_2$ solution, followed by immersion in a ~1 m<u>M</u> solution of a bisphosphonated compound.[27,28] The addition of subsequent layers is then accomplished with alternate zirconation and bisphosphonation steps. Perhaps the single most important step in determining the extent of organization and density of the layers is the chemistry used in the preparation of the substrate. To determine the role of priming in multilayer growth, we have synthesized multilayers on silicon substrates where the initial phosphate or phosphonate functionality

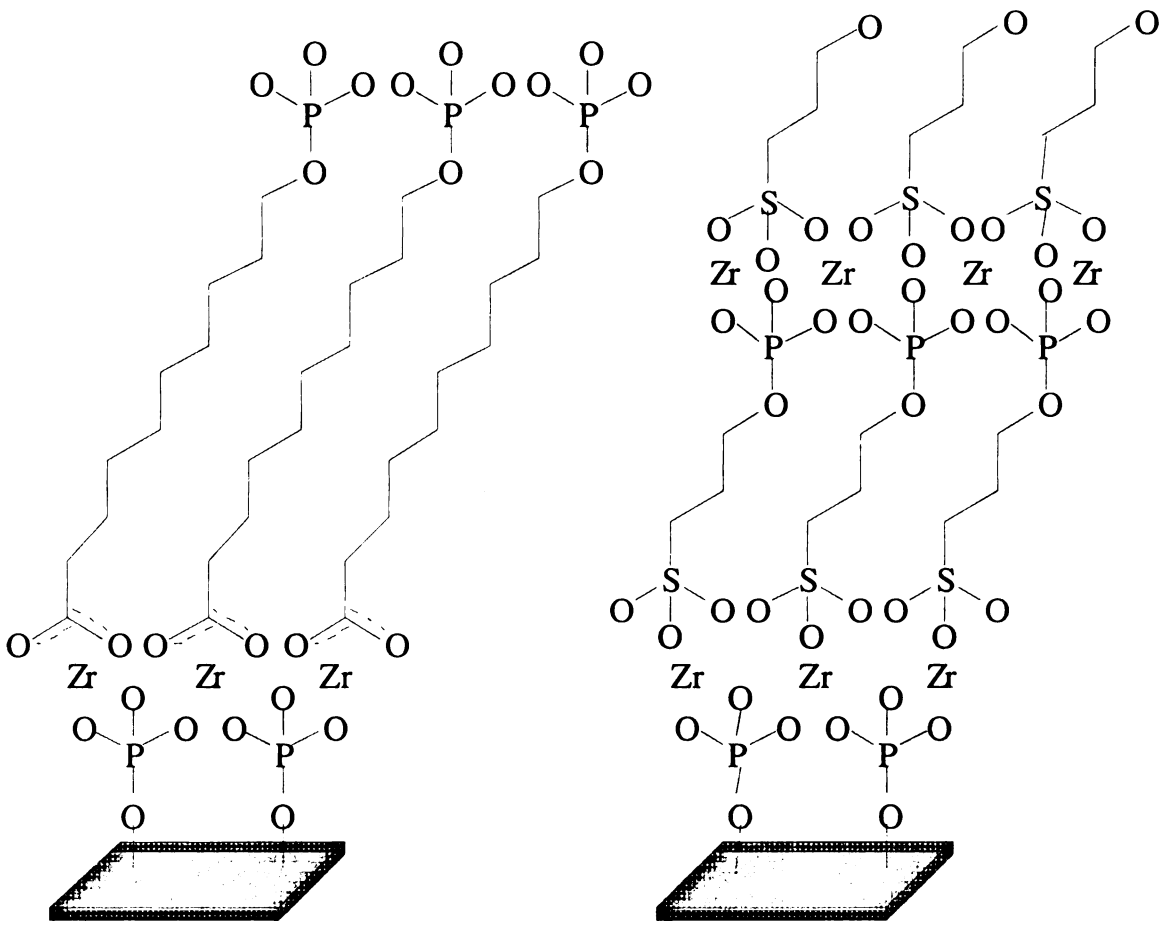

Figure 2.2. Schematic of the asymmetric multilayers we report here. Left: An oriented multilayer formed using HDA and reacted with $POCl_3$/collidine then H_2O. Right: An oriented multilayer formed using PSA and reacted with $POCl_3$/collidine then H_2O. These schematics are not intended to indicate the precise stoichiometry of the layered interfaces.

was created by two different routes. For both routes, the silicon substrates are first treated to produce a native oxide layer ~15 Å thick. The first method was as outlined above, and the second method was the direct treatment of the oxidized and hydrolyzed Si surface with $POCl_3$. We find no significant difference between the two surfaces in terms of the ellipsometric data, Figure 2.3. The surfaces primed with the silane reagent first produced HDA layers with thicknesses of 14.4 ± 0.5 Å per layer and the $POCl_3$ treated silanol surface yielded a value of 14.6 ± 0.6 Å per layer. The intercepts were 7.2 ± 2.1 Å and 9.6 ± 4.8 Å for the silane primed and $POCl_3$-treated silanol surfaces, respectively. We understand the 7.2 Å height for the silane-primed surface based on simple molecular mechanics predictions. The 9.6 Å thickness for the $POCl_3$-treated surface is possible evidence for the formation of polyphosphates resulting from the presence of residual water at the silanol surface, although further investigation is clearly needed to resolve this matter. We do note that the XPS data on Zr/P ratio are not consistent with the formation of polyphosphates (*vide infra*). The facile reaction of the surface silanols with $POCl_3$ is expected since, in oriented multilayer growth, the terminal OH-groups are phosphorylated directly with $POCl_3$ to yield phosphate functionalities[8,9,29] that facilitate adsorption of subsequent layers. Lukeš *et al.*[30] have phosphorylated the active silanol groups on the surface of silica gel with various phosphorus oxyacids in inert solvents (*e.g.* hexane, toluene) to produce surface-bound esters. Because the use of substrates where the surface silanol groups have been phosphorylated and hydrolyzed directly yields the same multilayers as those resulting from the more involved priming chemistry, we have used the simpler, direct surface treatment in the preparation of samples discussed in this paper.

The initial diagnostic tool we use to evaluate whether or not layers are deposited

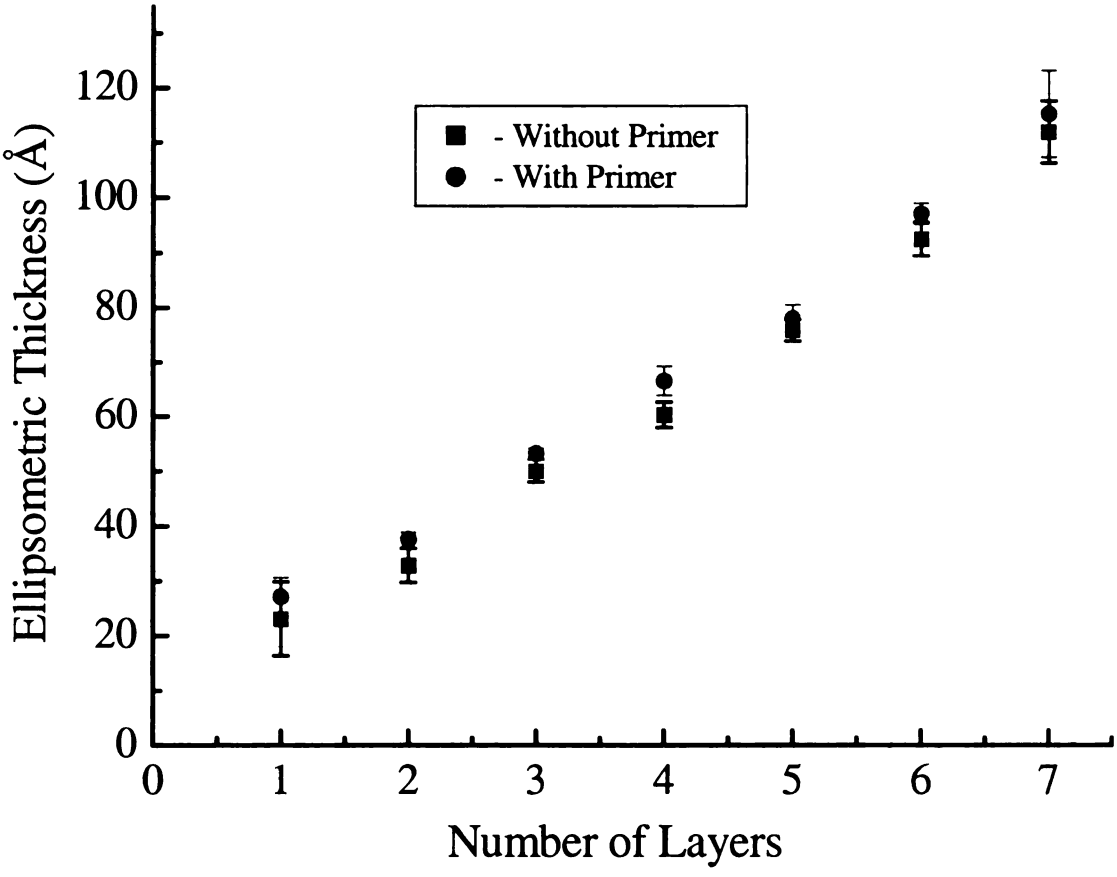

Figure 2.3. Ellipsometric thickness of 10-hydroxydecanoic acid (HDA) with and without a primer.

on silicon substrates is optical null ellipsometry. Ellipsometry is a convenient technique for determining the thickness of SAMs on various substrates.[31] Figure 2.4 shows linear growth of seven layers of HDA and seven layers of PSA with slopes of 14.4 ± 0.5 Å/layer and 5.7 ± 0.2 Å/layer, respectively. We note that the number of layers we report in Figure 2.4 is not the upper limit to our ability to grow them. We expect that, as with the metal bisphosphonate layers, the formation of up to 100 layers is easily attainable. The average thickness of these layers, as measured by ellipsometry, when compared to the values predicted by molecular mechanics of 17.7 and 9.5 Å respectively, indicates that our layers are either tilted or coverage is incomplete. From our absorption measurements on multilayers grown using a biphenyl-containing ligand, the surface loading density we recover is consistent with essentially full coverage to within our ability to make this determination (*vide infra*). The tilt angles we calculate are 38° ± 1° for HDA and 53° ± 2° for PSA. The calculated tilt angle for HDA is consistent with other measurements on metal phosphonates made by our group and others. The tilt angle for PSA, however, is significantly different. We consider that the calculated angle is equal to the magic angle, within the experimental uncertainty because of significant disorder within the layers. Because the aliphatic portions of the layer constituents are only C_3 in length, it is not possible to achieve organization mediated by van der Waals interactions that is sufficiently strong to overcome thermal effects. It is well known, for example, that the aliphatic organization seen for alkanethiols is present only for thiols greater than C_9 because of the additive nature of the van der Waals interactions.[32]

The disordered conformation indicated by ellipsometry is not unique to our

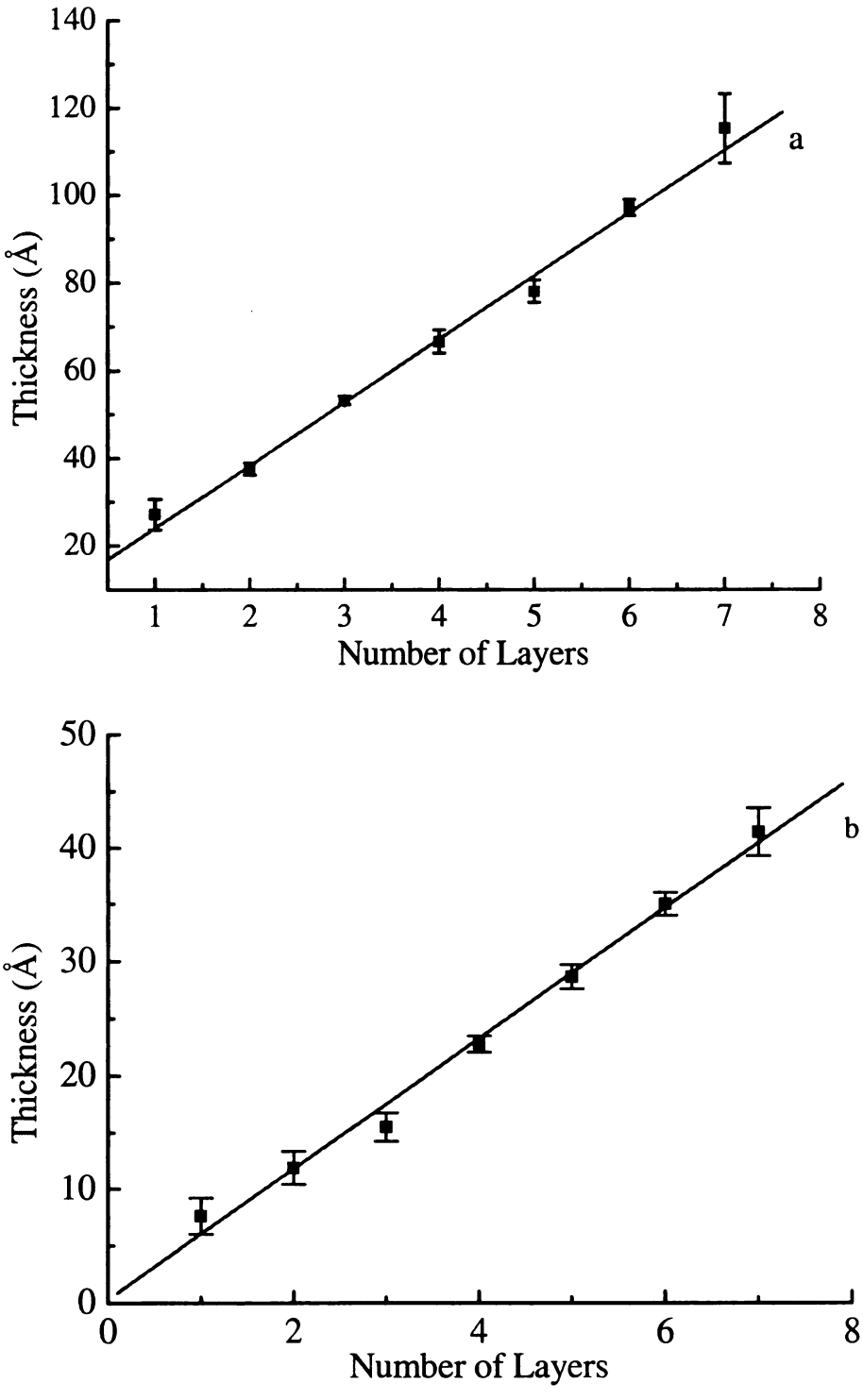

Figure 2.4. Ellipsometric thickness of the interfaces as a function of number of layers added. (a) Layers formed using HDA and Zr^{4+}. The slope of the best-fit line is 14.4 ± 0.4 Å/layer. (b) Layers formed using PSA and Zr^{4+}. The slope of the best-fit line is 5.7 ± 0.2 Å/layer.

systems, but has been observed by others for a variety of mono- and multilayer systems.[17,33-38] The limited extent of organization in these systems has been attributed to partial surface coverage and steric factors that preclude mesoscopic organization. As the aliphatic chain length of the layer constituents increases however, the interchain interactions can become sufficiently strong to result in order within the layers. Our data indicate that HDA multilayers are relatively more ordered than the PSA multilayers, consistent with the relative lengths of the two layer constituents.

FTIR spectroscopy is particularly useful for characterizing organization in layered assemblies containing aliphatic constituents. Extensive studies on a variety of alkane systems have well-established relationship between band energy and local environment. The asymmetric stretch for liquid alkanes is centered at 2928 cm^{-1} and in crystalline alkanes this band shifts to ~2918 cm^{-1} while for the symmetric stretch, the disordered limit is ~2858 cm^{-1} and the crystalline band position is 2848 cm^{-1}. For both bands, the extent of organization is taken to be related to band position, although there is no scale upon which "organization" is based. The C-H stretching region of up to eight layers of HDA (Figure 2.5a) contains characteristic asymmetric and symmetric CH_2 stretching resonances at 2923 cm^{-1} and 2852 cm^{-1} respectively. Similar results were obtained for substrates treated with PSA (Figure 2.5b). Thus, the ellipsometry data suggest limited organization for HDA and little or no organization for PSA, and the FTIR data indicate little or no crystalline organization in either system. We do not attempt to extract quantitative layer growth information from these data because the external reflection sample geometry is not as reproducible as is needed for quantitation and because UV-visible absorption and optical null ellipsometry data both provide the quantitative

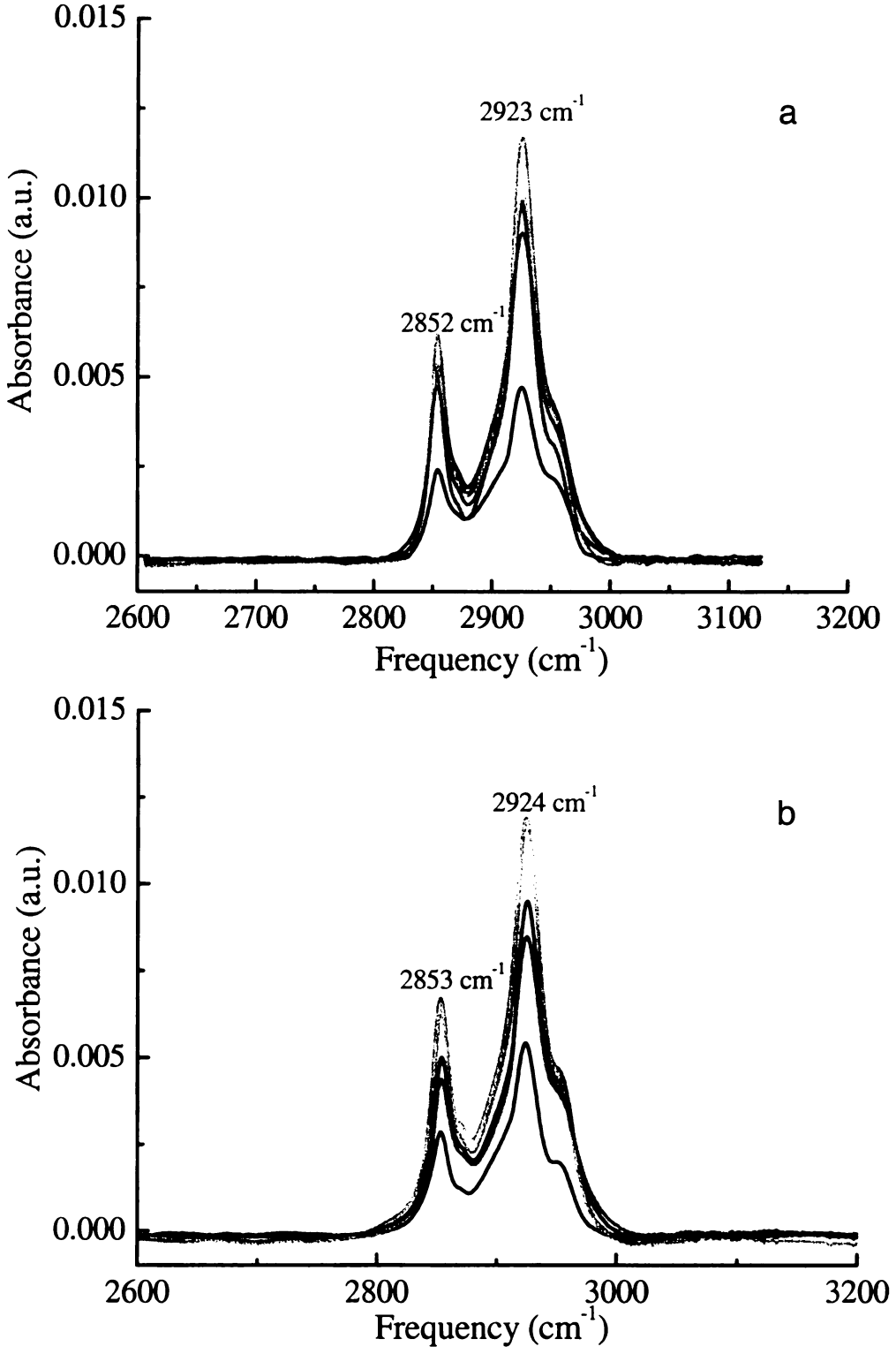

Figure 2.5. (a) FTIR spectra of the CH stretching region for 3 through 8 layers of HDA. (b) FTIR spectra of the CH stretching region for 3 through 8 layers of PSA. No band shifts are found for either interface as a function of number of layers added.

information we need.

In addition to the CH stretching region, there is significant structural information available from other IR spectral regions. The HDA monolayer exhibits two broad bands at 1610 - 1650 cm^{-1} and near 1450 cm^{-1} (Figure 2.6a). These bands are the asymmetric and symmetric carboxylate stretches, respectively.[25] Free carboxylic acids have a characteristic resonance at ~1740 cm^{-1} and the absence of this band indicates essentially complete chemisorption (complexation and deprotonation) of a layer. To evaluate the extent of carboxylate complexation by Zr^{4+} in multilayers, we have synthesized five layers of 1,16-hexadecanedioic acid ($HO_2C(CH_2)_{14}CO_2H$) on silicon and the FTIR spectrum (Figure 2.6b) shows, in addition to carboxylate bands at 1466 cm^{-1} and 1591 cm^{-1}, a prominent free C=O band at 1742 cm^{-1}. This is expected because of the free terminal -CO_2H group. When zirconated and capped with a layer of HDA, the 1742 cm^{-1} resonance almost completely disappears (Figure 2.6c). We take this as evidence of coordination of the (deprotonated) carboxylate group to Zr^{4+}. Following the addition of this capping layer, there is a small residual signal at 1728 cm^{-1}, which we attribute to the presence of a limited number of defects in the layer.

Evidence of carboxylate multilayer growth was also demonstrated using absorption measurements to quantitate growth of 4'-hydroxy-4-biphenylcaboxylic acid ($HOC_6H_4C_6H_4CO_2H$, HBPCA) layers on quartz. The synthetic procedure for the growth of these layers is the same as described for HDA and PSA. For these measurements, a linear increase in absorbance, 0.005 a.u./bilayer (one layer grown on each side of the substrate), at $\lambda_{max} \cong 284$ nm was observed as the number of layers was increased from 1 to 7 (Figure 2.7). We use these data to estimate the loading density of layer constituents.

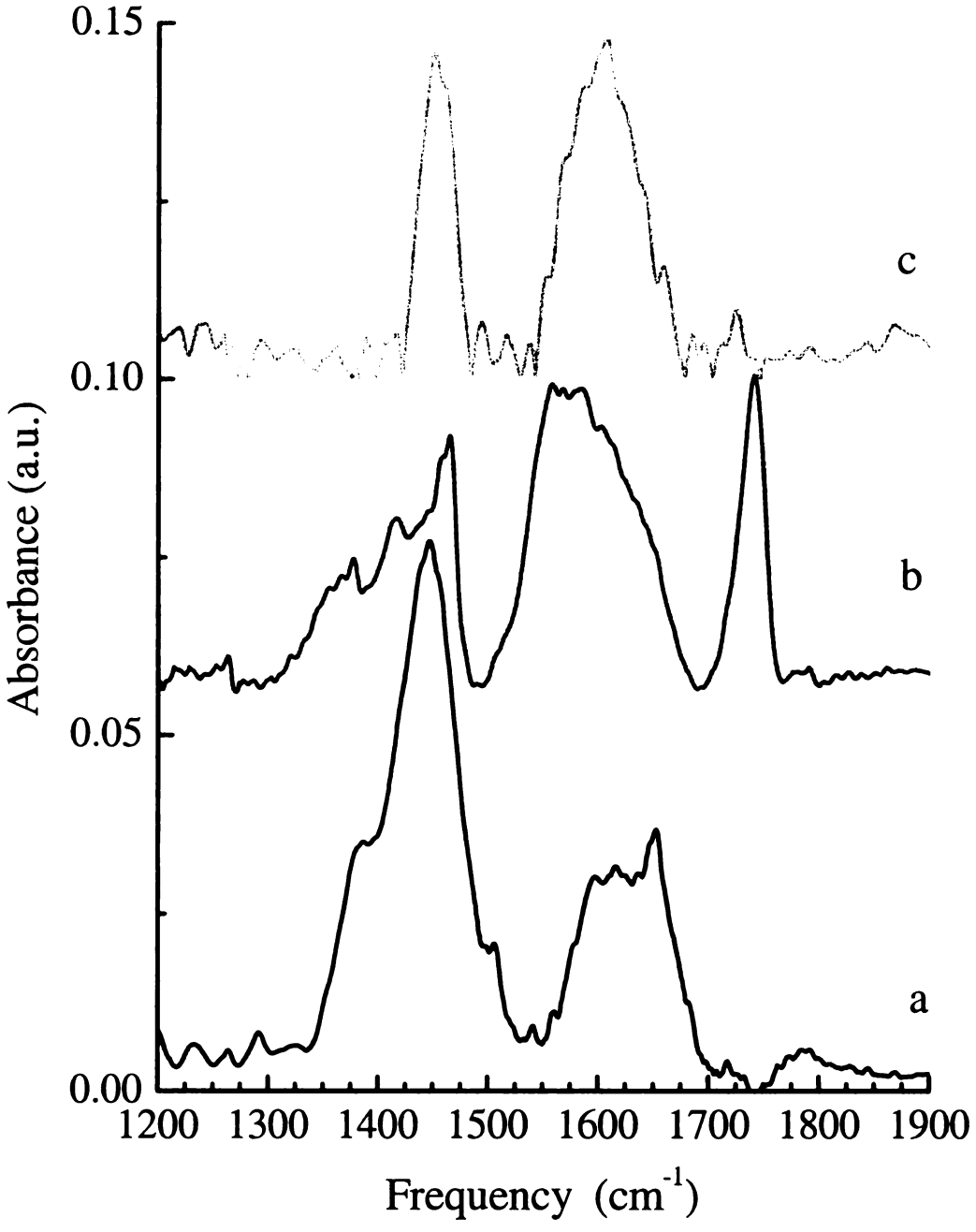

Figure 2.6. (a) FTIR spectrum of the C=O stretching region of a 6-layer assembly of HDA. (b) FTIR spectrum of a 6-layer assembly of Zr-bis(1,16-hexadecanedioate). The prominent resonance at 1742 cm^{-1} results from the uncomplexed terminal $-CO_2H$ functionality. (c) FTIR spectrum of the multilayer shown in (b) but capped with a single layer of HDA. The absence of the free $-CO_2H$ resonance indicates essentially complete capping of the surface.

For the biphenyl chromophore, we take the extinction coefficient at 284 nm to be 18,000 L/mol-cm,[39] corresponding to an absorption cross section of $3x10^{-17}$ cm^2/mlc. The absorption data yield a surface density of $8.4x10^{13}$ mlc/cm^2, approximately a factor of two less than what we have observed for ZP polymer layers on quartz.[40] One possibility for this comparatively low density is that the number of surface silanol groups was not maximized for these substrates prior to layer growth. In any event, it is instructive to have an estimate of the density of the layers. The linearity of the absorbance signal as a function of number of layers indicates that the growth of the layers occurs such that each layer is registered with respect to its underlayer, *i.e.* the reactions used to form each layer go essentially to completion.

To confirm that complexation was occurring in the HDA multilayers via carboxylate coordination, ^{13}C NMR spectra of a monolayer of ^{13}C-labelled stearic acid, ($CH_3(CH_2)_{16}{}^{13}CO_2H$) adsorbed on primed and zirconated silica gel were taken both in the solid state and by dispersion of the sample in $CDCl_3$. The data show an upfield shift in signal of the carbonyl carbon (C=O) from 179 ppm, observed for pure, uncomplexed stearic acid in $CDCl_3$, to 175 ppm for the adsorbed acid. This shift is consistent with complexation. Gajda-Schrantz *et al.* observed ^{13}C signals at 172.54 ppm to 176.10 ppm for the carbonyl carbon of a (α,ω)-sulfonylcarboxylic acid complexed with di-*n*-butyltin(IV).[41] For multilayers formed from PSA, we do not have analogous NMR data. For PSA layers, the sulfonate linkage was established by the appearance of a band at 1070 cm^{-1} in the IR spectrum of the layers. This feature is consistent with the SO stretching mode seen in multilayers linked by S-S bonds,[42] and the existence of this band demonstrates the existence of the sulfonate functionality within the layered assembly.

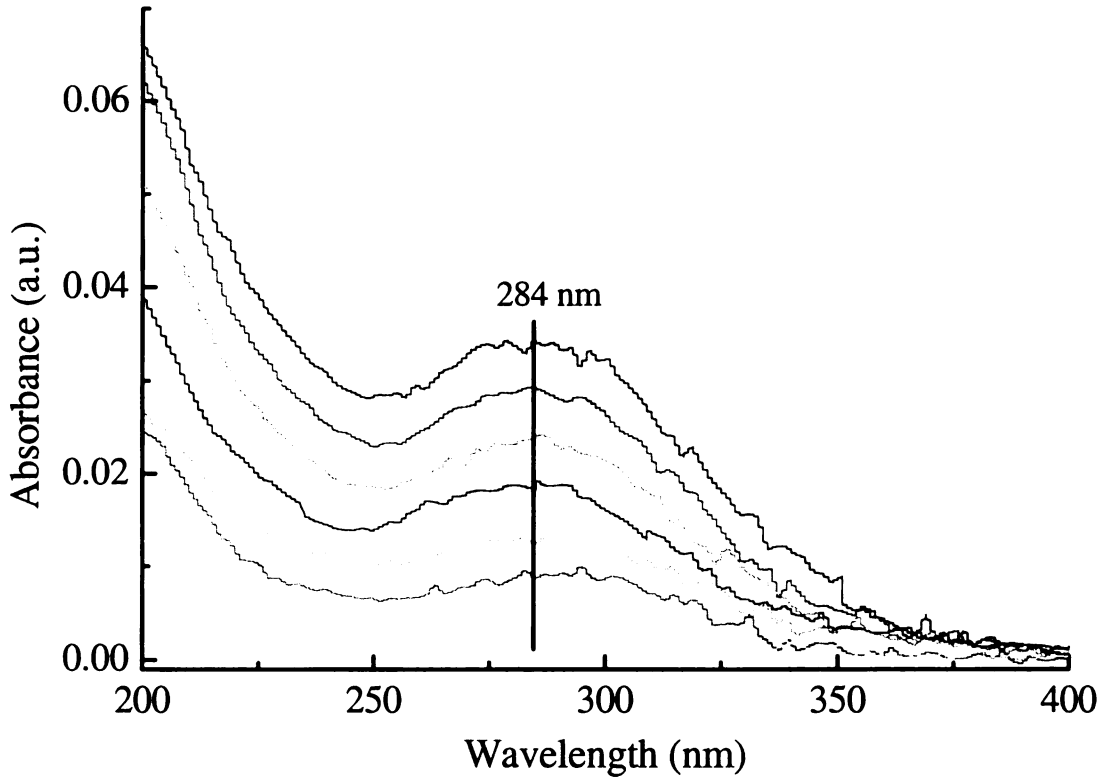

Figure 2.7. Absorption spectra of biphenyl chromophores as a function of number of layers for 1 to 7 layers. These data are linear in number of layers and can be used to estimate the surface density of the layer constituents. See text for a discussion.

So far, we have considered the structural properties of the multilayers in the context of macroscopic layer thickness and aliphatic chain order, as sensed by ellipsometry and FTIR, respectively. It is also important to consider the intrinsic constraints on the metal coordination with these layered materials because of the need to maintain charge neutrality. The crux of the issue is that the RSO_3^- or RCO_2^- moieties are necessarily present at the same concentration as the $ROPO_3^{2-}$ groups because of the use of (α,ω)-bifunctional alkanes in the synthesis of the layers. We observe a linear dependence of multilayer thickness on the number of ligand deposition cycles, and conclude from this finding that the density of ligands is essentially the same in each layer. Therefore the coordination about the metal center must be of the form $\{ROPO_3^{2-} - Zr^{4+} - {}^-O_2CR\}^+$ or $\{ROPO_3^{2-} - Zr^{4+} - {}^-O_3SR\}^+$. The formation of an explicitly neutral structure of the form $\{ROPO_3^{2-} - Zr^{4+} - ({}^-O_2CR)_2\}^0$ or $\{ROPO_3^{2-} - Zr^{4+} - ({}^-O_3SR)_2\}^0$ is not possible based on the ellipsometric (Figure 2.4) and linear optical response data (Figure 2.7) we present here. The XPS data on these multilayers reveal a ~1:1 stoichiometric ratio of Zr/P, and this situation is possible only for 1:1 translayer stoichiometry. To maintain charge neutrality and 1:1 translayer ligand stoichiometry, there must be free anionic species present in the metal coordination layers. Because we used $ZrOCl_2$ for the zirconation reaction(s), the free anion within the layers could be either Cl^- or OH^-. The XPS data on HDA and PSA multilayers are shown in Figure 2.8. These data do not contain any Cl resonances, leaving OH^- as the only possible anion that can be present to enforce charge neutrality.

Having established the synthesis of multilayers using the carboxylate and sulfonate functional groups, we investigated the resistance of these assemblies to solvent exposure. Because there is limited literature on the solubility of Zr salts, it is not clear

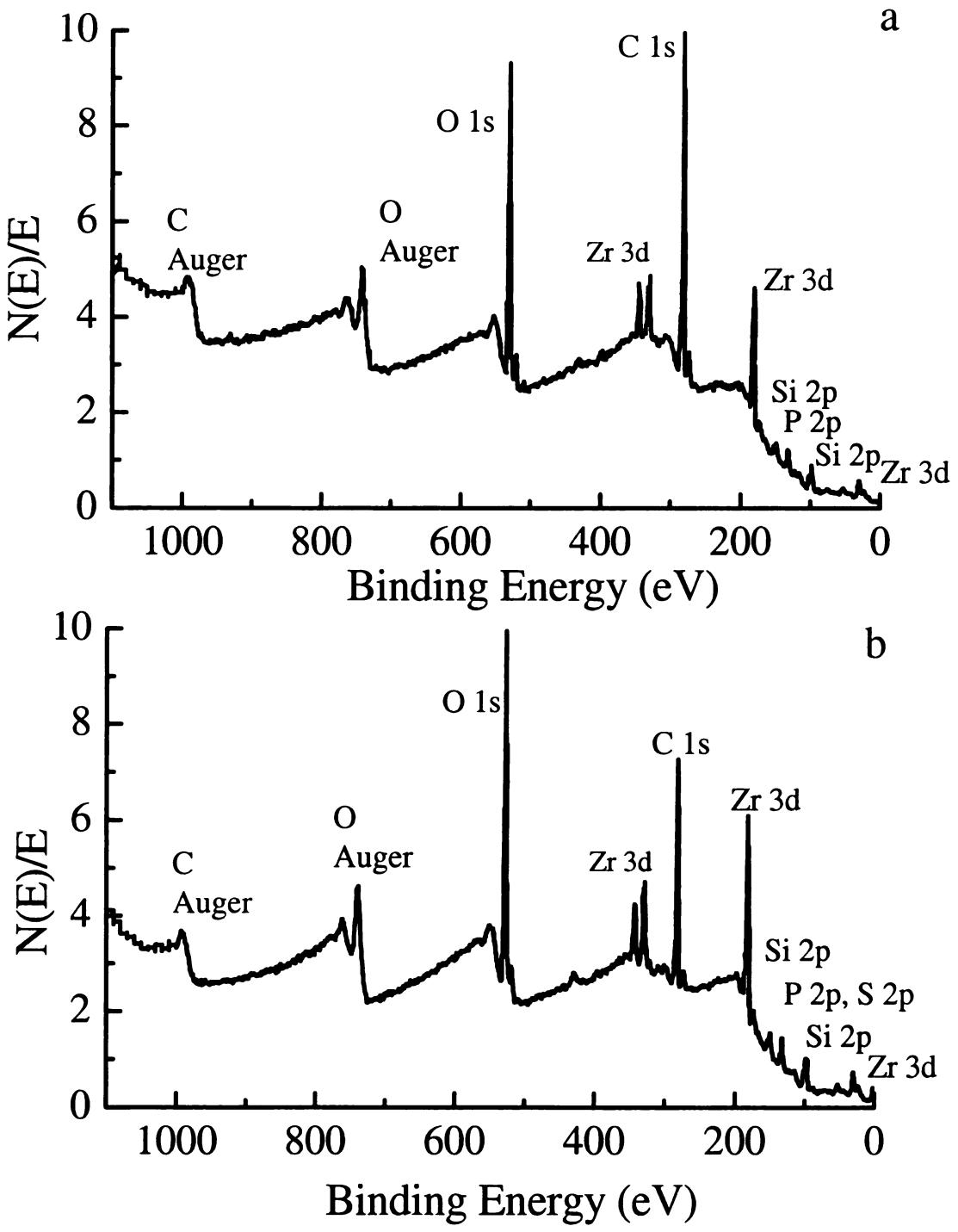

Figure 2.8. XPS spectra of the multilayer assemblies. (a) Spectrum of a five layer sample of HDA. (b) Spectrum of a five layer sample of PSA. In both spectra, band assignments are indicated.

whether the carboxylate or sulfonate compounds will be soluble to a significant extent in certain solvents. We are particularly interested in the integrity of the layers as a function of exposure to ethanol because this solvent is used in the formation of the layers. We measured the thickness of six-layer assemblies of HDA after heating in ethanol at 80 °C for up to 72 minutes and for PSA, after exposure for up to 62 minutes. In all cases, no significant decrease in thickness of the layers was observed, indicating that these new systems are stable to ethanol exposure. In addition to ethanol, we have examined the stability of these layers upon exposure to hexane, methylene chloride, tetrahydrofuran and 0.5 M KCl at temperatures between 66° C and 80° C for variable periods of time. These data are summarized in Tables 2.1 and 2.2. Again, no change in ellipsometric thickness was noted for either multilayer assembly. We also examined the solvent-exposed layers using FTIR and found no evidence for significant solvent permeation.

The vast majority of multilayer chemistry based on metal bisphosphonate interlayer linking strategies is done using Zr^{4+}. While there are several divalent metals that work well for this purpose in alcohol solvents,[13] the rule of thumb for choosing a metal ion is to combine high charge with small ionic radius. As a demonstration that Zr^{4+} is not the only metal ion that can be used for this application, we have also constructed oriented multilayer assemblies of HDA and PSA using Hf^{+4}. We find the same regular build-up of layers with ellipsometric thickness of 14.4 ± 0.7 Å and 6.4 ± 0.4 Å, respectively, for up to six layers (Figure 2.9). These thicknesses are the same as those we observe for the layers grown with Zr^{4+}. Solvent exposure studies show no significant decrease in thickness when Hf-HDA and Hf-PSA were heated to 80° C in ethanol for 30 minutes. Upon exposure to hexane, methylene chloride, tetrahydrofuran, and 0.5 M KCl

Solvent/solution	Number of Zr-HDA layers	Exposure conditions	Ellipsometric thickness (Å)
C_2H_5OH	6	80°C, 17 min.	90 ± 5
C_2H_5OH	6	80°C, 28 min.	86 ± 4
C_2H_5OH	6	80°C, 40 min.	87 ± 3
C_2H_5OH	6	80°C, 57 min.	84 ± 4
C_2H_5OH	6	80°C, 72 min.	82 ± 4
C_2H_5OH	8	25°C, 12 hrs.	110 ± 4
n-C_6H_{14}	8	25°C, 2 hrs.	114 ± 3
CH_2Cl_2	8	25°C, 2 hrs.	109 ± 4
C_4H_8O	8	25°C, 12 hrs.	109 ± 5
0.5 M KCl(*aq*)	8	25°C, 12 hrs.	113 ± 3

Table 2.1. Ellipsometric thickness of HDA assemblies (using Zr) as a function of exposure to selected solvents and solutions.

Solvent/solution	Number of Zr-PSA layers	Exposure conditions	Ellipsometric thickness (Å)
C_2H_5OH	7	25°C, 40 min.	40 ± 2
C_2H_5OH	7	80°C, 40 min.	39 ± 2
n-C_6H_{14}	7	69°C, 20 min.	38 ± 2
CH_2Cl_2	7	40°C, 40 min.	37 ± 2
C_4H_8O	7	66°C, 50 min.	39 ± 1
C_2H_5OH	14	80°C, 0 min.	79 ± 4
C_2H_5OH	14	80°C, 10 min.	75 ± 6
C_2H_5OH	14	80°C, 20 min.	77 ± 6
C_2H_5OH	14	80°C, 62 min.	88 ± 5
C_2H_5OH	18	25°C, 12 hrs.	98 ± 4
n-C_6H_{14}	18	25°C, 2 hrs.	101 ± 5
CH_2Cl_2	18	25°C, 2 hrs.	104 ± 8
C_4H_8O	18	25°C, 12 hrs.	101 ± 4
0.5 M KCl(*aq*)	18	25°C, 12 hrs.	104 ± 3

Table 2.2. Ellipsometric thickness of PSA assemblies (using Zr) as a function of exposure to selected solvents and solutions.

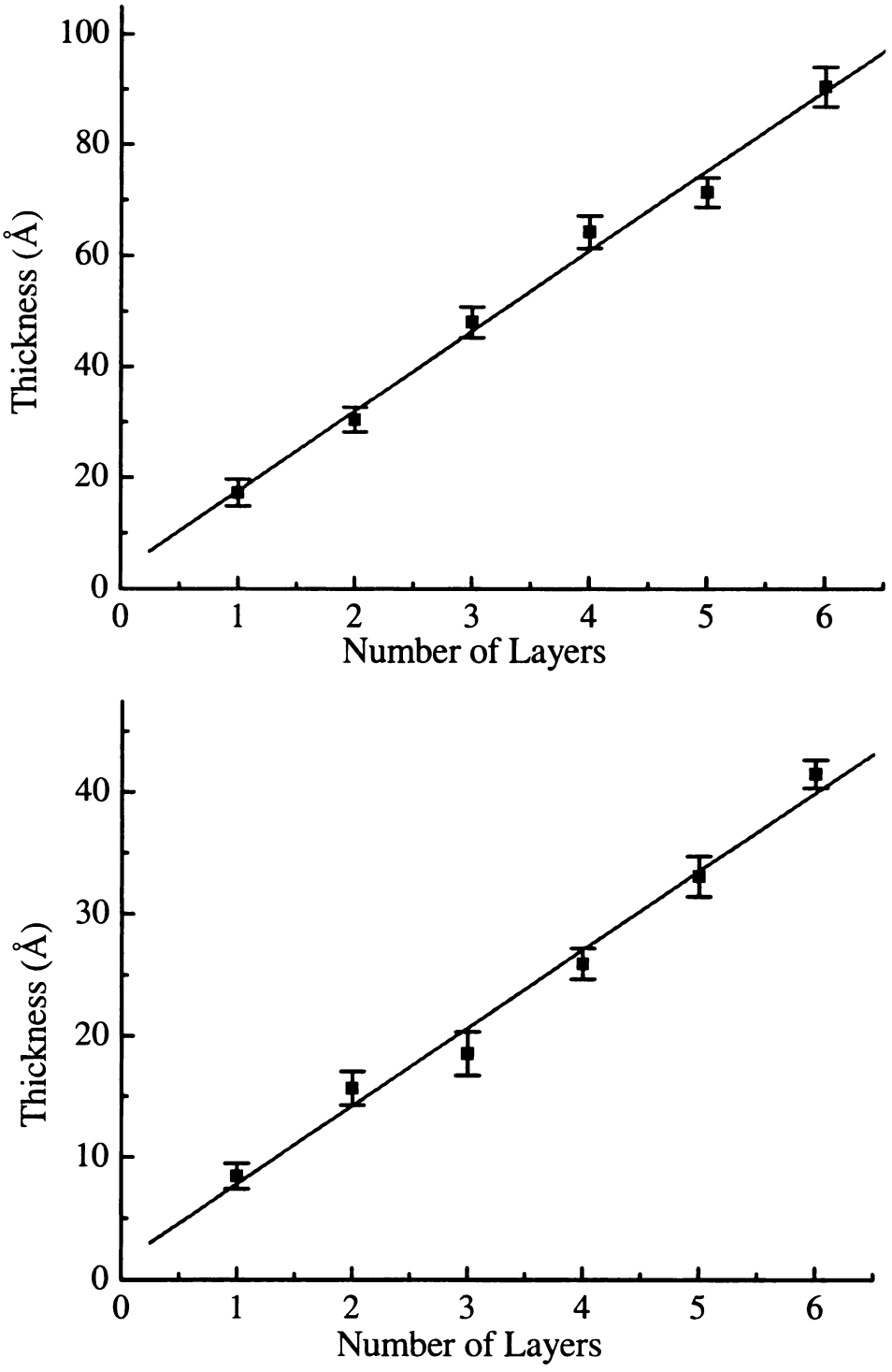

Figure 2.9. Ellipsometric thickness of the interfaces as a function of number of layers added. (a) Layers formed using HDA and Hf^{4+}. The slope of the best-fit line is 14.4± 0.7 Å/layer. (b) Layers formed using PSA and Hf^{4+}. The slope of the best-fit line is 6.4 ± 0.4 Å/layer.

at 25° C for 12 to 24 hours, we find these systems to be still very stable. These data are summarized in Tables 2.3 and 2.4. HDA and PSA multilayers formed using Hf^{4+} are essentially identical to those synthesized using Zr^{4+} and this result is fully consistent with the work reported by the Page group using Hf^{4+} in the construction of bisphosphonate layered materials.[43] The value of being able to select different metal ions lies primarily in the ability to modify the polarizability of the asymmetric coordinated metal sheets within these layers.

Solvent/solution	Number of Hf-HDA layers	Exposure conditions	Ellipsometric thickness (Å)
C_2H_5OH	6	25°C, 2 min. rinse	91 ± 4
C_2H_5OH	6	25°C, 48 hrs.	90 ± 3
C_2H_5OH	6	80°C, 30 min.	89 ± 5
n-C_6H_{14}	6	25°C, 12 hrs.	93 ± 4
CH_2Cl_2	6	25°C, 12 hrs.	88 ± 5
C_4H_8O	6	25°C, 24 hrs.	89 ± 4
0.5 M KCl(*aq*)	6	25°C, 24 hrs.	90 ± 5

Table 2.3. Ellipsometric Thickness of HDA Assemblies (using Hf) as a Function of Exposure to Selected solvents and Solutions.

Solvent/solution	Number of Hf-PSA layers	Exposure conditions	Ellipsometric thickness (Å)
C_2H_5OH	6	25°C, 2 min. rinse	42 ± 1
C_2H_5OH	6	25°C, 48 hrs.	43 ± 1
C_2H_5OH	6	80°C, 30 min.	42 ± 2
n-C_6H_{14}	6	25°C, 12 hrs.	43 ± 1
CH_2Cl_2	6	25°C, 12 hrs.	42 ± 2
C_4H_8O	6	25°C, 24 hrs.	43 ± 1
0.5 M KCl(*aq*)	6	25°C, 24 hrs.	42 ± 1

Table 2.4. Ellipsometric Thickness of PSA Assemblies (using Hf) as a Function of Exposure to Selected solvents and Solutions.

2.4 Conclusions

We have synthesized multilayers that exhibit asymmetric coordination chemistry, imparting directionality to the resulting assembly. We use carboxylate and sulfonate functionalities for this purpose, and the resulting assembly possesses many of the same physical properties of Zr-bisphosphonate films. Orientation of the coordination chemistry was controlled layer-by-layer using a three step synthetic approach that required activation of the top-most layer before subsequent layers could be formed. Using optical null ellipsometry and FTIR, we showed that organic layer constituents did not exhibit the quasi-crystalline order seen for alkanethiol/gold monolayers. This result is the same as that seen for ZP multilayers. Calculation of the average tilt angle (38° for HDA and 53° for PSA) reveals more extensive disorder for the shorter chain sulfonic acid system. We attribute the more extensive disorder in this system as being the result of the aliphatic chains being too short to permit significant van der Waals attractive interactions. Work is currently in progress to use these oriented multilayers to determine their $\chi^{(2)}$ nonlinear optical response.

2. 5 Literature Cited

1. Sun, L., Kepley, L. J., Crooks, R. M. *Langmuir*, **1992**, *8*, 2101.
2. Yang, H. C., Dermody, D. L., Xu, C., Ricco, A. J., Crooks, R. M. *Langmuir*, **1996**, *12*,726.
3. Wells, M., Dermody, D. L., Yang, H. C., Kim, T., Ricco, A. J., Crooks, R. M. *Langmuir*, **1996**, *12*,1989.
4. Kaschak, D. M., Mallouk, T. E. *J. Am. Chem. Soc.*, **1996**, *118*, 4222.
5. Batchelder, D. N., Evans, S. D., Freeman, T. L., Haussling, L., Ringsdorf, H., Wolf, H. *J. Am. Chem. Soc.* **1994**, *116*, 1050.
6. Tarlov, M. J., Burgess, D. R. F., Gillen, G. *J. Am. Chem. Soc.*, **1993**, *115*, 5305.
7. Katz, H. E., Wilson, W. L., Scheller, G. R. *J. Am. Chem. Soc.*, **1994**, *116*, 6636.
8. Putvinski, T. M., Schilling, M. L., Katz, H. E., Chidsey, C. E. D.,Mujsce, A. M., Emerson, A. B. *Langmuir*, **1990**, *6*, 1567.
9. Katz, H. E., Scheller, G. J., Putvinski, T. M., Schilling, M. L., Wilson, W. L., Chidsey, C. E. D. *Science*, **1991**, *254*, 1485.
10. Lee, H., Kepley, L. J., Hong, H. G., Akhter, S., Mallouk, T. E. J. *Phys. Chem.*, **1988**, *92*, 2597.
11. Lee, H., Kepley, L. J., Hong, H. G., Mallouk, T. E. *J. Am. Chem. Soc.*, **1988**, *110*, 618.
12. Thompson, M. E. *Chem. Mater.*, **1994**, *3*, 521.
13. Yang, H. C.; Katsunori, A.; Hong, H. G.; Sackett, D. D.; Arendt, M. F.; Yau, S. L.; Bell, C. M.; Mallouk, T. E.; *J. Am. Chem. Soc.*, **1993**, *115*, 11855.

14. Touwslager, F. J., Sondag, A. H. M. *Langmuir*, **1994**, *10*, 1028.

15. Allara, D. L., Nuzzo, R. G. *Langmuir*, **1985**, *1*, 52.

16. Sondag, A. H. M., Raas, M. C., *Applied Spectroscopy*, **1989**, *43*, 107.

17. Sondag, A. H. M., Raas, M. C. *J. Chem. Phys.*, **1989**, *91*, 4926.

18. Bandyopadhyay, K., Patil, V., Vijayamohanan, K., Sastry, M. *Langmuir*, **1997**, *13*, 5244.

19. Chen, S. H.; Frank, C. W.; *Langmuir*, **1989**, *5*, 978.

20. Allara, D. L., Swalen J. D. *J. Phys. Chem.* **1982**, *86*, 2700.

21. Cohen, S. R., Naaman, R., Sagiv, J. *J. Phys. Chem.*, **1986**, *90*, 3054.

22. Chau, L. K.; Porter, M. D.; *Chem. Phys. Lett.*, **1990**, *167*, 198.

23. Smith, E. L.; Porter, M. D.; *J. Phys. Chem.*, **1993**, *97*, 8032.

24. Lu, G., Purvis, K. L., Schwartz, J., Bernasek, S. *Langmuir*, **1997**, *13*, 5791.

25. Aronoff, Y. G., Chen, B., Lu, G., Seto, C., Schwartz, J., Bernasek, S. L. *J. Am. Chem. Soc.* **1997**, *119*, 259.

26. VanderKam, S. K, Bocarsly, A. B., Schwartz, J. *Chem. Mater.* **1998**, *10*, 685.

27. Horne, J. C., Blanchard, G. J. *J. Am. Chem. Soc.*, **1996**, *118*, 12788.

28. Buscher, C. T., McBranch, D., Li, D. *J. Am. Chem. Soc.* **1996**, *118*, 2950.

29. Katz, H. E., Schilling, M. L., Ungashe, S., Putvinski, T. M., Chidsey, C. E. D., in Supramolecular Chemistry, T. Bien, Ed., *American Chemical Society Symposium Series 499*, Washington DC, **1992**, p. 24

30. Lukeš, I., Borbaruah, M., Quin, L. D. *J Am. Chem. Soc.*, **1994**, *116*, 1737.

31. Ulman, A. An Introduction to *Ultrathin Organic Films from Langmuir- Blodgett to Self-Assembly*; Academic Press: Boston, MA, **1991**

32. Dubois, L. H.; Nuzzo, R. G.; *Annu. Rev. Phys. Chem.*, **1992**, *43*, 437.

33. Zamborini, F. P., Crooks, R. M. *Langmuir*, **1998**, *14*, 3279.

34. Porter, M. D., Bright, T. B., Allara, D. L., Chidsey, C. E. D. *J. Am. Chem. Soc.*, **1987**, *109*, 3559.

35. Maoz, R., Sagiv, J. *J. Colloid Interface Sci.* **1984**, *100*, 465.

36. Miller, W. J., Abbott, N. L. *Langmuir*, **1997**, *13*, 7106.

37. Allara, D. L., Nuzzo, R. G. *Langmuir*, **1985**, *1*, 45.

38. DuBois, L. H., Zegarski, B. R., Nuzzo, R. G. *Langmuir*, **1986**, *2*, 412.

39. Berlman, I. B.; Handbook of Fluorescence Spectra of Aromatic Molecules, Second Edition, Academic Press, New York, 1971.

40. Kohli, P.; Blanchard, G. J.; *Langmuir*, **1999**, *15*, 1418.

41. Gajda-Schrantz, K.; Nagy, L.; Kuzmann, E.; Vertes, A.; Holecek, J.; Lycka, A., *J. Chem. Soc., Dalton Trans.*, **1997**, 2201.

42. Kohli, P., Taylor, K. K., Harris, J. J., Blanchard, G. J. *J. Am. Chem. Soc.* **1998**, *120*, 11962.

43. Neff, G. A.; Mahon, T. M.; Abshere, T. A.; Page, C. J.; *Mat. Res. Soc. Symp. Proc.*, **1996**, *435*, 661.

Chapter 3

Surface Second Harmonic Generation from Asymmetric Multilayer Assemblies: Gaining Insight into Layer-Dependent Order

Summary

We report on the use of surface second harmonic generation (SHG) measurements to probe microscopic organization in asymmetrically-bound aliphatic multilayer assemblies. The use of layers that are bound asymmetrically using metal ion coordination chemistry allows the orientation of the individual layer constituents to be controlled, and the asymmetric coordination makes the assemblies $\chi^{(2)}$-active. We find that, for the systems we report here, the surface second-order nonlinear response increases in proportion to the square of the number of layers initially, then saturates and decreases with additional adlayers. Optical null ellipsometry and FTIR data point to regular growth in terms of thickness and chromophore density while the surface SHG data point to increasing disorder with the adsorption of additional layers. The FTIR data suggest a subtle decrease in overall order of these chains with increasing number of layers, but this trend is not as pronounced as that seen in the surface SHG data. We interpret these data in the context of an increase in the distribution of nonlinear chromophore orientations with layer growth and not a change in the average orientation angle.

3.1 Introduction

Controlling and altering the chemical and physical properties of interfaces using self-assembly techniques has gained substantial interest in the materials community because of the broad potential utility of this approach to interface property control. The ability to control the structure and composition of organic thin films makes this structural motif attractive for tailoring surface properties such as friction,[1-3] wetting and adhesion,[4-6] electron transfer,[7,8] and corrosion protection.[9] Through rational design, synthesis, and the use of specific adsorbates, layered interfaces have also found application in electronics and microelectronics and applications that depend on these technologies.[10] Such uses include chemical sensors,[11-13] electro-optic devices,[14,15] second order nonlinear optics,[16,17] and pattern definition.[18-20]

Controlling the molecular structure and macroscopic organization of molecular interfaces now lies within the realm of routine chemical preparation.[21-23] In multilayer assemblies, the individual layers can be connected through physisorption,[24,25] ionic association chemistry[26,27] or through the formation of covalent bonds.[28,29] The latter two structural motifs are substantially more robust than physisorbed Langmuir-Blodgett (LB) films. The most widely studied and best-characterized self-assembling systems are the alkanethiols on gold.[21,30-32] Recent work has demonstrated the labile nature of these materials and the relatively modest thermodynamic driving force responsible for their formation.[33,34] The metal-bisphosphonate multilayer assemblies pioneered by the Mallouk, Thompson, and Katz groups have also received a great deal of research attention because of their ease of formation and robustness.[16,26,27,35] The formation of these assemblies relies on inorganic ionic association chemistry where dissociation is

inefficient. This approach produces very robust layers and is a versatile means of constructing moderately well ordered multilayer interfaces. While the metal phosphonates are in wide use, they are not ideal candidate materials for all interfacial applications and, as a result, multiple different interlayer linking strategies have been demonstrated. Among these alternative linking strategies are those developed from silane coupling agents on silicon,[36,37] glass,[38] and quartz,[39,40] and the use of carboxylic and sulfonic acid complexation with various metal ions.[41-43] Novel hybrid multilayer assemblies have also been demonstrated where the layers are linked by either ionic or covalent chemistry within a given multilayer assembly.[28,29,44] There is a wide range of chemistry that can be brought to bear on the regular growth of multilayer assemblies.

One of the most appealing aspects of self-assembling multilayer structures is the combination of exquisite control over the thickness and chemical identity of the layer constituents combined with the experimental simplicity of the layer formation. High quality thin films are needed for most optoelectronic applications of organic materials[45] and ordered interlayer covalent bonding is expected to facilitate electron transfer between layers in molecular electronic devices. Densely packed SAMs function as nearly impermeable dielectrics[46-48] and as patternable monolayer resists.[49,50] For essentially any application of these materials, the extent and nature of organization within the material is critical but, in many cases, the information available on molecular-scale organization is indirect.

The basis for the uncertainty in layer organization lies in the contribution of both kinetic and thermodynamic factors in determining the growth of these materials. Organization within multilayer interfaces depends on the strength of intermolecular

interactions within the layer and with underlayers, with the initial growth being determined by the kinetics of formation of the interlayer chemical linking functionality.[29,31] While the thermodynamic factors are determined by the chemistry used, substantial kinetic control can be exerted over the growth of interfacial materials and it is important to develop means to characterize the organization intrinsic to the resulting interfaces. We report here on our use of surface second harmonic generation to characterize layer-dependent changes in the organization of multilayer assemblies. The basis for our ability to relate order in layered materials to surface SHG signal intensity is built upon the well-established foundation built by a number of groups.[51-54] Recently, Simpson and Rowlen have placed much of this work on unified ground by relating second harmonic signal intensity to the chromophore average orientation angle and distribution width.[55-58] For a layered interface to be $\chi^{(2)}$-active, the microscopic (molecular) as well as the macroscopic structure of the interface must be noncentrosymmetric. We have designed and demonstrated a family of structurally simple multilayer assemblies with predetermined orientation. We achieve this organization by means of asymmetric ionic complexation and report on the characterization of these materials using optical null ellipsometry, FTIR and surface second harmonic generation to elucidate the microscopic, layer-dependent organization within these systems. Our data point to the average tilt angle of the adlayer constituents remaining approximately constant with multilayer growth, but the orientational distribution width of the molecules within the layers increases substantially with layer growth.

3.2 Experimental

Reagents and Materials: 10-Hydroxy-1-decanoic acid (HDA), 3-hydroxy-1-propanesulfonic acid sodium salt (PSA), zirconyl chloride octahydrate, phosphorus oxychloride, 6-mercaptohexanoic acid, 2,4,6-collidine, 11-bromo-1-undecanol, and bromotrimethylsilane were obtained from Aldrich. Other reagents used were bromotrimethylsilane (United Chemical Technologies, Inc), hydrogen peroxide (J. T. Baker), sulfuric acid, hydrochloric acid (Columbus Chemical Industries, Inc), acetyl chloride (Mallickrodt), sodium bicarbonate (Spectrum Quality Products. Inc.), and d-chloroform (99.8 % with 1% TMS). Anhydrous acetonitrile (99+ %), reagent grade acetonitrile, hexanes, anhydrous dichloromethane, toluene, and ethanol were obtained from Aldrich and tetrahydrofuran was obtained from EM Science. All reagents were obtained in the highest purity grade available and used as received.

Synthesis of 11-hydroxy-1-undecylphosphonic acid (HUDPA): HUDPA was synthesized using a Michaelis-Arbuzov type reaction on the bromo functionality of 11-bromo-1-undecanol where the hydroxyl group was first protected by reaction with acetyl chloride in dry dichloromethane (*vide infra*).[59] Reagent grade dichloromethane was dried by washing, 4 times, with aqueous 5% $NaHCO_3$, dried over anhydrous $CaCl_2$, and then stirred with CaH_2 for two hours. The resulting product was then vacuum distilled and stored under argon.[60]

Hydroxyl group protection with acetyl chloride in dry dichloromethane **(1).** 11-Bromo-1-undecanol (4.96 g, 19.8 mmol) was stirred in 10 mL of anhydrous CH_2Cl_2 at 0°C under argon for 10 minutes. Acetyl chloride (3.60 g, 45.8 mmol) was added drop wise over 15 minutes and after the solution was stirred for an additional 15 minutes at

0°C, the solution was allowed to warm to room temperature over two hours. The solution was stirred at room temperature until ^{1}H NMR analysis of the reaction mixture showed the disappearance of the peak at δ = 3.62 ppm (HO-$^*CH_2$) and the appearance of the peak at δ ~ 4.02 ppm (CH_3O-$^*CH_2$-). One 25 mL portion of 5 % $NaHCO_3$, then two 25 mL portions of water were used to wash the organic phase, which was then dried over anhydrous Na_2SO_4 and the organic solvent removed by rotary evaporation to give 5.22 g (17.8 mmol) of a colorless liquid (89.9 % yield, pure by NMR). ^{1}H NMR ($CDCl_3$) δ = 4.02 (t, 2H, CH_2O), 3.37 (t, 2H, CH_2Br), 2.01 (s, 3H, CH_3), 1.74 –1.86 (q, 2H, $^*CH_2CH_2O$), 1.52 – 1.64 (q, 2H, $^*CH_2CH_2Br$), 1.18 – 1.44 (m, 14H).

***11-Hydroxy-1-undecylphosphonic acid* (2):** 5.033 g (17.7 mmol) of **1** was refluxed in excess triethylphosphite under argon at 150°C for 5 hours and the excess triethylphosphite removed by vacuum distillation to give a light yellow, oily product. The disappearance of the ^{1}H NMR resonance at δ = 3.37 ppm ($^*CH_2Br$) indicated the completion of the reaction. 6 M aqueous HCl (20 mL) was added to the product and the solution was refluxed for 12 hours, producing a white precipitate of **2** (3.011 g, 11.9 mmol, 67 % yield, pure by NMR) that was collected by vacuum filtration. ^{1}H NMR (DMSO-d_6) δ = 7.24 (s, broad, 1H, OH), 4.02 (t, 2H, HO-*CH_2-), 1.16 – 1.52 (m, 20H).

Surface Preparation: Multilayers used for second harmonic generation (SHG), FTIR, and ellipsometry measurements were grown on quartz, gold, and silicon substrates respectively. The surfaces of 15 x 15 x 1 mm precut Si(100) wafers (Multi Crystal Optics, Inc.) and quartz substrates were prepared using a slight modification of a procedure reported previously for ZP layers.[41] Si substrates were cleaned in piranha solution (3:1 H_2SO_4:H_2O_2. *Caution-strong oxidizer!*) for 15 minutes, rinsed with distilled

water, and dried under a stream of N_2. The surface silanol groups of the cleaned Si substrates were phosphorylated directly by reaction with 20 mM $POCl_3$ in the presence of 20 mM 2,4,6-collidine in 10 mL anhydrous acetonitrile under an argon atmosphere at room temperature. After 15 minutes the substrates were removed, rinsed with reagent grade acetonitrile and then water, dried with a stream of N_2, and zirconated by immersion for 10 minutes in a 5 mM $ZrOCl_2$ in 60 % aqueous ethanol. The resulting surfaces were rinsed with water and dried with N_2. Gold substrates were cleaned with a UV/ozone cleaner for 15 minutes and immersed in a 5 mM solution of 6-mercaptohexanoic acid in 60 % aqueous ethanol for 30 minutes. The resulting carboxylate-terminated surface was zirconated by exposure to 5 mM $ZrOCl_2$ in 60:40 ethanol:water for 10 minutes, followed by rinsing with water and drying with a stream of N_2.

Layer Deposition: HDA, PSA, and HUDPA were deposited on zirconated surfaces from saturated solutions (~0.2 mM) of the appropriate molecules in 60 % aqueous ethanol solutions at ~ 60 °C for 20 minutes with stirring. The resulting interfaces were rinsed twice with ethanol and dried with a stream of N_2. Subsequent layers were deposited in the same manner following phosphorylation and zirconation of the OH-terminated interfaces as described above. In all cases, terminal OH groups were phosphorylated before measurements were made.

Surface characterization: ^{1}H NMR measurements were performed on a Varian Gemini-300 MHz NMR spectrometer. Multilayer thickness was measured using an optical null ellipsometer (Rudolph AutoEL-II) operating λ = 632.8 nm with a 70° angle of incidence. Software supplied by Rudolph (DAFIBM) was used to calculate layer thickness where the refractive index of the oxide layer was taken as to be $\mathbf{n} = 1.462 + 0i$

and $\mathbf{n} = 1.540 + 0i$ was used for the ZP layers. Each data point reported here is an average of 5 to 9 measurements from different locations on each substrate. FTIR spectra of multilayers on gold were obtained using a Nicolet Magna 750 FTIR spectrometer equipped with an external reflectance accessory, operating at an IR beam incidence angle of ~80° with respect to the surface normal.[61] Spectra were averaged over at least 256 scans at 4 cm^{-1} resolution against a background of bare gold.

Surface second harmonic generation laser system: The laser system used for this work has been described in detail[62] and we recap its salient features here. The source laser is a Q-switched, mode-locked Nd:YAG laser (Quantronix model 416) operating at 1064 nm. The mode-locked laser pulses are ~100 ps in duration with a 12 ns spacing. The Q-switched envelope duration is ~2 μs and the repetition rate of the Q-switch is set to 500 Hz. The polarization condition of the incident fundamental light incident on the sample was set to TM using a half-wave plate and any second harmonic light generated by the optics prior to the sample was filtered using a RG-630 color filter. The second harmonic light generated in transmission mode from the sample (~100 μm beam spot diameter) was passed through three dichroic filters and a monochromator to remove residual fundamental light and the second harmonic signal was detected with a PMT (Hamamatsu type 466).

3.3 Results and Discussion

A number of techniques have been developed for characterizing mono- and multilayer molecular assemblies. Because of the very small quantity of material present in a monolayer (~$5x10^{14}$ mlc cm^{-2} for alkanethiols on Au),[63] it is difficult to elucidate detailed structural information about such assemblies. For multilayer systems, layer growth is often taken to be "regular" when the increase in ellipsometric layer thickness and (IR or UV-visible) absorbance with number of layers are both linear. In contrast to this simplistic test for "regular" layer growth, chromophore-containing multilayers have been shown to exhibit changes in average orientation angle as a function of surface coverage.[64-66] These outwardly contrasting pieces of information suggest that the growth of multilayers is a more complex process than simple intuition would indicate. For chromophore-containing systems, the chromophores themselves may perturb the organization intrinsic to the layered materials, and this is an issue that remains to be resolved fully.

One technique that is emerging as an effective tool in the investigation of orientational order in layered interfacial structures is surface second harmonic generation (SSHG).[51,66-69] The form and polarization-dependence of the surface SHG signal can be related to the average orientation of adlayer molecules at an interface, provided they are deposited in an orientationally-specific manner.[53]

We are interested in understanding the organization intrinsic to layered multilayer assemblies and how that organization depends on the deposition of sequential layers. Surface SHG measurements provide a useful means to study this matter and the data from these measurements, when combined with results from linear techniques (FTIR,

ellipsometry) provide information on the changing orientational properties of the interfaces with layer growth.

The key to the success of this work lies in the materials we use. We are interested in the organization of ionically-bound multilayer structures. Surface second harmonic generation spectroscopy is a technique that relies on the intrinsic symmetry properties of the interface. For the most widely studied ionically-bound interfaces, the metal bisphosphonates, the interlayer linking moiety possesses a center of inversion, making these materials $\chi^{(2)}$-inactive to within the dipole approximation. One way to circumvent this limitation is to incorporate nonlinear chromophores in the layer structure, between the interlayer linking functionalities.[15,16,62] This approach is useful for a variety of applications of these interfaces, but it is limited in its ability to elucidate the fundamental growth and organization issues that remain largely unresolved in alkanebisphosphonate systems. To overcome this problem, we have devised and demonstrated a family of oriented multilayer structures using structurally simple (α,ω)-bifunctional alkanes where the nonlinear chromophore is the asymmetrically coordinated metal ion center between layers.[41] We show a schematic for the oriented growth of these assemblies in Figure 3.1. The use of bifunctional alkanes allows the interrogation of systems with structures that likely mimic that of the metal bisphosphonates. We use three different measurements to provide insight into the organization of these layered materials. We consider the ellipsometric information first, then the FTIR data on these layers. The use of these two bodies of data together provides limited but useful information on the average tilt angle of the layer constituents, and we use this information in the interpretation of the surface SHG data.

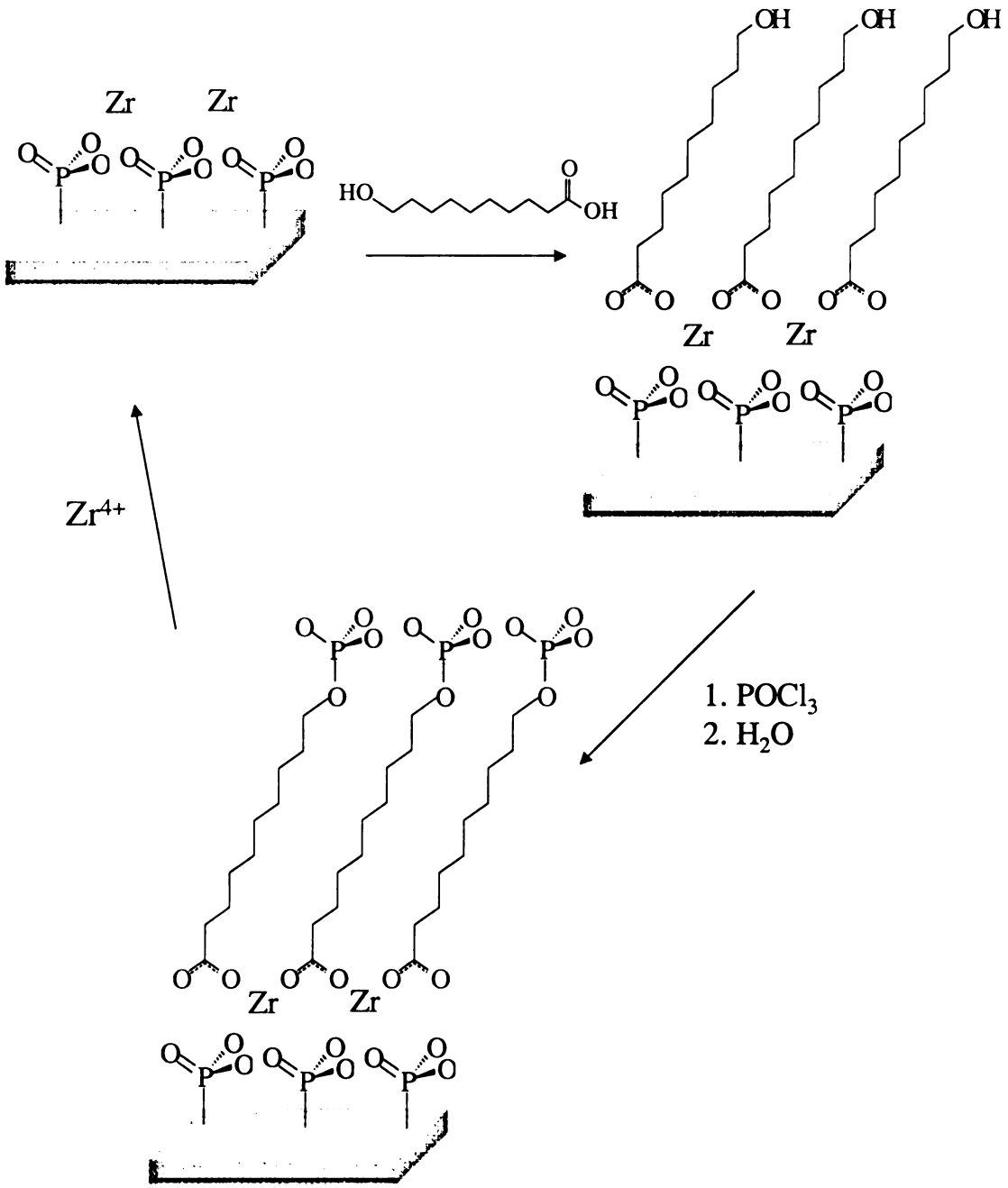

Figure 3.1. Diagram of oriented layer synthesis using asymmetric metal ion complexation. The adlayer constituent shown is 10-hydroxy-1-decanoic acid. Details of the synthetic procedure is provided in the text.

We have used three different asymmetric layered structures; those based on 10-hydroxy-1-decanoic acid (HDA), 11-hydroxy-1-undecylphosphonic acid (HUDPA), and 3-hydroxy-1-propanesulfonic acid (PSA), (Figure 3.2). Using these materials and the oriented synthetic approach described in the Experimental section, we constructed multilayer structures of HDA, HUDPA and PSA. These multilayer interfaces were constructed on oxidized silicon and fused silica substrates, depending on the measurement to be performed. The ellipsometric data, by themselves, are useful in demonstrating the growth of the layered assemblies and we show these data in Figure 3.3. In all cases, we observe linear growth for these assemblies, with the slope of the ellipsometric data depending on the identity of the adlayer constituent. We recover best-fit slopes of 14 ± 1 Å/layer for HDA, 17 ± 1 Å/layer for HUDPA, and 5.5 ± 1 Å/layer for PSA. These results are in intuitive agreement with the structures of the molecules adsorbed; the all-*trans* length of the adlayer species is predicted by molecular mechanics to be 17.7 Å for HDA, 20.5 Å for HUDPA and 9.5 Å for PSA. The calculated lengths are longer than the observed thickness, indicative of either tilting of the molecules within the layers or incomplete coverage. To separate the average tilt angle from the loading density for these layers, we need to be able to characterize one of these system properties using an alternate means. We could use the FTIR data we present below for this purpose if we knew the extinction coefficients for the various IR bands with reasonable accuracy. Because this information is not generally available for the adlayer molecules we study here, we use the FTIR data for structural characterization and not quantitation. For quantitation, we rely on surface loading density data we obtained previously from absorbance measurements of multilayers grown using biphenyl-containing analogues.[41]

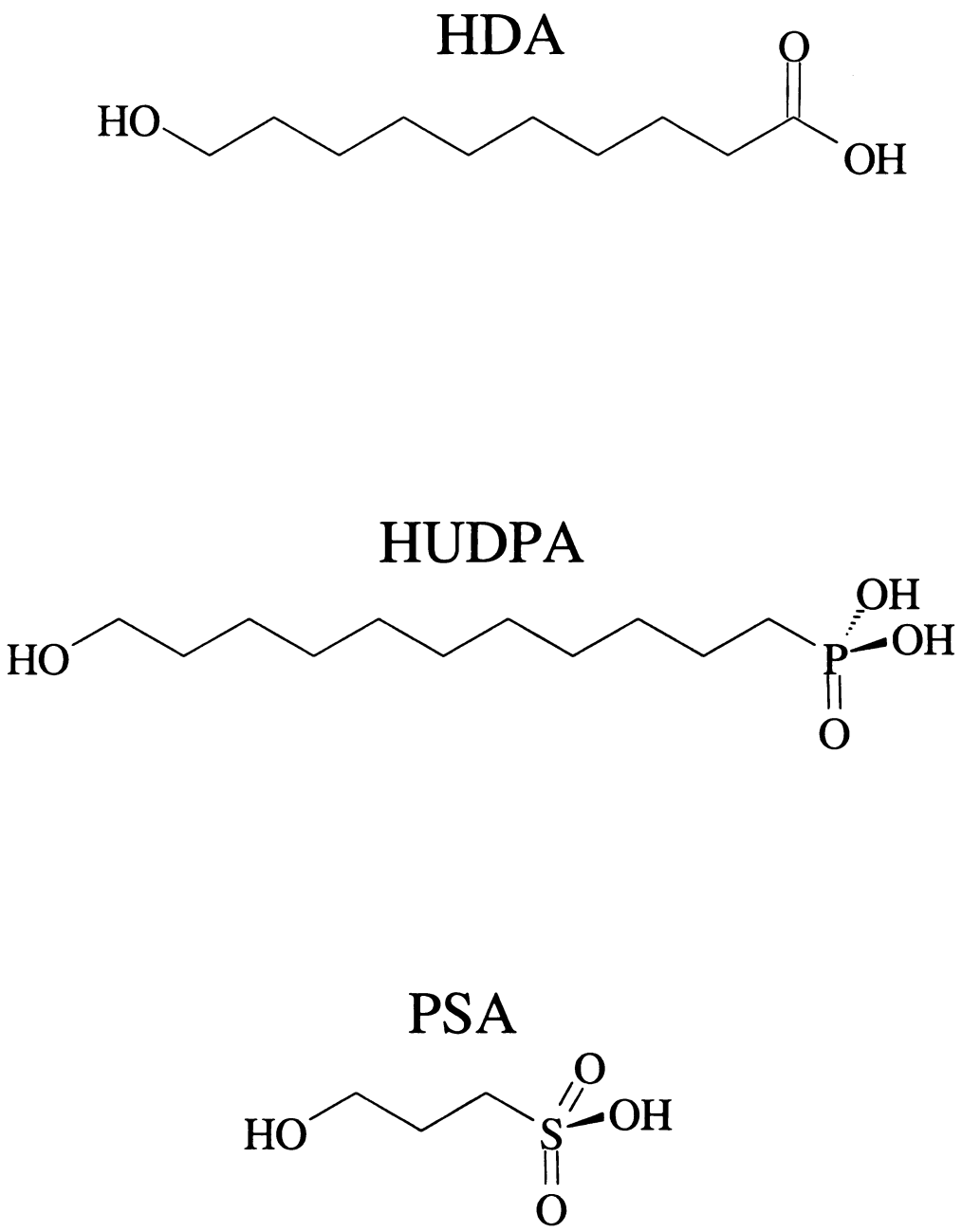

Figure 3.2. Structures of adlayer constituents. HDA = 10-hydroxy-1-decanoic acid, HUDPA = 11-hydroxy-1-undecylphosphonic acid, PSA = 1-hydroxy-3-propane sulfonic acid.

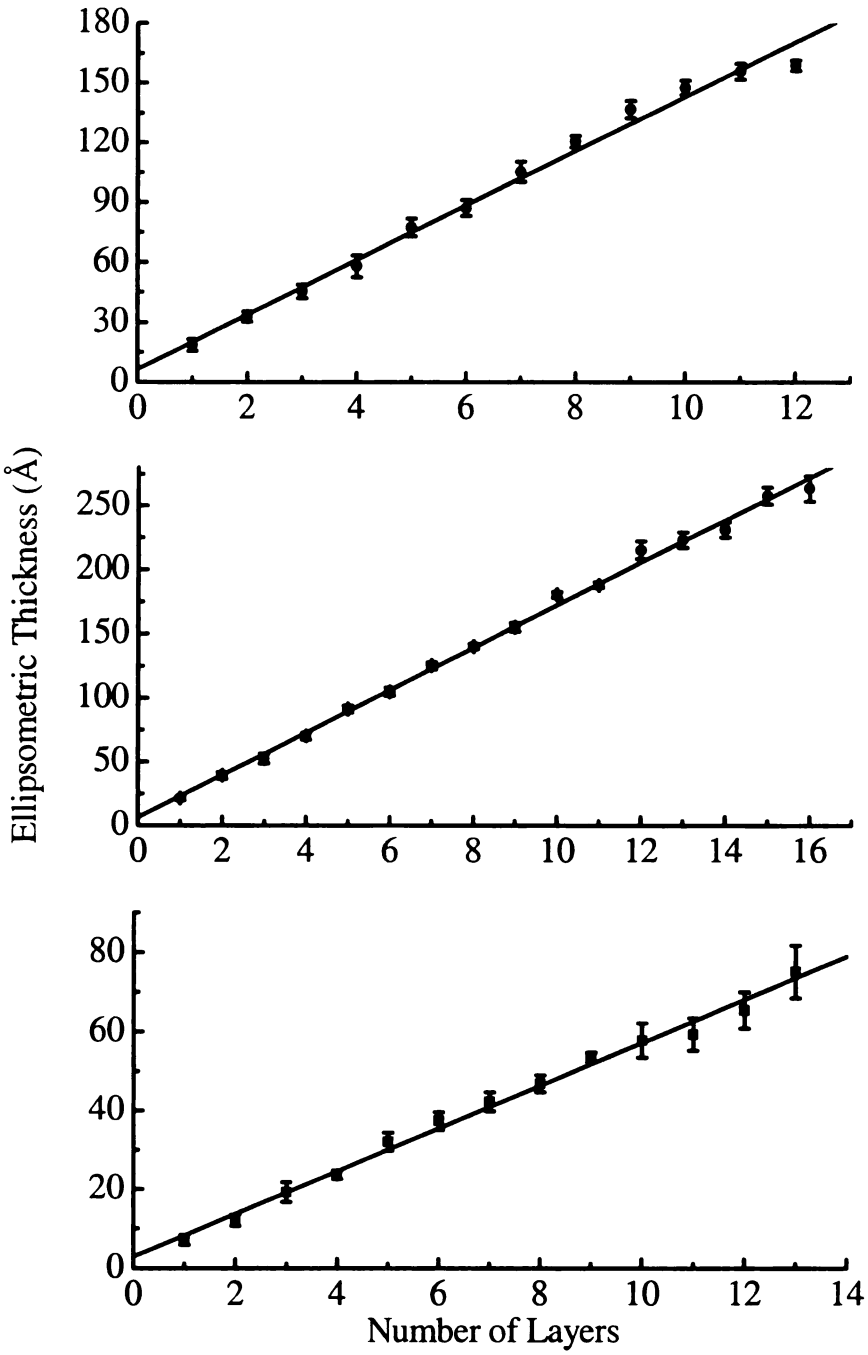

Figure 3.3. Ellipsometric thicknesses of multilayer assemblies. (a) data for HDA, with the best-fit regression of the data yielding a thickness of 14 ± 1 Å/layer. (b) data for HUDPA, with the best-fit regression of the data yielding a thickness of 17 ± 1 Å/layer. (c) data for PSA, with the best-fit regression of the data yielding a thickness of 5.5 ± 1 Å/layer.

Our data for bifunctional alkane adlayers are the same as those we reported in that work and, based on this correspondence, we can calculate the average tilt angle of HDA to be 39 ± 3° with respect to the surface normal, for HUDPA, 32 ± 2° and for PSA, 55 ± 10°. The results for HDA and HUDPA are consistent with other reports on growth of metal bisphosphonates. We interpret the 55° tilt angle recorded for PSA as a measurement of the magic angle for this system, indicating the absence of order within the layer. This is not a surprising result given the shortness of the alkyl chain and thus the absence of strong van der Waals interchain interactions in these adlayers.[22]

For layered interfaces containing aliphatic constituents, FTIR is particularly useful for characterizing the local environment of the methylene functionalities. While the experimental data contain information on both average orientation and local environment, we concentrate on the band positions and not their relative intensities in this work. We present in Figure 3.4a the FTIR spectra of HDA showing the CH_2 stretching mode region. The resonance at ~2926 cm^{-1} is the asymmetric stretch and the 2854 cm^{-1} band is the symmetric CH_2 stretch. Based on extensive studies on a variety of alkane systems, there is a well-established relationship between band energy and local environment. For liquid alkanes, the asymmetric stretch is centered at 2928 cm^{-1} and in crystalline alkanes this band shifts to ~2918 cm^{-1}. For the symmetric stretch, the disordered limit is ~2858 cm^{-1} and the crystalline band position is 2848 cm^{-1}. For both bands, the extent of organization is taken to be related to band position, although there is no scale upon which "organization" is based. We show in Figure 3.4b the dependence of the asymmetric and symmetric band positions on the thickness of the layers. For HDA, there is a small and correlated variation in position with number of layers (within the

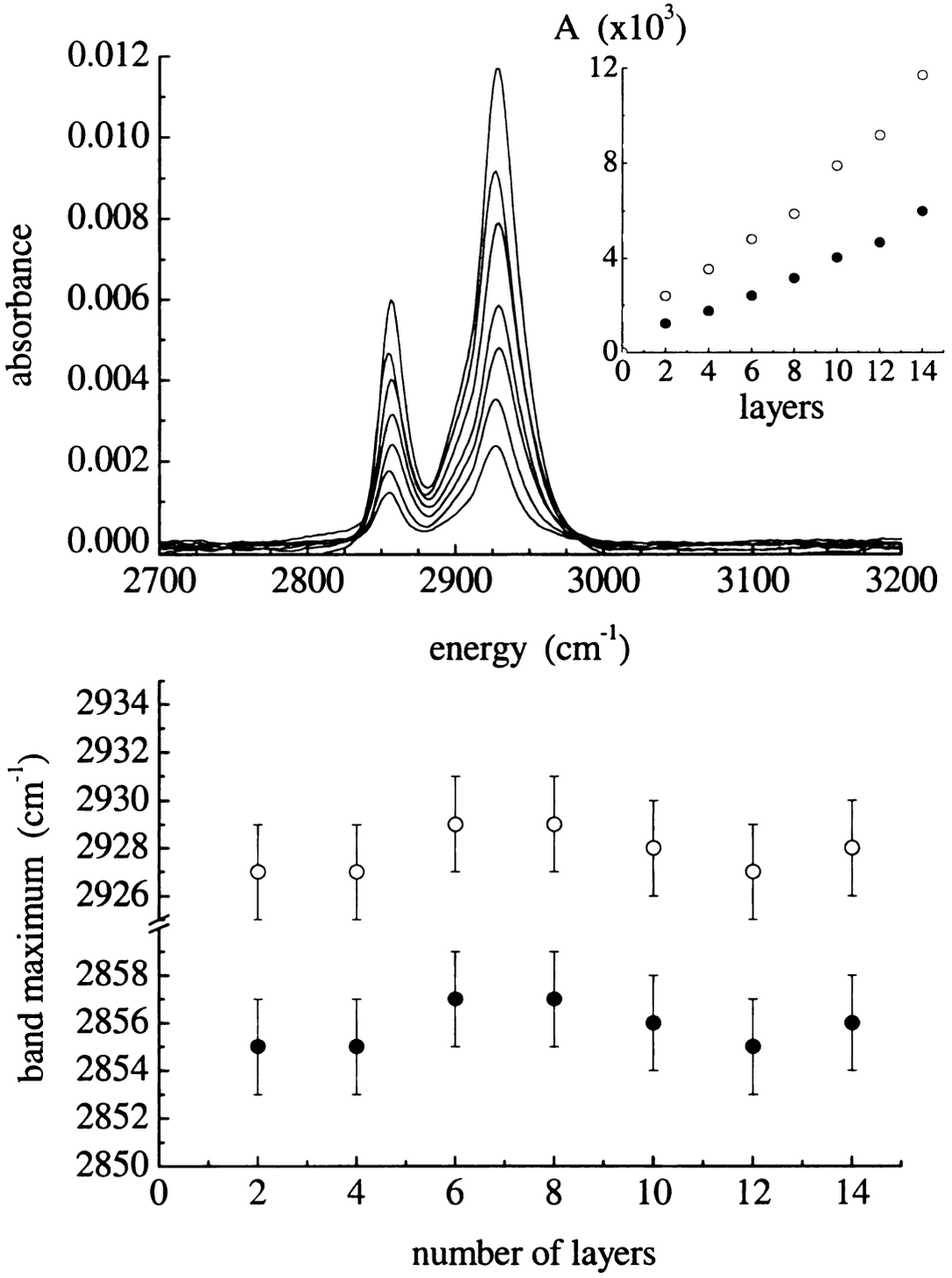

Figure 3.4. FTIR data for HDA multilayers. The top panel contains FTIR spectra of the CH_2 stretching region for multilayers containing 2 – 14 layers. Inset: Beer's law dependence of symmetric (●) and asymmetric (○) stretching resonances. The bottom panel shows the band maxima for the two resonances as a function of number of layers.

experimental resolution), but, significantly, there is no trend to these data. It is important to consider that these data are not the sequential spectra of the individual layers as they are deposited, but rather the average of all the layers present for each measurement. Thus, we would expect any trends, if they exist, to be smoothly varying and subtle. We conclude from the band positions and layer-dependence that the average environment *sensed by the aliphatic chains* does not change significantly with the growth of additional layers.

We present the FTIR spectral data for HUDPA in Figure 3.5a and the layer-dependence of the band positions in Figure 3.5b. We observe no trend in these data outside the uncertainty. The band positions of ~2928 cm^{-1} and 2856 cm^{-1} suggest that the aliphatic chains experience a disordered environment regardless of the number of layers. This finding is significant in light of the surface SHG data we discuss below.

For PSA, the first layers are characterized by band positions at 2928 cm^{-1} and 2857 cm^{-1} and with the addition of more layers, the bands shift to 2934 cm^{-1} and 2864 cm^{-1} (Figure. 3.6). These latter positions lie outside the values typically used in the interpretation of CH_2 stretching bands and this is not a surprising result given the shortness of the alkyl chain for PSA. Because of the proximity of the CH_2 groups to the terminal polar functionalities, a measurable shift of the CH_2 band positions is expected. Despite this offset, we assert that the systematic change in band position with increasing number of layers is related to the organization of the adlayer. Our surface SHG data support this assertion (*vide infra*). The IR data indicate limited organization for our systems even though plots of absorbance vs. number of layers are nominally linear (see insets in Figures 3.4 - 3.6).

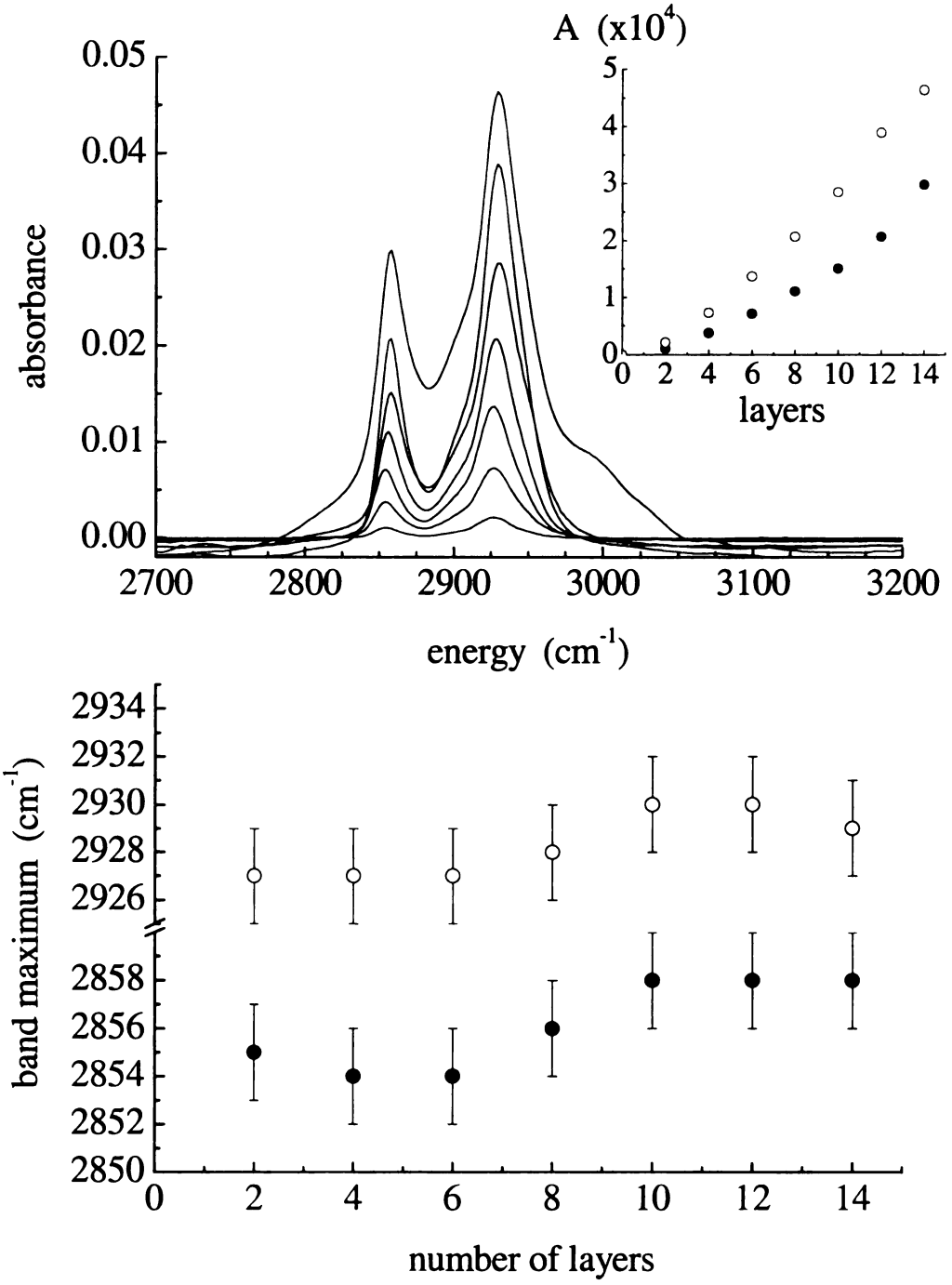

Figure 3.5. FTIR data for HUDPA multilayers. The top panel contains FTIR spectra of the CH_2 stretching region for multilayers containing 2 – 14 layers. Inset: Beer's law dependence of symmetric (•) and asymmetric (○) stretching resonances. The bottom panel shows the band maxima for the two resonances as a function of number of layers.

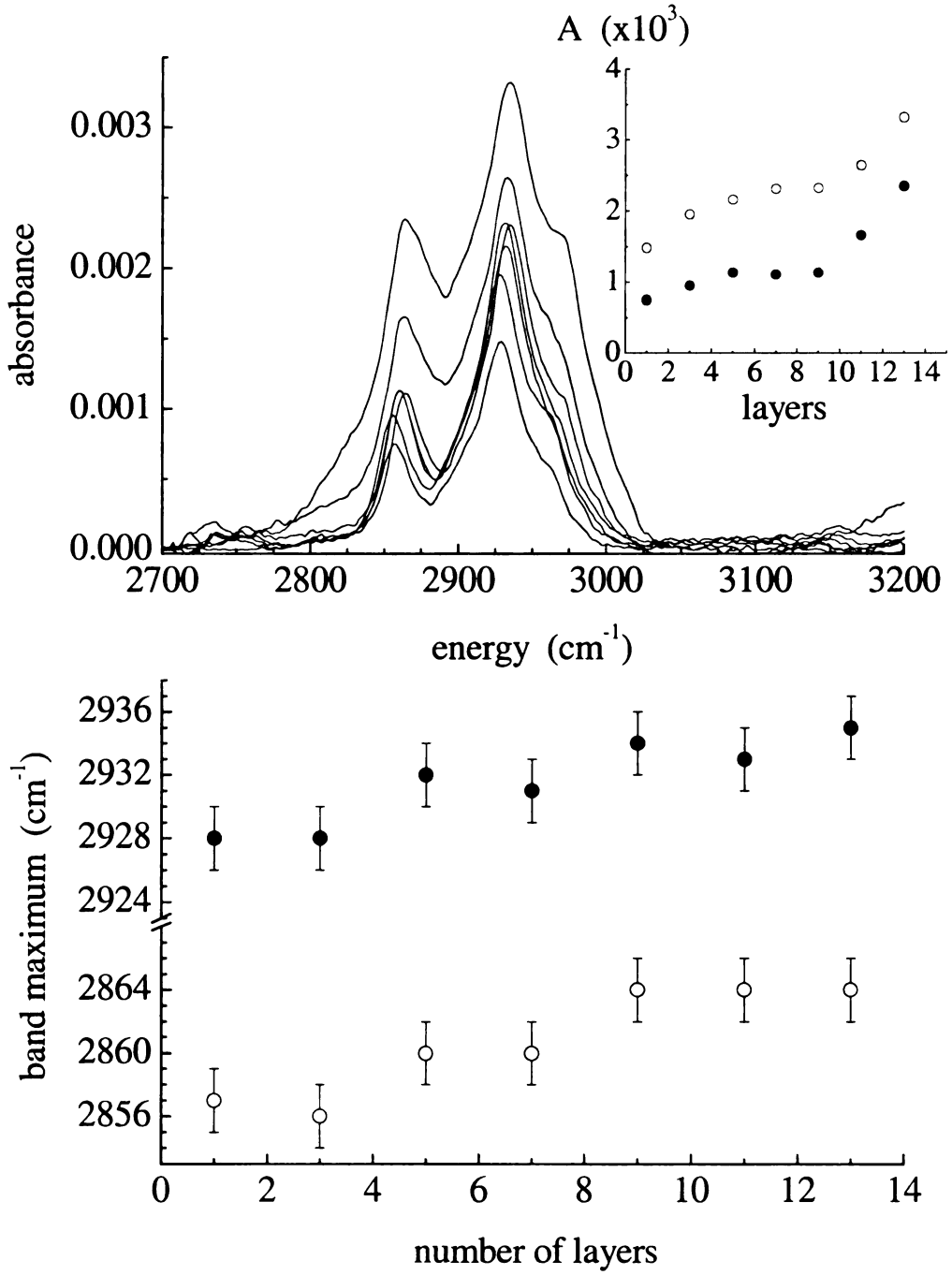

Figure 3.6. FTIR data for PSA multilayers. The top panel contains FTIR spectra of the CH_2 stretching region for multilayers containing 1 – 13 layers. Inset: Beer's law dependence of symmetric (•) and asymmetric (○) stretching resonances. The bottom panel shows the band maxima for the two resonances as a function of number of layers.

With the basic characterization provided by the linear response data, we are in a position to consider the results of our surface SHG studies. It is important to note that surface SHG measurements sense the organization of the asymmetrically coordinated metal ion centers and not that of the aliphatic chains. This is significant because the correspondence between aliphatic chain order and interlayer connection order may not be direct and thus there is no reason to assume, *a priori*, that the FTIR and surface SHG data will provide information that is directly comparable. Before discussing the meaning of the SHG data, we consider the form of our experimental signal because it is important in understanding the information we extract. Because we perform our surface SHG measurements in transmission mode, we sense the second harmonic signal generated at both the front and back faces of the sample.[62] Interference between light generated at these two interfaces leads to a signal that oscillates as a function of the angle of incidence of the fundamental beam and we understand this interference effect quantitatively.[70] Once this interference effect is taken into account, the dependence of the second harmonic signal on the incidence angle of the fundamental light can be related to several experimental parameters. The intensity of the second harmonic light scales as the square of the active $\chi^{(2)}$ tensor element(s) accessed for a given polarization condition and the square of the intensity of the incident fundamental light.

$$I_{2\omega} \propto \left|\chi^{(2)}_{total}\right|^2 I_{\omega}{}^2 \tag{3.1}$$

where

$$\chi^{(2)}_{total} = \chi^{(2)}_{bulk} + \chi^{(2)}_{surf} + \chi^{(2)}_{adlayer} \tag{3.2}$$

In Eq. 3.2, $\chi^{(2)}{}_{bulk}$ refers to the second order response of the bulk substrate and is dominated by contributions from the electric-quadrupole and magnetic dipole terms.

Both of these terms are significantly smaller than the surface ($\chi^{(2)}_{surf}$) and adlayer ($\chi^{(2)}_{adlayer}$) contributions.[71] The surface $\chi^{(2)}$ term can and does contain substantial contributions from both quadrupolar and dipolar terms. The adlayer term depends on the average orientation angle of the nonlinear chromophore relative to the surface normal as well as the orientational distribution of the nonlinear chromophore ensemble. We have discussed these issues in detail in a previous paper[62] and we treat the experimental signal as being separable into two components. These are the interference effect, which is physical in nature and contains information on the thickness of the substrate, and the "envelope function" – the experimental signal without the interference effect. The shape of the envelope function depends sensitively on the mechanism of the nonlinear response as well as the nonlinear chromophore average tilt angle and distribution width.[56]

We use TM-polarized light for these measurements and thus the experimental signal contains contributions from both the quadrupolar and dipolar components of the $\chi^{(2)}$ tensor. We use these two contributions to advantage in determining the magnitude of the adlayer nonlinear response (*vide infra*). The basis for separating the dipolar and quadrupolar contributions to the experimental signal lies in their different dependencies on the incidence angle of the fundamental light. For a dipolar response, which is the dominant term for the adlayer, we expect on geometric grounds to see a negligible signal for the incident electric field propagating normal to the substrate plane. The interaction between the adlayer and the incident electric field increases with the angle between the substrate normal and the fundamental electric field propagation axis. This incidence-angle dependence is the result of the in-plane cancellation of the adlayer dipole moment in systems characterized by small (relative to the laser beam spot size), randomly oriented

domain structure.[62] The quadrupolar response is not affected by the same cancellation effects in the plane of the substrate and thus senses both in-plane and out-of-plane contributions to the $\chi^{(2)}$ response. The quadrupolar response, which for symmetry reasons, lies in the plane of the substrate, is maximum when the incident fundamental electric field is propagating along the substrate normal. For the quartz substrates we use in this work, the quadrupolar response has been determined to be ~ five times larger than the dipolar response.[72] The signal seen for small sample rotation angles is dominated by the quadrupolar response and for higher rotation angles, the dipolar response of the nonlinear chromophore determines the experimental signal. We can use the substrate quadrupolar signal as an internal standard for the calibration of the adlayer $\chi^{(2)}$ response.

We show in Figure 3.7 the experimental angle-dependence of the surface SHG signal for the bare substrate and selected multilayers of HDA. The functional form of the analogous data for HUDPA and PSA are the same. As discussed above, the signal near zero degrees sample rotation angle is dominated by the substrate quadrupolar contribution to the $\chi^{(2)}$ response and the signal at higher incidence angles is produced primarily by the asymmetrically-coordinated adlayers. We show the layer-dependence of the surface SHG intensity of HDA at 60° sample rotation angle in Figure 3.8a. For a multilayer assembly with uniform growth characteristics (*i.e.* each layer is characterized by order identical to the layer beneath it), we would expect to see a linear dependence of the square root of the surface second harmonic signal on the number of layers. We do not observe this trend experimentally. We present these same data for HUDPA in Figure 3.8b and PSA in Figure 3.8c. In all cases, we obtain the same general form of the signal, with subtle, system-dependent changes in the number of layers at which the experimental

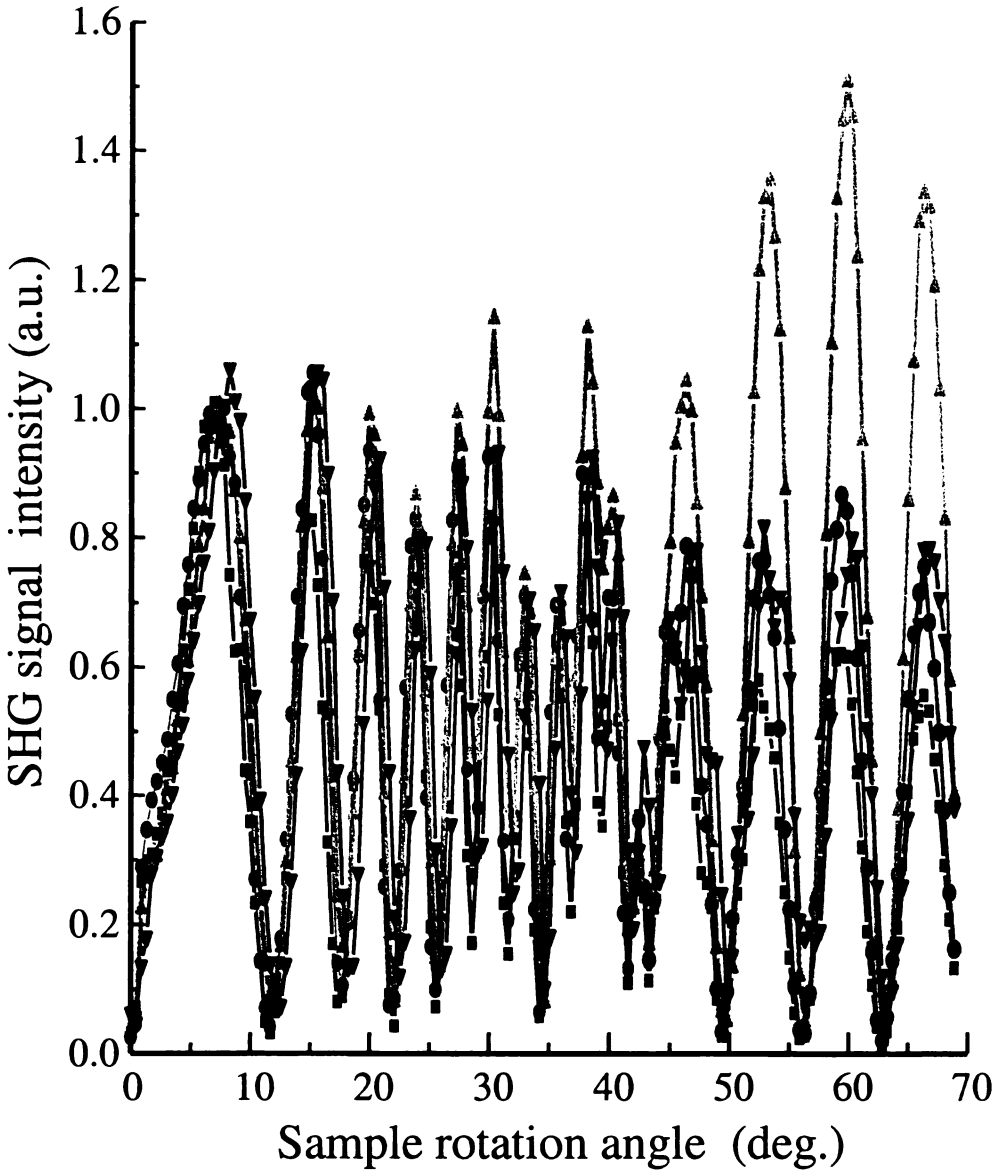

Figure 3.7. Surface second harmonic generation intensity as a function of sample rotation angle for HDA. The data points are for the bare substrate (■), five bilayers (●), ten bilayers (♦) and fifteen bilayers (▲). Data on bilayers is reported because of the use of a transparent (SiO_x) substrate. Deposition of adlayers proceeded uniformly on both sides of the substrate.

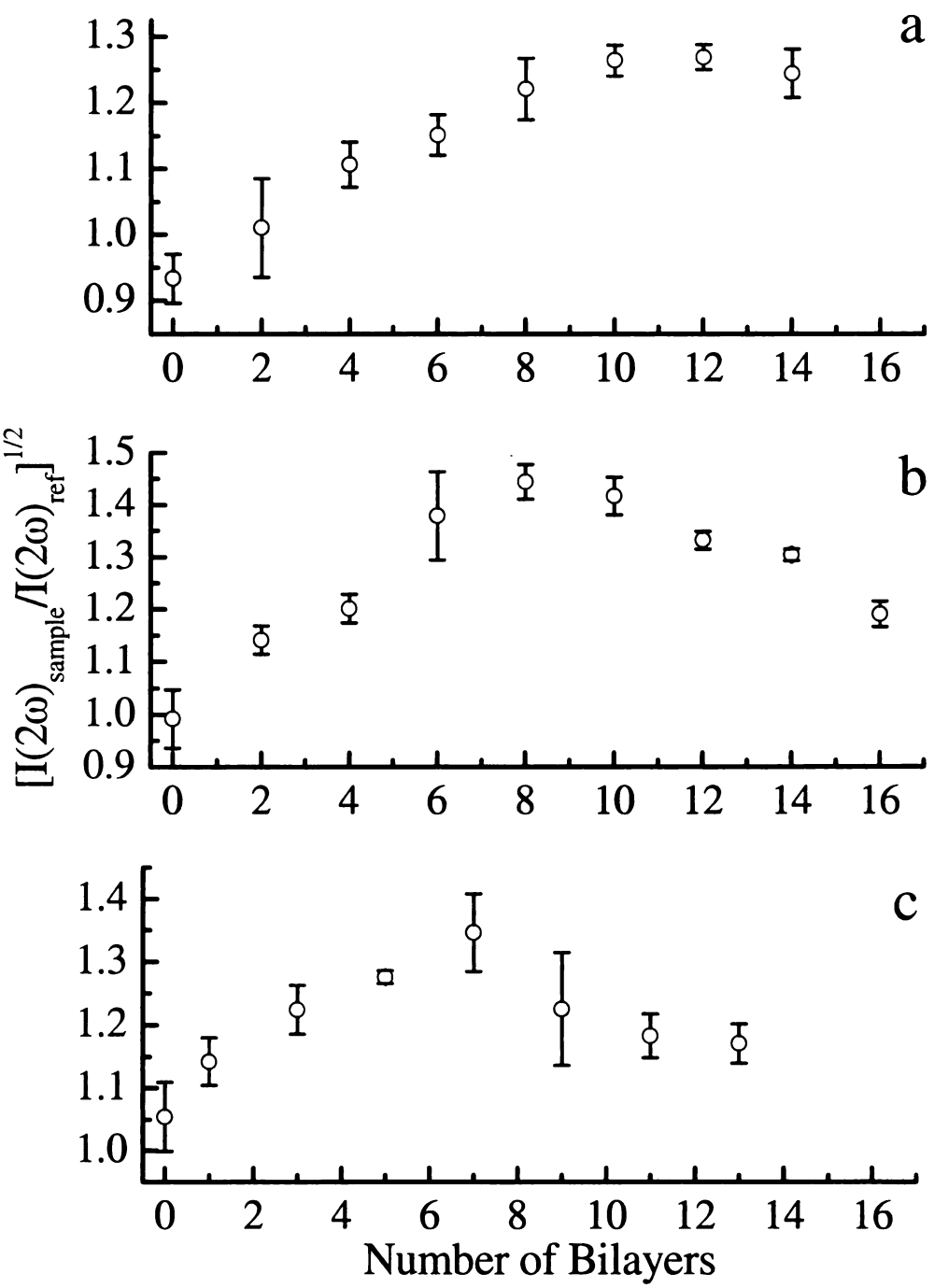

Figure 3.8. (a) Second harmonic signal intensity for HDA at 60° sample rotation angle as a function of adlayer number. (b) Second harmonic signal intensity for HUDPA at a sample rotation angle of 60° as a function of number of adlayers. (c) Second harmonic signal intensity for PSA at 60° sample rotation angle as a function of adlayer number.

signal at 60° rotation angle reaches a maximum. There are several possible explanations for these data.

It is useful to first estimate the nonlinear response for each adlayer. We assume that the response of the samples near 0° sample rotation is dominated by the quadrupolar contribution from the fused silica substrate, and we have estimated the value of χ^{Q} ~ 2.1×10^{-17} esu/cm^2.[62] For HDA, $\chi^{(2)} = \chi^{Q} \cdot [I_{2\omega}(\text{sample, } 60°)/n \cdot I_{2\omega}(\text{ref, } 0°)]^{1/2}$ ~ 3.3×10^{-18} esu/cm^2-layer where n is the number of layers. Similarly, for HUDPA, we recover $\chi^{(2)}$ ~ 3.8×10^{-18} esu/cm^2-layer and for PSA, $\chi^{(2)}$ ~ 4.1×10^{-18} esu/cm^2-layer. While it is tempting to offer an explanation for the relative magnitudes of these nonlinear responses, the structural complexity of the interlayer ionic linking chemistry precludes accurate modeling. In addition, given the uncertainty in the experimental data, it is not clear that these values of $\chi^{(2)}$ are different from one another. These data are important because they demonstrate the magnitude of the $\chi^{(2)}$ response for asymmetrically-coordinated metal ions to be small.

As discussed above, we are interested in understanding the layer-dependent organization of asymmetrically bound adlayer assemblies. The data in Figure 3.8 all show that the nonlinear response of the adlayers does not behave in the expected manner for thicknesses of greater than ~8 layers. There are several possible explanations for these data. The first is that the tilt angle of the layer constituents changes with number of layers. This may be expected based on the literature showing that ZP layers initially exhibit island growth but with the addition of layers, these islands grow together to form a reasonably uniform interface.[73] The explanation for this observation is that the ionic

complexation chemistry allows for growth at island edges with the addition of layers.[73,74] There are several pieces of information that suggest this explanation does not account for our data. The first is that we observe a linear ellipsometric dependence on number of layers, suggesting reasonably uniform layer density. Second, FTIR data exhibit a nominal Beer's law dependence of the CH stretching resonances (Figures 3.4 - 3.6), again arguing for approximately constant layer density. The third point that is not consistent with a change in average orientation angle with the addition of layers is the surface SHG data. We show in Figure 3.9 the dependence of the calculated SHG envelope function on the chromophore orientation angle.[62] The data shown in Figure 3.8 are for the fixed orientation angle of 60° with respect to the substrate normal. Over the range of sample tilt angles of 20° to 50°, we expect the magnitude of the envelope function to change very little at a sample tilt angle of 60°. Thus the deviation from the expected linear dependence of $I_{2\omega}^{1/2}$ on number of layers cannot be accounted for by a change in the chromophore tilt angle unless the tilt angle approaches 90° (parallel to the substrate) with increasing number of layers. This structural motif is inconsistent with known ZP layer growth behavior.[73]

If the experimental surface SHG data cannot be accounted for in terms of layer-dependent changes in the average chromophore tilt angle, we must consider changes in the width of the chromophore angular distribution. An increase in the distribution width with number of layers would correspond to a decrease in order with increasing number of layers. It has been established that the magic angle for $\chi^{(2)}$ processes is 39.2°, and that a large body of experimental surface SHG data reported in the literature yield an apparent chromophore tilt angle of 39 ± 2°.[58] If we assume that our apparent tilt angle for these

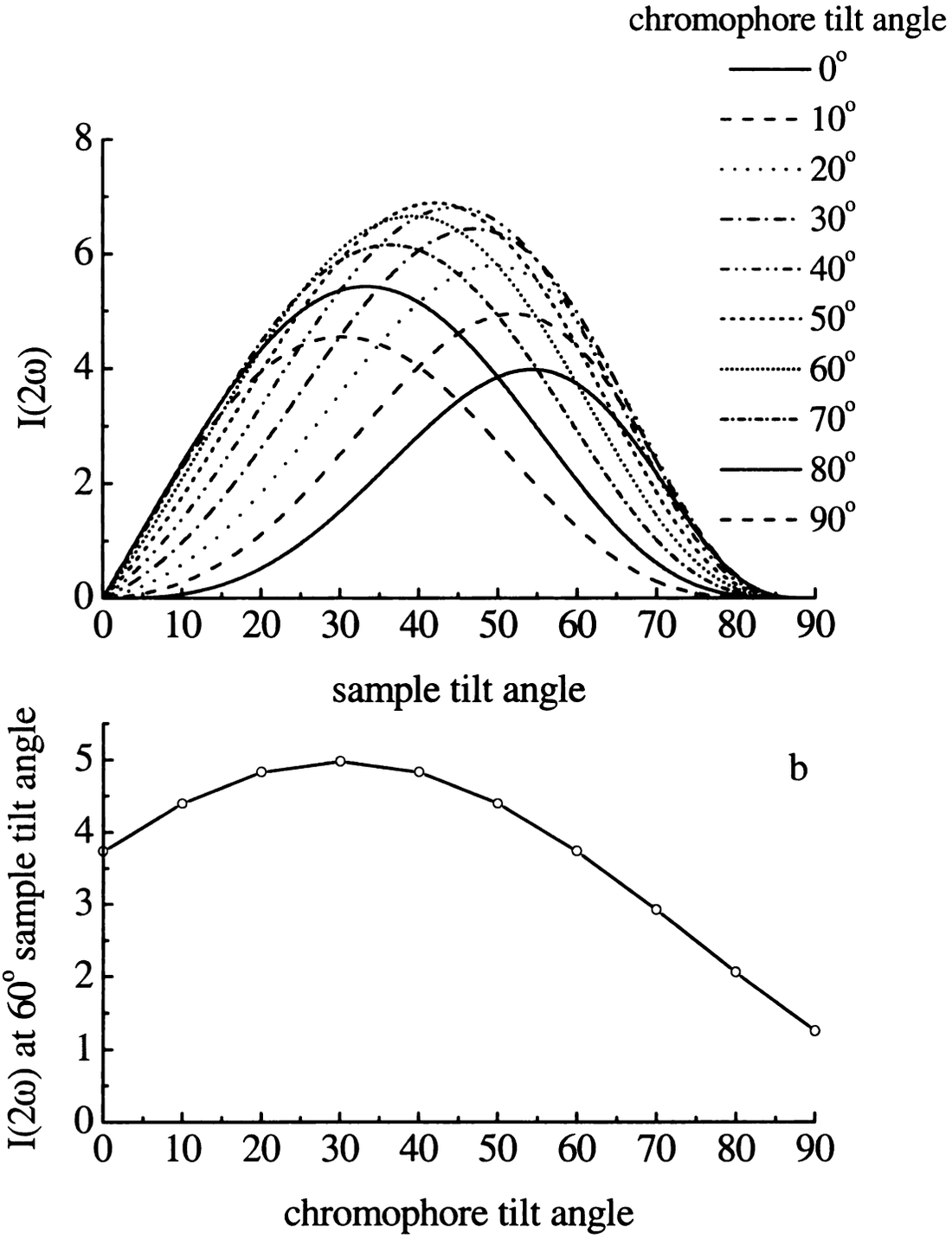

Figure 3.9. Top panel: Calculated SHG envelope function for chromophore tilt angles shown at right. The calculation is for the dipolar SHG response only. (b) Calculated surface SHG intensity taken at 60° sample rotation angle as a function of chromophore tilt angle.

data is 39°, the surface SHG signal intensity of a single adlayer will vary with distribution angle width as shown in Figure 3.10. These intensities are plotted on a log scale for clarity of presentation and show that, once the distribution width exceeds ~ 20°, the surface SHG signal per layer at 60° decreases monotonically with increasing distribution width. The negative deviations we see for more than 8 layers in Figure 3.8 can be accounted for in terms of a progressively increasing distribution width. While it may be tempting to extract quantitative changes in distribution width with increasing number of layers, the presence of the substrate response, which is dominated by a quadrupolar component of $\chi^{(2)}$ and the lack of knowledge regarding the form of the orientational distribution precludes modeling these data with any degree of confidence. We are left with the qualitative result that our data are consistent with an apparently constant average chromophore tilt angle and an increase in the tilt angle distribution width with increasing number of adlayers.

Surface second harmonic generation has, of course, been used before to understand organization in layered materials. For certain systems, second harmonic intensity has been shown to with increase with the square of the number of chromophore layers,[75,76] but those results are based on fewer than 10 layers. It is therefore difficult to make a direct connection between those data and ours because the strongest evidence for changes in layer order occur only for multilayer stacks with more than 8 layers. Also, the organization in those reports was for the organic constituents between the metal bisphosphate/phosphonate interlayer linking moieties and the relationship of the organization in these two regions of the adlayers remains to be established. There have

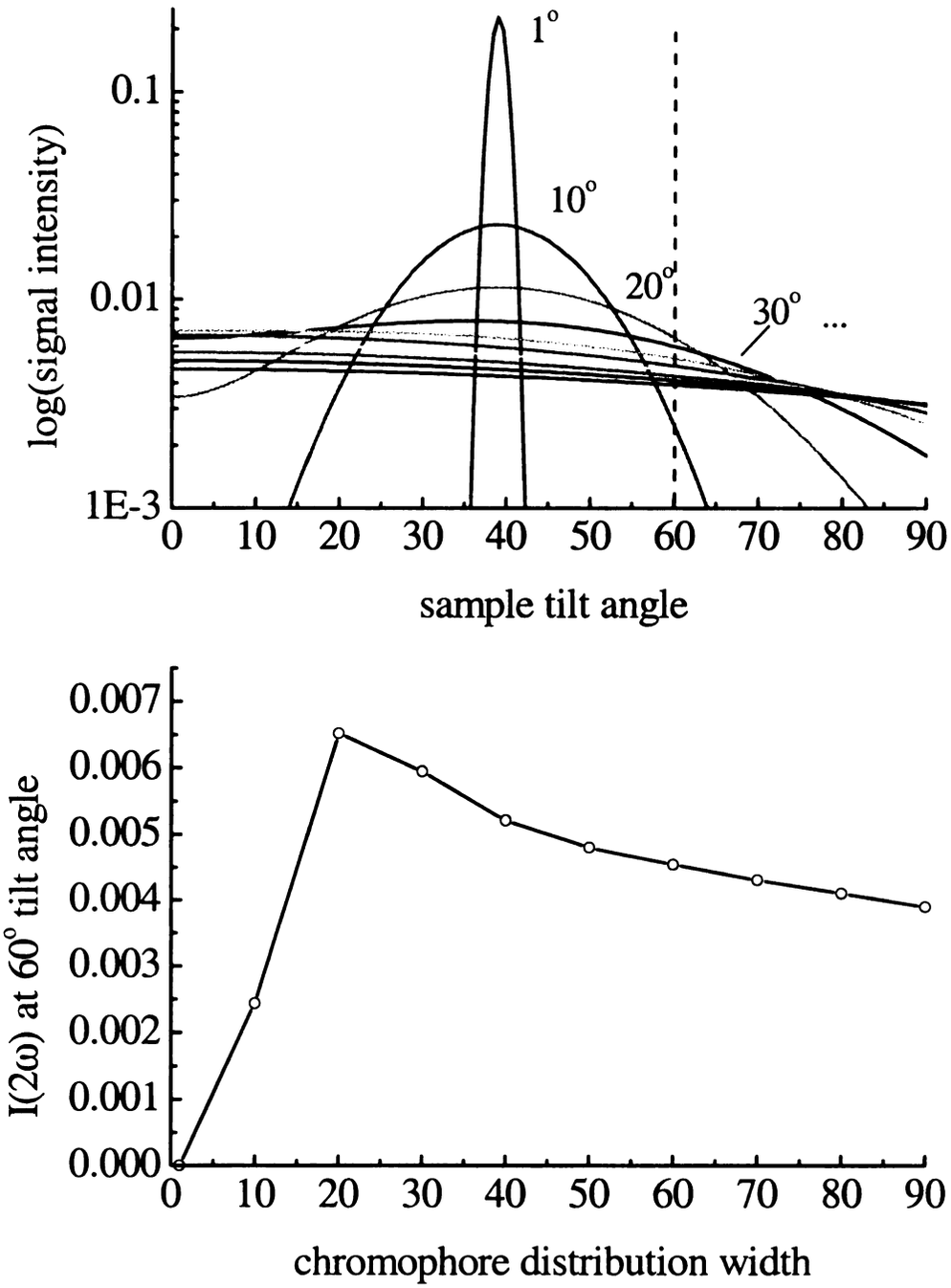

Figure 3.10. Top panel shows the calculated SHG envelope function at a function of sample rotation angle for different distribution widths starting at 1°, and then in 10° steps to 90°. The plot is on a logarithmic scale for clarity. Bottom panel: Dependence of the second harmonic signal at the fixed observation angle of 60° sample rotation as a function of sample orientational distribution width. These calculations were performed assuming an average chromophore tilt angle of 39° with respect to the substrate normal.

been other reports of saturation of the second harmonic intensity in layered materials but the authors did not offer a detailed explanation for the apparent discrepancy between theory and experiment.[77-79] Kikteva *et al.*[76] have reported increases in second harmonic intensity for up to five layers of Rhodamine 6G spin-cast on fused silica substrates, but the signal was found to decrease with the addition of more layers. In that work, the disorder intrinsic to a spin-cast film can be used to explain their findings.

The work we report here provides insight into the magnitude of the $\chi^{(2)}$ contribution of the inorganic interlayer for ionically-bound multilayer systems. In most ZP multilayer systems where bisphosphonates are used in the layer assembly, a center of inversion is created at the metal centers, therefore precluding this part of the multilayer assembly from generating any $\chi^{(2)}$ response. Investigating the SH response of Zr- 1,10-decane-bis(phosphonic acid) multilayers grown on a Hf-functionalized silicon substrate, Neff *et al.*[75] observed no measurable difference between those films and the metal-primed substrates. This is not an unexpected result since hydrocarbon chains do no contribute measurably to second order nonlinear optical activity due to the small hyperpolarizability characteristic of σ bonds.[80]

3.4 Conclusions

We have shown that surface second harmonic generation in conjunction with asymmetric, oriented layer deposition is useful for probing molecular order in aliphatic multilayer assemblies. Optical null ellipsometry and FTIR show regular layer deposition density and thickness but the organic constituents do not exhibit quasi-crystalline order. This finding is consistent with other reports on ZP systems and likely is the result of fast deposition kinetics and a small desorption rate constant for the layer constituents. Our surface second harmonic generation data reveal a relatively small nonlinear optical activity for the inorganic interlayer constituents within these layers and the deviation of the $\chi^{(2)}$ response from the expected $\sqrt{I_{2\omega}}$ vs. number of layers is consistent with an increase in the distribution width of the nonlinear chromophore tilt angles with layer growth. Future work, including SHG imaging measurements, may shed light on the details of this layer-dependent organization phenomenon.

3.5 Literature Cited

1. Kim, H. I.; Graupe, B. J.; Oloba, O.; Koini, T.; Imaduddin, S.; Lee, T. R.; Perry, S.; *Langmuir*, **1999**, *15*, 3179.
2. Lee, S.; Shon, Y. S.; Colorado, R.; Guenard, R. L.; Lee, T. R.; Perry, S. S. *Langmuir*, **2000**, *16*, 2220.
3. Xiao, X.; Hu, J.; Charych, D. H.; Salmeron, M.; *Langmuir* **1996**, *12*, 235.
4. Laibinis, P. E.; Whitesides, G. M. *J. Am. Chem. Soc.* **1992**, *114*, 1990.
5. Bain, C. D. and Whitesides G. M. *Angew. Chem., Int. Ed. Engl.* **1989**, *28*, 506.
6. Abbott, N. L. and Whitesides, G. M. *Langmuir*, **1994**, *10*, 1493.
7. Guo, L. H.; Facci, J. S.; McLendon J. *J. Phys. Chem.* **1995**, *99*, 8458.
8. Hockett, L. A.; Creager, S. E. *Langmuir*, **1995**, *11*, 2318.
9. Laibinis, P. E.; Whitesides, G. M. *J. Am. Chem. Soc.* **1992**, *114*, 9022.
10. Carter, F. L. *Molecular Electronic Devices II*, Maecel Dekker, New York, **1987.**
11. Everhart, D. S. *Chemtech,* **1999**, *4*, 30.
12. Yang, H. C.; Dermody, D. L.; Xu, C.; Ricco, A. J.; Crooks, R. M. *Langmuir*, **1996**, *12*, 726.
13. Wells, M.; Dermody, D. L.; Yang, H. C.; Kim, T.; Crooks, R. M.; Ricco, A. J.; *Langmuir*, **1996**, *12*, 1989.
14. Batchelder, D. N., Evans, S. D., Freeman, T. L., Haussling, L., Ringsdörf, H., Wolf, H.; *J. Am. Chem. Soc.* **1994**, *116*, 1050.
15. Katz, H. E., Wilson, W. L., Scheller, G. R. *J. Am. Chem. Soc.*, **1994**, *116*, 6636.

16. Katz, H. E., Scheller, G. J., Putvinski, T. M., Schilling, M. L., Wilson, W. L., Chedsey, C. E. D. *Science*, **1991**, *254*, 1485.

17. Putvinski, T. M., Schilling, M. L., Katz, H. E., Chidsey, C. E. D.; Mujsce, A. M., Emerson, A. B. *Lungmuir*, **1990**, *6*, 1567.

18. Kumar, A.; Biebuyck, H. A.; Abbott, N. L.; Whitesides, G. M. *Langmuir*, **1994**, *10*, 1498.

19. Tarlov, M. J.; Burgess, D. R. F.; Gillen, G. *J. Am. Chem. Soc.* **1993**, *115*, 5305.

20. Lewis, M.; Tarlov, M. J.; Carron, K. *J. Am. Chem. Soc.* **1995**, *117*, 9574.

21. Ulman, A.; *Chem. Rev.*, **1996**, *96*, 1533.

22. Dubois, L. H.; Nuzzo, R. G., *Annu. Rev. Phys. Chem.*, **1992**, *43*, 437.

23. Linford, M. R.; Fenter, P.; Eisenberger, P. M.; Chidsey, C.E. D. *J. Am. Chem. Soc.*, **1995**, *117*, 3145.

24. Langmuir, I.; *J. Am. Chem. Soc.* **1917**, *39*, 1848.

25. Blodgett, K. B. *J. Am. Chem. Soc.*, **1935**, *57*, 1007.

26. Lee, H.; Kepley, L. J.; Hong, H. G.; Mallouk, T. E. *J. Am. Chem. Soc.*, **1988**, *110*, 618.

27. Lee, H.; Kepley, L. J.; Hong, H. G.; Akhter, S.; Mallouk, T. E. *J.Phys. Chem.*, **1988**, *92*, 2597.

28. Kohli, P.; Taylor, K. K.; Blanchard, G. J. *J. Am. Chem. Soc.*, **1998**, *120*, 11962.

29. Kohli, P. and Blanchard, G. J. *Langmuir*, **2000**, *16*, 4655.

30. Nuzzo, R. G.; Allara, D. L. *J. Am. Chem. Soc.*, **1983**, *105*, 4481.

31. Ulman, A. *An Introduction to Ultrathin Films: From Langmuir-Blodgett to Self-Assembly*; Academic Press, Inc.: New York, **1991**.

32. Nuzzo, R. G.; Dubois, L. H.; Allara, D. L. *J. Am. Chem. Soc.*, **1990**, *112*, 558.

33. Karpovich, D. S.; Blanchard, G. J., *Langmuir*, **1994**, *10*, 3315.

34. Schessler, H. M.; Karpovich, D. S.; Blanchard, G. J.; *J. Am. Chem. Soc.*, **1996**, *118*, 9645.

35. Thompson, M. E. *Chem. Mater.*, **1994**, *3*, 521.

36. Sagiv, J. *J. Am. Chem. Soc.*, **1980**, *102*, 92.

37. Silberzan, P.; Leger, L.; Ausserre, D.; Benattar, J. J. *Langmuir*, **1991**, *7*, 1647.

38. Le Grange, J. D.; Markham, J. L.; Kurjian, C. R. *Langmuir*, **1993**, *9*, 1749.

39. Brandriss, S.; Margel, S. *Langmuir*, **1993**, *9*, 1232.

40. Mathauser, K.; Frank, C. W. *Langmuir*, **1993**, *9*, 3002.

41. Bakiamoh, S. B.; Blanchard, G. J. *Langmuir*, **1999**, *15*, 6379.

42. Allara, D. L., Nuzzo, R. G. *Langmuir*, **1985**, *1*, 52.

43. Bandyopadhyay, K., Patil, V., Vijayamohanan, K., Sastry, M. *Langmuir*, **1997**, *13*, 5244.

44. Kohli, P. and Blanchard, G. J. *Langmuir*, **1999**, *15*, 1418.

45. Ledoux, I.; Zyss, J., *in Novel Optical Materials and Applications*, edited by I. C. Khoo, F. Simoni, and C. Umeton, Wiley, New York, **1997**, 1-48.

46. Becka, A. M.; Miller, C. J.; *J. Phys. Chem.*, **1992**, *96*, 2657.

47. Miller, C. J.; Gratzel, M.; *J. Phys. Chem.*, **1991**, *95*, 5225.

48. Miller, C. J.; Cuendet P.; Gratzel, M.; *J. Phys. Chem.* **1991**, *95*, 877.

49. Corbitt, T. S.; Crooks, R. M.; Ross, C. B.; Hampden-Smith, M. J.; Schoer, J. K.; *Adv. Mat.*, **1993**, *5*, 935.

50. Xia, Y.; Mrksich, M.; Kim, E.; Whitesides, G. M.; *J. Am. Chem. Soc.*, **1995**, *117*, 9576.

51. Corn, R. M.; Higgins, D. A.; *Chem. Rev.*, **1994**, *94*, 107.

52. Eisenthal, K. B.; *J. Electrochem. Soc.*, **1988**, *135*, C385.

53. Heinz, T. F.; Tom, H. W. K.; Shen, Y. R.; *Phys. Rev. A*, **1983**, *28*, 1883.

54. Richmond, G. L.; *Surf. Sci.*, **1984**, *147*, 115.

55. Simpson, G. J.; Rowlen, K. L.; *Accts. Chem. Res.*, **2000**, *33*, 781.

56. Simpson, G. J.; Westerbuhr, S. G.; Rowlen, K. L.; *Anal. Chem.*, **2000**, *72*, 887.

57. Simpson, G. J.; Rowlen, K. L.; *Chem. Phys. Lett.*, **1999**, *309*, 117.

58. Simpson, G. J.; Rowlen, K. L.; *J. Am. Chem. Soc.*, **1999**, *121*, 2635.

59. Bhattachrya, A. K.; Thyagarajan, G.; *Chem Rev.*, **1981**, *81*, 415.

60. Strazzolini, P.; Giumanini, A. G.; Verardo, G.; *Tetrahedron*, **1994**, *50*, 217.

61. Porter, M.D.; Bright, T. B.; Allara, D. L.; Chidsey, C. E. D.; *J. Am. Chem. Soc.* **1987**, *109*, 3559.

62. Flory, W. C.; Mehrens, S. M.; Blanchard, G. J.; *J. Am. Chem. Soc.*, **2000**, *122*, 7976.

63. Flink, S.; va Veggel, F. C. J. M.; Reinhoudt,D. N.; *Adv. Mater.*, **2000**, *12*, 1315.

64. Inoune, T.; Moriguchi, M.; Ogawa, T.; *Thin Solid Films*, **1999**, *350*, 238.

65. Lin S.; Meech, S. R.; *Langmuir*, **2000**, *16*, 1167.

66. Zimdars, D.; Eisenthal, K. B.; *J. Phys. Chem.*, **1999**, *103*, 10567.

67. Simpson, G. J.; Westerbuhr, S. G.; Rowlen, K. L.; *Anal. Chem.*, **2000**, *72*, 887.

68. Shen, Y. R. *The Principles of Nonlinear Optics*, Wiley, New York, **1992**.

69. Lukpe, G.; Marowaky, G.; Sieverdes, F. *In Organic Molecules for Nonlinear Optics and Photonics*, Messier, J. *et al.*, Kluwer Academic Publishers, Amsterdam, **1991**.

70. Li, D.; Ratner, M. A.; Marks, T. J.; *J. Am. Chem. Soc.*, **1990**, *112*, 7389.

71. Berkovic, G.; Shen, Y. R.; *Opt. Soc. Am. B,* **1989**, *6*, 205.

72. Guyot-Sionnest, P.; Shen, Y. R.; *Phys. Rev. B*, **1987**, *35*, 4420.

73. Byrd, H.; Snover, J. L.; Thompson, M. E.; *Langmuir*, **1995**, *11*, 4449.

74. Kaschak, D. M.; Johnson, S. A.; Hooks, D. E.; Kim, H.-Y.; Ward, M. D.; Mallouk, T. E.; *J. Am. Chem. Soc.*, **1998**, *120*, 10887.

75. Neff, G. A.; Helfrich, M. R.; Clifton, M. C.; Page, C. J.; *Chem. Mater.*, **2000**, *12*, 2363.

76. Kikteva, T.; Star, D.; Zhao, Z.; Baisley, T. L.; Leach, G. W.; *J. Phys. Chem. B,* **1999,** *103*, 1124.

77. L'vov, Y.; Yamada, S.; Kunitake, T.; *Thin Solid Films,* **1997**, *300*, 107.

78. Balasubramanian, S.; Wang X.; Wang H. C.; Yang, K.; Kumar, J.; Tripathy, S. K.; Li, L.; *Chem. Mater.*, **1998**, *10*, 1554.

79. Roberts, M. J.; Lindsay, G.A.; Herman, W. N.; Wynne, K. J.; *J. Am. Chem. Soc.* **1998,** *120*, 11202.

80. Chemla, D. S.; Zyss, J.; *Nonlinear Optical Properties of Organic Molecules and Crystals* Academic Press, **1987.**

Chapter 4

Characterizing Metal Phosphonate Surface Coverage using Surface Second Harmonic Generation. The Coexistence of Ordered and Disordered Domains

Summary

We report on the use of surface second harmonic generation (SHG) intensity measurements to understand the molecular details of potentially heterogeneous surface coverage. Using a rigid chromophore with a large second order nonlinear susceptibility ($\chi^{(2)}$) and an adlayer diluent molecule with negligible nonlinear response, the incidence angle-dependence of the SHG intensity was determined as a function of surface chromophore coverage. The SHG data at fixed incidence angle suggest that the average orientation of the adsorbed chromophores does not change significantly with surface coverage, resulting in the expected square-law relationship between SHG intensity and loading density. The form of the SHG data point to the presence of two distinct domains in the monolayer. The dominant domain is characterized by chromophores oriented along the surface normal and the minority domain is comprised of a nominally random orientational distribution, with the relative amount of the disordered domain decreasing with increasing fractional chromophore coverage.

4.1 Introduction

The field of interfacial materials holds much promise for a variety of technologies, ranging from chemical separations[1,2] to nonlinear optics and electro-optics,[3-5] because of the ability to control macroscopic properties by chemical means. A number of methods have been used in the assembly of ultrathin interfaces with the aim of achieving control over their molecular-scale structure and mesoscopic organization. The most widely studied and best-characterized interfacial materials are alkanethiol self-assembled monolayers on gold, (SAMs), pioneered by Allara and Nuzzo in the early 1980s.[6,7] These materials possess substantially greater order than alkylsiloxane[8,9] self-assembled-monolayers and are more robust than physisorbed Langmuir-Blodgett (LB) films.[10,11] Due to the modest driving forces responsible for their formation, alkanethiol/gold SAMs are relatively labile.[12,13] In an effort to create robust and structurally versatile layered assemblies, Mallouk and coworkers demonstrated layered self-assembly based on ionic complexation between transition metal ions (*e.g.* Zr^{4+}) and anionic functionalities such as phosphate or phosphonate.[14,15] The first demonstrations of metal phosphonate layered growth used symmetric α,ω-alkanebisphosphonates. To achieve orientational control within the layers, Katz and coworkers[16] used ω-hydroxyorgano phosphonates to enforce macroscopic orientation of the layers by means of the three-step sequence of surface activation, adlayer adsorption, and conversion of the terminal hydroxyl groups to phosphates. Other interface linking strategies include the use of carboxylic and sulfonic acid complexation with various metal ions,[17,18] and novel hybrid structures where layers can be linked either ionically or covalently.[19-21]

Molecular-scale organization at an interface can be significantly different from that of the corresponding bulk material and, while our understanding of intermolecular interactions in the bulk phase is relatively mature, the same level of understanding remains to be achieved for most interfaces, where substrate morphology can play a significant role. The limited structural information available on interfacial systems stems from the small amount of material present in an interfacial layer and the limited number of surface-specific techniques capable of probing molecular structural properties. Techniques available for the study of surfaces and interfaces include particle scattering[22,23] and photon-based measurements.[24-26] The electron-based methods must be performed under high vacuum while the optical techniques can be performed under ambient laboratory conditions. Second order nonlinear optical methods are inherently surface-selective and have proven to be quite useful for investigating a variety of surfaces and interfaces.[27-30] Second harmonic generation (SHG) is the conversion of two photons of frequency ω to a single photon of frequency 2ω which, in the electric dipole approximation, requires a noncentrosymmetric medium such as a surface.[31-33] Surface SHG measurements are nondestructive, sensitive, and applicable to any interface accessible to light. This technique has been used to study solid/air,[34,35] solid/liquid,[34,36] liquid/vapor,[34,37] and liquid/liquid[38,39] interfaces. The combination of sensitivity and surface selectivity has led to the use of SHG in the study of a variety of interfacial phenomena, including electron-transfer reactions,[30,40] electrostatic properties,[29] surface symmetry,[41,42] organization and orientation of chemisorbed and physisorbed molecules, [43-47] adsorption and desorption kinetics,[48-50] and surface coverage.[51,52]

We report on the use of surface SHG intensity measurements to elucidate the details of ZP adsorption chemistry under conditions where the surface coverage can be

heterogeneous, owing either to substrate non-uniformity or adsorbate aggregation. For this work, we use two molecules capable of oriented interfacial deposition; the $\chi^{(2)}$ chromophore ((4-(4-(4-(4-((2-hydroxyethyl)sulfonyl)phenyl)azo)phenyl)piperazinyl). phenyl)phosphonic acid), **C1**, and (12-hydroxyl-1-dodecylphosphonic acid), HDPA, an aliphatic diluent with the same terminal functionalities as the chromophore. The structures of **C1** and HDPA are shown in Figure 4.1. We create interfaces of controlled composition by adsorption from solutions containing predetermined concentrations of the chromophore and the diluent. We monitor the surface **C1** loading density using UV-visible absorption spectroscopy and we investigate adsorbate distribution using surface SHG intensity measurements. The chromophore concentration-dependence of the surface SHG response points to the existence of two chromophore domains, one characterized by significant order and the other largely disordered, with the contribution from the disordered domain decreasing with increasing chromophore concentration. Our findings are consistent with interface heterogeneity sensed by surface SHG measurements being mediated by adlayer intermolecular interactions.[53,54] This interfacial heterogeneity appears to be in addition to the intrinsic heterogeneity of the interface arising from the non-uniform distribution of surface silanol functionalities.

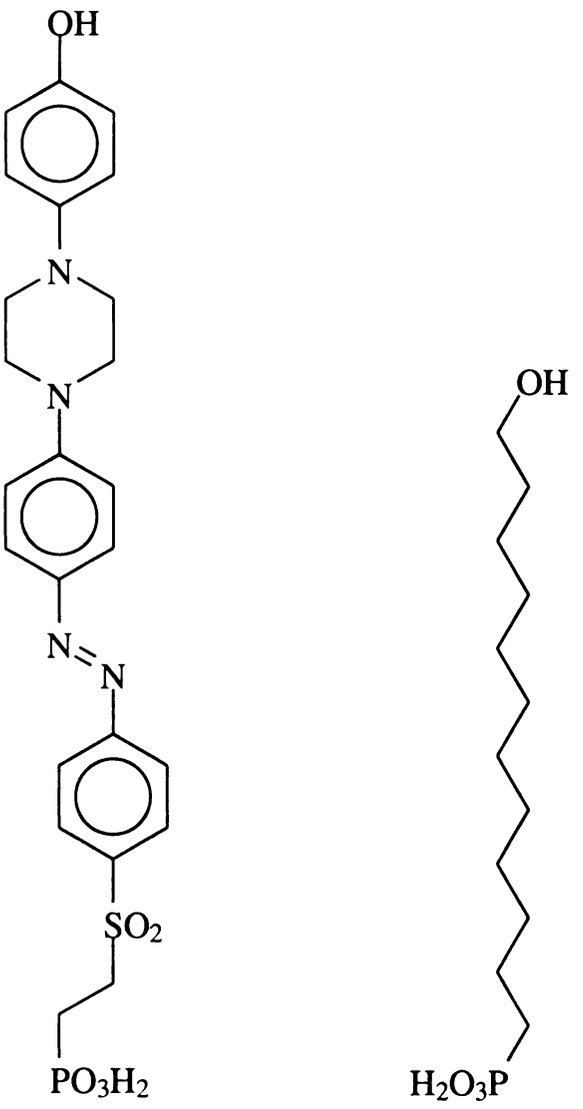

C1 HDPA

Figure 4.1. Structures of $\chi^{(2)}$ chromophore **C1** (left) and HDPA monolayer diluent (right).

4.2 Experimental Section

Reagents and Materials. 12-bromo-1-dodecanol, 4-bromoaniline, *n*-butyl lithium, diethylchlorophosphate, $CDCl_3$, triisopropylphosphite, sodium metal, 4-acetamidobenzene sulfonyl chloride, zirconyl chloride octahydrate, 2-chloroethanol, 2,4,6-collidine, $CDCl_3$, DMSO-d_6, bromotrimethylsilane, dimethylformamide, ethanol, methylene chloride, diethylether, tetrahydrofuran, benzene, ethanol, and acetonitrile were obtained from Sigma-Aldrich Chemical Co. in the highest purity available and used without further purification. Other reagents used were silica gel, sodium iodide, sodium bicarbonate, *p*-toluenesulfonyl chloride, ethylene glycol (Spectrum Quality Products, Inc.), sodium nitrite, sodium acetate, sodium bicarbonate, hydrogen peroxide (J. T. Baker), sulfuric acid, hydrochloric acid (Columbus Chemical Industries, Inc.), propanoic acid (Fluka), and N,N-bis(2-chloroethyl) aniline (Frinton Laboratories).

Chromophore synthesis: The synthesis of the $\chi^{(2)}$ chromophore **C1**, (4-(4-(4-(4-((2-hydroxyethyl)sulfonyl)phenyl)azo)-phenyl)piperazinyl)phenyl)phosphonic acid), has been reported previously.[55] The synthesis of the bifunctional alkane diluent 12-hydroxy-1-dodecylphosphonic acid, HDPA, has been reported previously.[56] In this procedure, the hydroxyl group was protected by reacting the 12-bromo-1-dodecanol with acetyl chloride at 0°C, followed by refluxing the ω-bromoester with excess triethylphosphite at 150°C for 5 hours.[57,58] The product was treated with bromotrimethylsilane at 20°C for 24 hours to hydrolyze the phosphoester bonds, followed by acid hydrolysis of the ester functionality using 6 M HCl. White crystalline product was collected by vacuum filtration and was pure by NMR. ^{1}H NMR (DMSO-d_6): δ = 7.24 (s, broad, 1H, OH), 4.02 (t, 2H, HO-$^*CH_2$-), 1.16 -1-53 (m, 22H).

Preparation of solutions for adlayer deposition: **C1** (27.0 mg, 5 mmol) and HDPA (14.0 mg, 5 mmol) were placed in two separate 10 mL volumetric flasks and about 5 mL of DMF were added. The flasks were shaken until the contents were dissolved, and then filled to the mark with DMF. The solutions used for layer deposition contained specific concentrations of both **C1** and HDPA and were made from the stock solutions. The total volume of each solution was 18 mL, made up of 2 mL 95% ethanol, 12 mL acetonitrile and 4 mL DMF. For example, a solution made to deposit an adlayer comprised of 10% **C1** solution and 90% HDPA was made with 0.36 mL of stock **C1** solution, 3.24 mL of stock HDPA solution, 0.40 mL DMF, 2 mL ethanol, and 12 mL acetonitrile. The volumes of stock **C1** and HDPA solutions used for layer deposition and the corresponding adlayer **C1** concentrations are shown in Table 4.1.

Adlayer formation: Quartz substrates (15 x 15 x 1 mm precut) used for monolayer syntheses were cleaned in piranha solution ($3H_2SO_4$:$1H_2O_2$. *caution: strong oxidizer!*) for 15 min, rinsed with flowing distilled water for 1 min, and dried with a stream of N_2.[59] Monolayers were deposited on the cleaned substrates using a slight modification of a procedure outlined previously.[56] The surface silanol groups were phosphorylated directly by reaction with 20 m$\underline{M}$ $POCl_3$ in 10 mL anhydrous acetonitrile containing 20 m$\underline{M}$ 2,4,6-collidine under argon at room temperature. After 15 minutes, the substrates were rinsed with reagent grade acetonitrile, then with flowing water for 30 sec., and then reacted with a 5 m$\underline{M}$ $ZrOCl_2$ solution in 60% ethanol (*aq*) for 10 min. Monolayers were deposited by immersion of zirconated surfaces into the working solutions (Table 4.1) in 50-mL round bottomed flasks at ~ 50°C for 1 hour, rinsed in warm ethanol, then water, and dried under a stream of N_2.

C1			HDPA		
Volume of **C1** stock (mL)	**[C1]** in deposition solution (mM)	Adlayer **[C1]** (%)	Volume of HDPA stock (mL)	[HDPA] in deposition solution (mM)	Adlayer [HDPA] (%)
0.00	0.00	0	3.60	1.00	100
0.36	0.10	10	3.24	0.90	90
0.72	0.20	20	2.88	0.80	80
1.08	0.30	30	2.52	0.70	70
1.44	0.40	40	2.16	0.60	60
1.80	0.50	50	1.80	0.50	50
2.16	0.60	60	1.44	0.40	40
2.52	0.70	70	1.08	0.30	30
2.88	0.80	80	0.72	0.20	20
3.24	0.90	90	0.36	0.10	10
3.60	1.00	100	0.00	0.00	0

Table 4.1. Compositions of solutions used for adlayer deposition.

Surface characterization: The solution phase **C1** concentrations used for monolayer deposition and the resultant adlayer **C1** loading densities were measured using UV-visible absorption spectroscopy (Cary 300 Bio UV-visible spectrophotometer). The scan rate for all measurements was 300 nm/min and the spectral resolution was 1 nm. The data were acquired using Cary WinUVscan® software and processed using Microcal Origin® v 6.1 software. The laser system used for this work has been described in detail elsewhere.[56,60] Surface SHG intensity measurements were performed using a Q-switched, mode-locked Nd:YAG laser (Quantronix model 416) operating at 1064 nm and 500 Hz Q-

switching rate with ~100 ps mode-locked pulse duration (41 MHz mode-locking frequency). The Q-switched envelop is ~2 μs. The incident fundamental light was TM polarized and any second harmonic generated by the optics prior to the sample removed using a RG-630 color filter. The second harmonic generated in the transmision mode from ~100 μm beam spot diameter was detected using a PMT (Hamamatsu type 466) after removing transmitted fundamental light with three dichroic filters and a monochromator.

4.3 Results and Discussion

The purpose of this work is to investigate the deposition behavior of monolayer interfaces containing multiple constituents. At heart is whether or not adlayer formation in ZP systems is random and, if not, what is the nature of the domains that form. We use surface SHG intensity measurements to examine the deposition of adlayers where there is the potential for heterogeneous surface coverage. We monitor the nonlinear optical response of a rigid chromophore with a large hyperpolarizability, β, deposited from a solution containing specified concentrations of the chromophore and a spacer. The steady state spectroscopic data indicate that we have macroscopic control over adlayer composition and the functional form of the surface SHG intensity data demonstrate there to be two characteristic domains. We consider first our steady state spectroscopic data, then treat the surface SHG data.

As detailed in the Experimental Section, we prepare solutions containing specified concentrations of **C1** and HDPA and determine the **C1** concentration in each using UV-visible absorption spectroscopy (Figure 4.2). The absence of spectral shifts over the concentration range used suggests the absence of solution phase aggregation phenomena. The key to the success of our work lies in our ability to deposit the same **C1**/HDPA ratio onto the substrate as we have in solution. This correspondence requires that the solubility of **C1** and HDPA be essentially the same in the solvent system used. We have determined empirically that a solvent system comprised of 4 DMF:2 ethanol:12 acetonitrile (v/v/v) allows us to make linear correspondence between solution phase concentration and adlayer loading density. We note that the absorption maximum of adsorbed **C1** blue-shifts with increasing surface chromophore concentration. The shift is as large as ~ 20 nm over

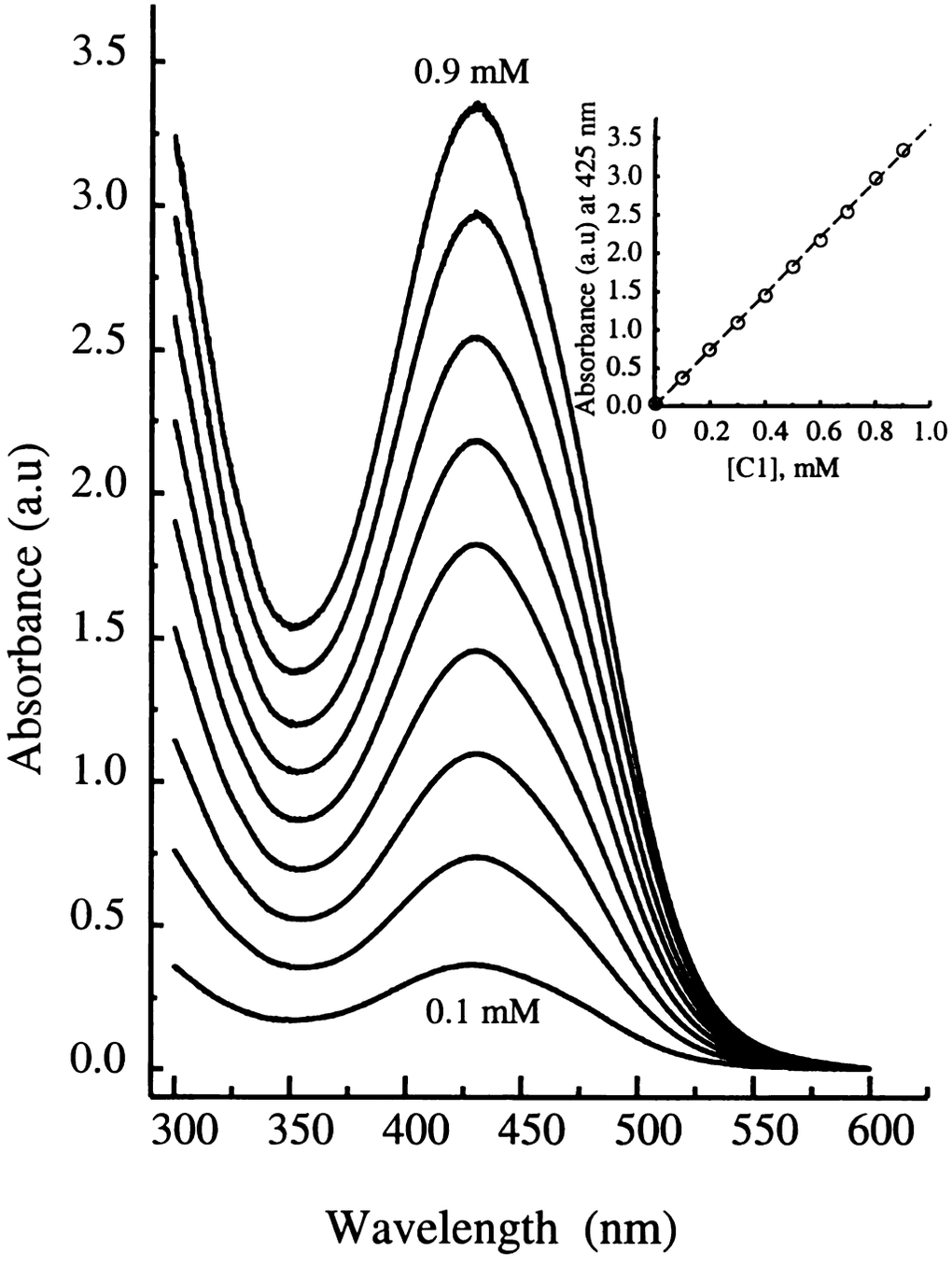

Figure 4.2. Absorbance spectra of solutions used for monolayer deposition. Total phosphonate concentration is 1 mM for all solutions. **C1** concentrations range from 0.1 mM (bottom spectrum) to 0.9 mM (top spectrum). Inset: Beers law plot of **C1** absorbance in solution.

the range of surface coverage of $0.1 \leq \theta \leq 1$,[30,39] indicating significant intermolecular interactions. We discuss the significance of this finding following consideration of the surface SHG data. The absorbance of adsorbed **C1** increases linearly with deposition solution concentration (Figure 4.3). Based on these data, it is not possible to discern whether or not the adlayer is comprised of a random distribution of adsorbed chromophore molecules. From solution phase UV-visible spectra we extract ε_{max} = 21,966 L/mol-cm for **C1** and, using the experimental absorbance data for one monolayer (A_{max} = 0.031 a.u for 100 % **C1**) shown in Figure 4.3, we estimate the surface loading density to be 8.5 x 10^{14} cm^{-2}-$layer^{-1}$. The density of silanol groups on the surface of silica or quartz is typically taken to be 2 – 8 $\mu mol/m^2$, corresponding to ~(1.25 – 5) x 10^{14} cm^{-2}, depending of the details of the surface preparation.[61-63] We acknowledge that the calculated loading density approaches or slightly exceeds the theoretical maximum packing density and we attribute this to uncertainty associated with the estimation of the extinction coefficient, ε_{max}, or unaccounted-for ordering of the **C1** adlayer yielding a higher than expected absorbance. The ability to achieve full surface coverage is attributed to the use of a rigid, rod-like chromophore capable of strong associative intermolecular interactions, combined with facile surface attachment chemistry.

The steady state absorbance data shown to this point indicate that we can control the bulk loading density of **C1** on SiO_x surfaces based on solution concentration. These data do not address the nature of the spatial distribution of **C1** on the surface. In an effort to address this issue, we examine the surface SHG response of monolayers containing a range of **C1** concentrations. The experimental data we present here is the dependence of the surface SHG intensity on the angle of incidence of the fundamental beam. The form

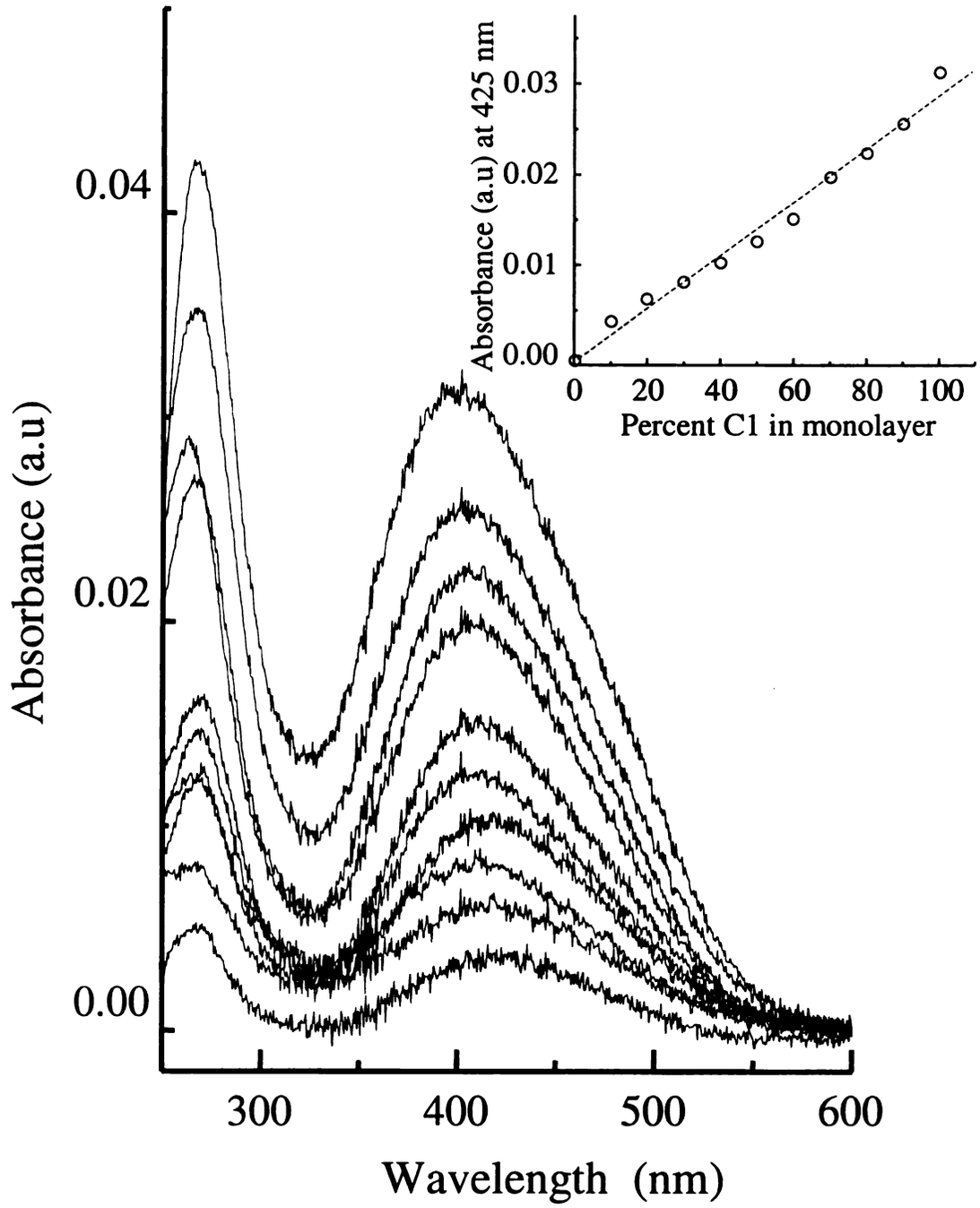

Figure 4.3. Absorbance spectra of adlayers of HDPA + C1 on SiOx substrates. Bottom spectrum is for a monolayer comprised of 10% **C1** and 90% HDPA. Top spectrum is for a monolayer comprised of 100% C1. The absorption maximum shifts from 430 nm to 417 nm over this adlayer **C1** concentration range. Inset: Beers law plot of adsorbed **C1**.

of our experimental signal has been discussed in detail elsewhere[56,60] and we recap only the salient points briefly below. In all cases, the incident fundamental electric field is TM-polarized and both TE- and TM-polarized second harmonic light is detected. The surface SHG measurements are performed in transmission mode and we detect the second harmonic signal generated from adlayers on both faces of the substrate.

$$E^{2\omega}(\theta) = \left(E^{\omega}\right)^2 \sum_{i=1}^{2} F_i \left(\frac{4\pi\chi^{(2)}}{{}_{\omega}n_i^2 - {}_{2\omega}n_i^2} \right) \exp(i\phi_i) \exp(i2\omega\ell_i/c) \left({}_{\omega}n_i \cos\theta_i^{\omega} - {}_{2\omega}n_i \cos\theta_i^{2\omega} \right) - 1$$

$$F_1 = {}_{\omega}T_{12}^2 \cdot {}_{\omega}R_2^2 \cdot {}_{2\omega}T_{23} \cdot {}_{2\omega}R_2 \cdot {}_{2\omega}T_{34} \cdot {}_{2\omega}R_4 \qquad (4.1)$$

$$F_2 = {}_{\omega}T_{12}^2 \cdot {}_{\omega}R_2^2 \cdot {}_{\omega}T_{23}^2 \cdot {}_{\omega}T_{34}^2 \cdot {}_{\omega}R_4^2 \cdot {}_{2\omega}T_{45} \cdot {}_{2\omega}R_4$$

where F_1 and F_2 are the Fresnel factors for the first and second interfaces. The sample is rotated through an angle θ, where $\theta = 0$ corresponds to the incident electric field propagating along the substrate normal. The thicknesses of the SHG-active layers are l_i and the terms ϕ_i are the relative phases of the second harmonic light generated at each interface.[64] The experimental signal exhibits interference between second harmonic light generated at the two sides of the substrate, [30,33,65] as seen in the experimental data.

$$\Delta I_{osc}(\theta) \propto \frac{2\omega d}{c} \left(n_{SiOx}^{2\omega} \cos\theta_{SiOx}^{2\omega} - n_{SiOx}^{\omega} \cos\theta_{SiOx}^{\omega} \right) \qquad (4.2)$$

The interference arises from dispersion in the SiO_x substrate. While this is largely a physical effect, the extent of cancellation depends on the organization of the adlayer(s), and we use this signal contribution to advantage in the interpretation of our data. The envelope function of the experimental data depend on both the average orientation angle of **C1** and the distribution of orientations that exist on the substrate. There are several contributions to the $\chi^{(2)}$ tensor that appears in Eq. 4.1; the susceptibility of the bulk substrate ($\chi^{(2)}_{bulk}$), the surface ($\chi^{(2)}_{surf}$), and the adlayer ($\chi^{(2)}_{adlayer}$) all contribute to the effective second-order response.

$$\chi^{(2)}_{eff} = \chi^{(2)}_{bulk} + \chi^{(2)}_{surf} + \chi^{(2)}_{ads} \quad (4.3)$$

Each of these contributions depends differently on the electric field angle of incidence and we can separate them to good approximation. Second-order processes are forbidden in centrosymmetric media within the dipole approximation.[31,33] We observe experimentally that the second harmonic signal arising from the (centrosymmetric) bulk substrate, $\chi^{(2)}_{bulk}$, is negligible based on the measurement of blank substrates. The second order nonlinear response of the blank substrate depends on $\chi^{(2)}$ contributions from the substrate surfaces, as seen from the oscillatory nature of the signal (Eq. 4.2, Figure 4.4). While dominated by the $\chi^{(2)}$ response of the surface, the signal from the blank substrate will contain contributions from both dipolar and quadrupolar terms in $\chi^{(2)}$. Guyot-Sionnest and Shen have shown that, for SiO_x, the quadrupolar component(s) of $\chi^{(2)}$ dominate over dipolar component(s).[66] The second order susceptibility of the air-fused silica interface is $\chi^{(2)} \sim 2.7\text{x}10^{-17}$ esu/cm^2, with the dipolar contribution being $\chi^{(2)}_{dip} \sim 5.7\text{x}10^{-18}$ esu/cm^2 and the quadrupolar contribution being $\chi^{(2)}_{quad} \sim 2.1\text{x}10^{-17}$ esu/cm^2. Because the angle-dependence of the quadrupolar and dipolar contributions to the substrate response differ, we can use $\chi^{(2)}_{quad}$ as an internal calibration for our measurements of adlayer-containing surfaces.[60]

The $\chi^{(2)}$ response of the HDPA is negligible compared to that of **C1**, [56,67] and we interpret our experimental data, especially at sample rotation angles substantially different from zero, to be dominated by **C1**. For these data, the SHG intensity depends on the **C1** surface number density, the average molecular orientation, and the distribution of orientation angles.[30,39,68-70] The experimental signal intensity, I(2ω), is proportional to the square of the surface nonlinear susceptibility, $(\chi^{(2)})^2$ and $\chi^{(2)}$ is related to the orientational

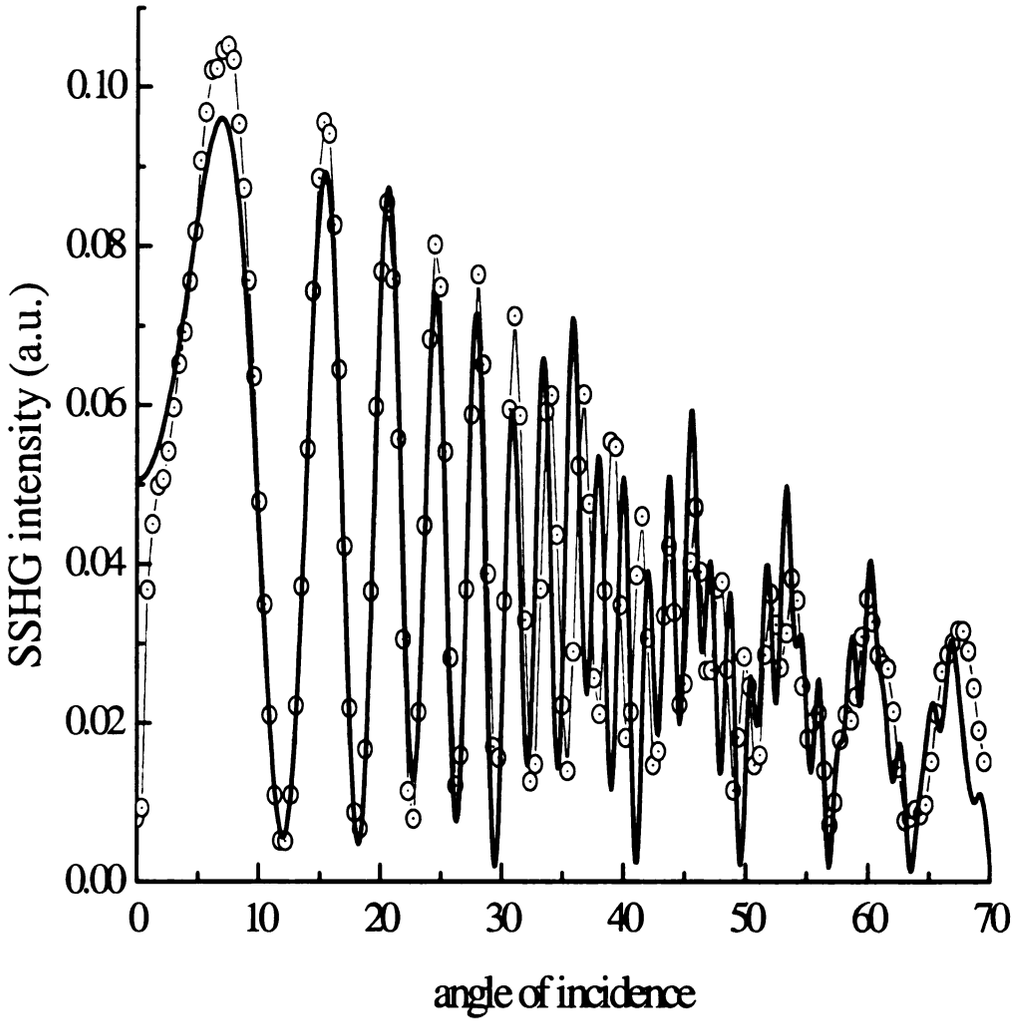

Figure 4.4. Experimental SSHG response of a SiO_x substrate (open circles) and fit of Eq. 1 to the data (solid line). For SiO_x, quadrupolar contributions to $\chi^{(2)}$ (near 0° incidence angle) dominate dipolar contributions (at higher incidence angles).

average of the molecular first hyperpolarizability, <β>, and the surface loading density, N_A,

$$\chi^{(2)} = N_A \langle \beta \rangle \tag{4.4}$$

Since I(2ω) is proportional to $|\chi^{(2)}|^2$ (Eq. 4.1) and $\chi^{(2)}$ is proportional to the number density, N_A (Eq. 4.4), the experimental second harmonic signal should increase with the square of the surface loading density, as long as the *average* molecular orientation does not change substantially with adlayer loading density (Figure 4.5). The data shown in Figure 4.5 are for a 60° sample rotation angle and any slight deviations from the linear dependence of $I(2\omega)^{1/2}$ on adlayer loading density reflect uncertainty in the experimental measurement. The *average* chromophore orientation on the surface does not change significantly with coverage, and we believe this finding to be consistent with our use of HDPA to provide full surface coverage over the range of **C1** loading densities studied. The interactions between the alkyl chains of HDPA and the relatively rigid **C1** molecule(s) determine the average chromophore orientations at lower surface coverage. These interactions are apparently not greatly different from the π-π interactions that likely dominate the chromophore orientations at high coverage. Several other groups have observed a constant adsorbate orientation with changes in adlayer density.[71-73]

One reason that the experimental data shown in Figure 4.5 are consistent with a constant average orientation is that the data are presented in a manner that is not particularly sensitive to adlayer orientation and orientational distribution. To gain a more complete understanding of the average orientation and distribution width of adlayer constituents, it is instructive to examine the sample rotation angle-dependence of the surface SHG signal. In particular, comparing the form of the experimental data to the

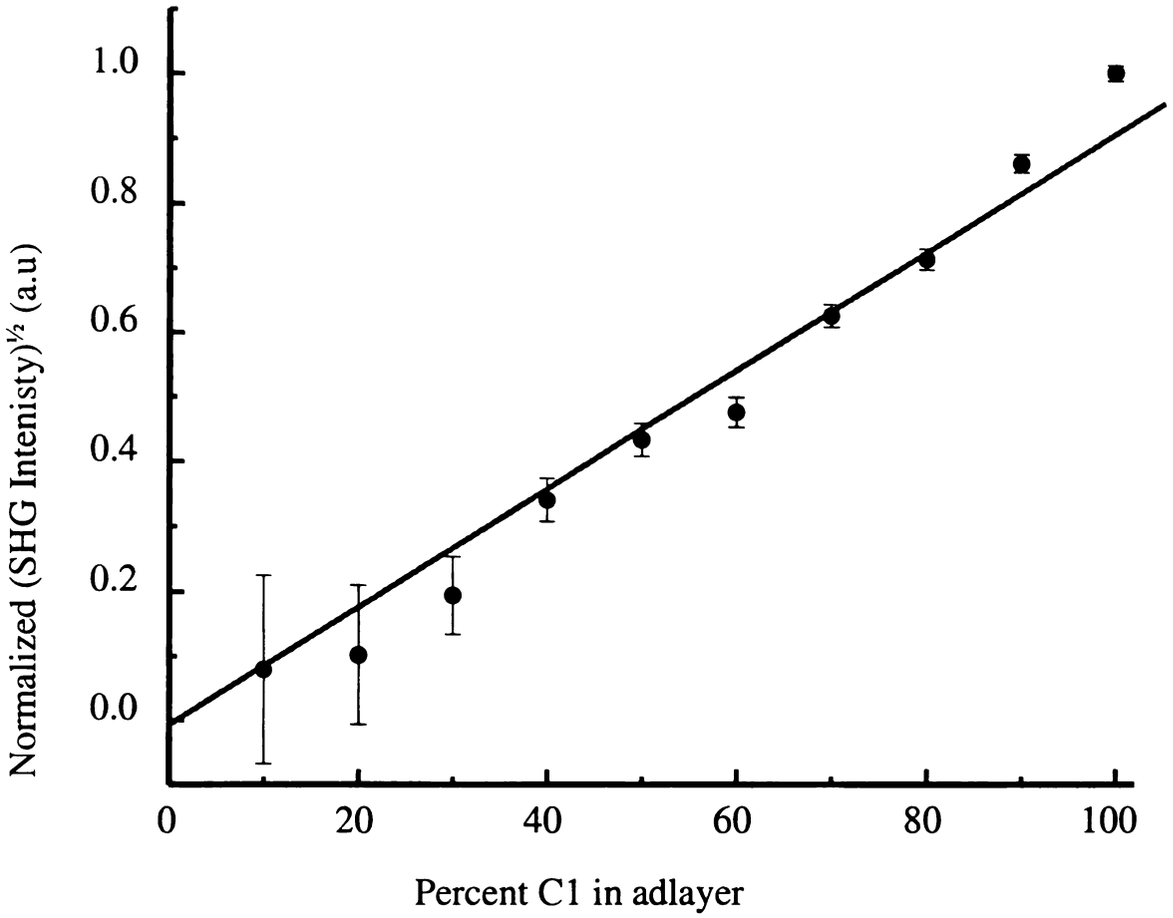

Figure 4.5 Dependence of surface SHG intensity at 60° angle of incidence as a function of **C1** loading density. The SSHG signal for each data point is normalized relative to the substrate $\chi(2)$ response. The data reveal the expected square-law dependence of signal intensity on loading density.

calculated SHG signal (Eqs. 4.1 and 4.2) allows information to be extracted on the average orientation of the chromophores within the adlayer. The orientation and distribution width information enter Eq. 4.1 through $\chi^{(2)}$ and the terms F_i. The completeness of cancellation in the oscillatory contribution to the experimental signal is determined by the extent to which the second harmonic signals from the two interfaces interfere with one another. If both interfaces contain only a single chromophore domain, essentially complete cancellation will result. In the case where there are multiple domains present within each interface, cancellation between front- and back-face SHG signals will be incomplete, especially in cases where the extent of order is very different for each domain type. The experimental data we recover for the series of adlayers with varying chromophore concentration do not exhibit complete cancellation of front- and back-face signals, and this finding cannot be reconciled with adlayers comprised of a single domain. The physical contributions to incomplete cancellation are accounted for in terms of the Fresnel factors F_i, and these terms do not provide agreement with the form of the experimental data.

The experimental SHG data for several adlayer loading densities are shown in Figures 4.6 – 4.8. For each of these bodies of data, we present fits of Eqs. 4.1 and 4.2 to the data, for the cases of one and two distinct domains within the adlayer. We treat the net SHG response of the sample as a linear superposition of the responses from multiple domains. In the cases of fitting the experimental data to a single adlayer domain, the model predicts almost complete cancellation of the experimental signal, consistent with identical and uniform monolayer deposition on both sides of the substrate.[74] We observe substantial regions where the calculated angle-dependent oscillations are not synchronized with the experimental data. Differences between the experimental and calculated signal intensities can arise from differences in the values of model parameters such as T, R, *n*,

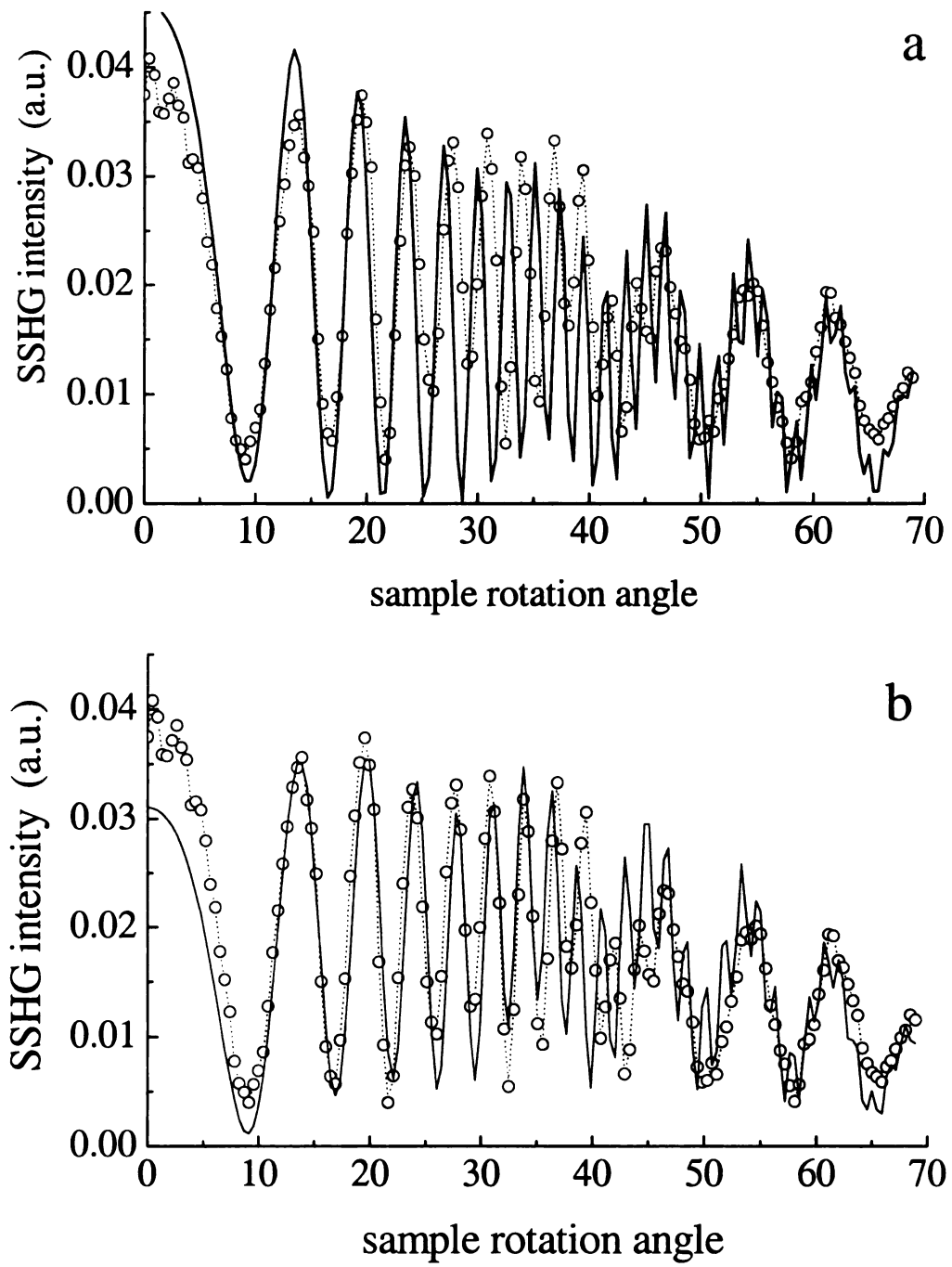

Figure 4.6. (a) Experimental SSHG data (open circles) and calculated signal (Eq. 1, solid line) for a monolayer comprised of 10% **C1** and 90% HDPA. The calculated signal is for a single domain. (b). Comparison of same experimental data to a calculated signal for two domains.

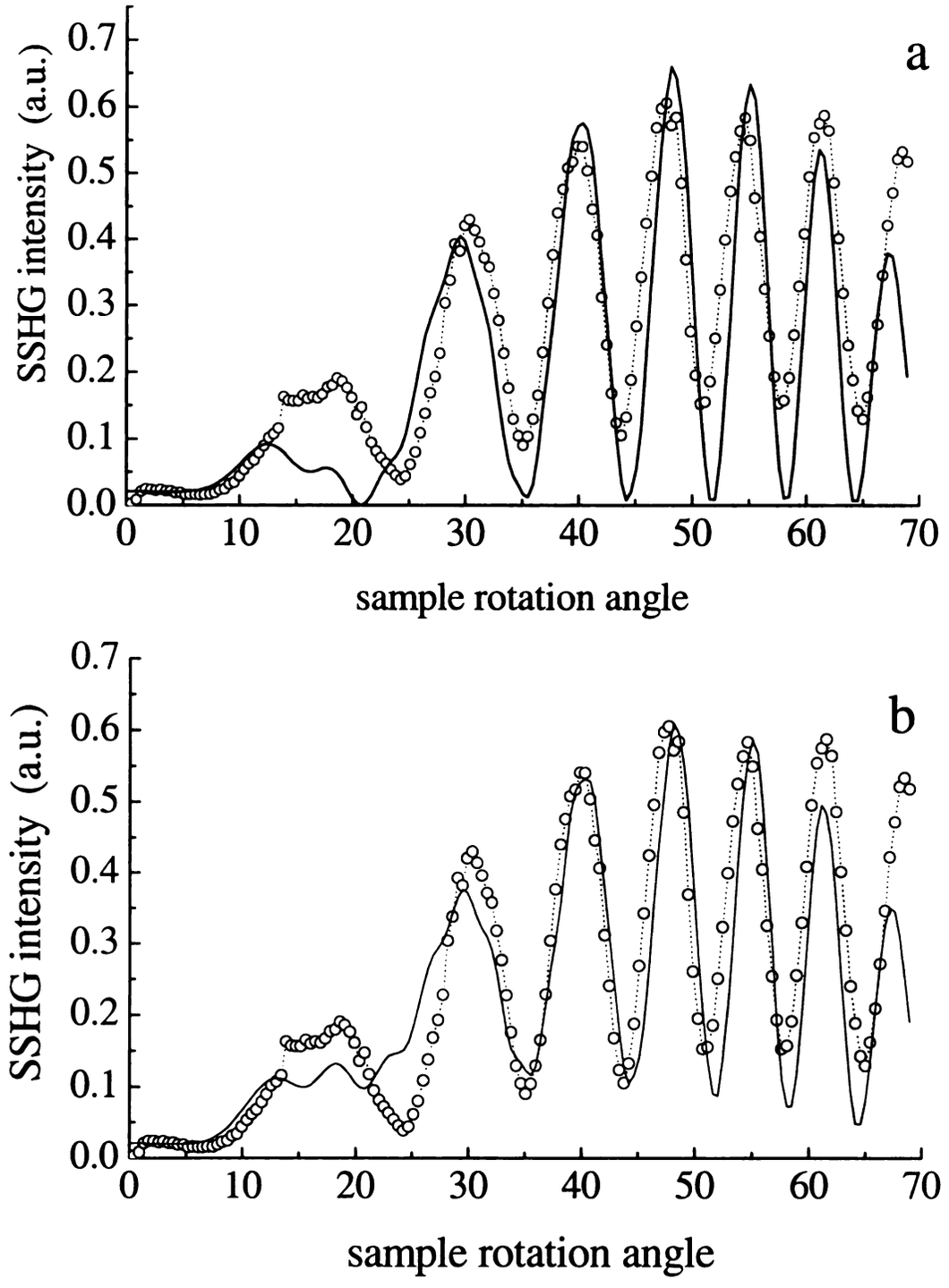

Figure 4.7. (a) Experimental SSHG data (open circles) and calculated signal (Eq. 1, solid line) for a monolayer comprised of 50% **C1** and 50% HDPA. The calculated signal is for a single domain. (b). Comparison of same experimental data to a calculated signal for two domains.

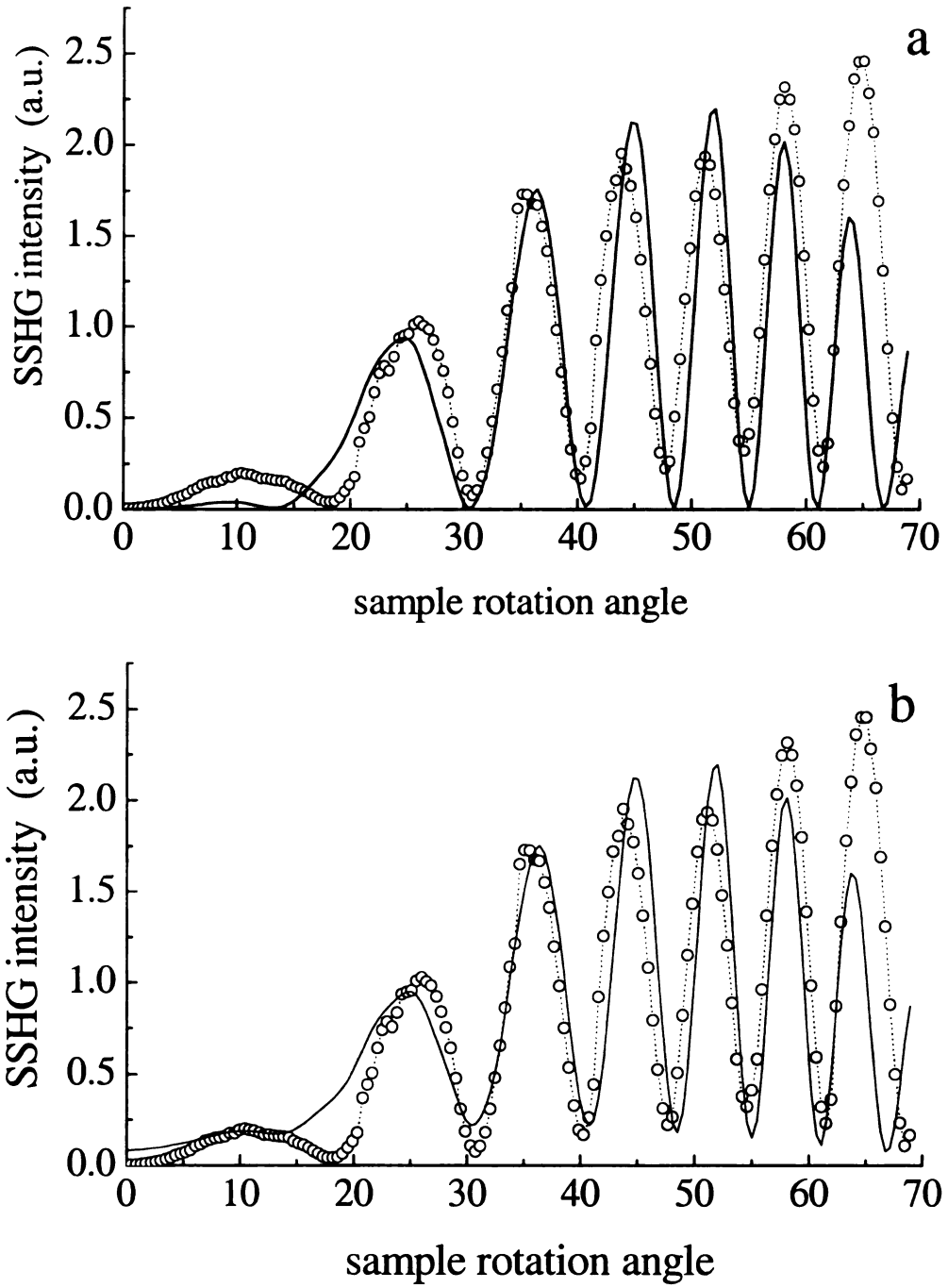

Figure 4.8. (a) Experimental SSHG data (open circles) and calculated signal (Eq. 1, solid line) for a monolayer comprised of 90% **C1** and 10% HDPA. The calculated signal is for a single domain. (b). Comparison of same experimental data to a calculated signal for two domains.

and $l_{i,,}$ but these quantities can be determined relatively easily and the dependence of the model on these quantities is relatively modest for the sample rotation angles that are in most serious disagreement with the experimental data. For example, the dependence of the calculated signal intensities on the terms F becomes significant only for relatively high incidence angles, and the most serious deviation(s) between experiment and calculation occur in the ~ 40° – 60° sample rotation angle region. We cannot bring the experiment and calculated signals into agreement by simply varying selected quantities in Eqs. 4.1 and 4.2. Inclusion of a second adlayer domain in the calculation provides agreement with the incomplete SHG cancellation and with the angle-dependence of the data. The experimental data for all adlayer loading densities can be accounted for by using two adlayer domains, where the dominant domain is comprised of chromophores oriented normal to the substrate plane and the second (minority) domain is characterized by an average chromophore tilt angle of 39°. The tilt angle of 39.2° is the "magic angle" for second order nonlinear optical experiments;[75] the implication of these fits to the data is that the first (dominant) domain is relatively well ordered while the second domain is characterized by substantial disorder.

The relative contribution of the ordered and disordered domains depends on the composition of the adlayer. A plot of fraction of random domain as a function of surface **C1** loading density is shown in Figure 4.9. Our fits of the experimental data to the model show that the random domain component of the surface structure decreases in a regular manner with increasing surface coverage. At the lowest **C1** loading densities (θ = 0.1 – 0.3), the data are fitted by iterative minimization of the difference between data and model to have ~85% of **C1** being in an ordered domain and ~ 15% residing in a disordered domain. For **C1** loading densities above 60%, ($\theta \geq 0.6$), ~ 5% resides in the disordered

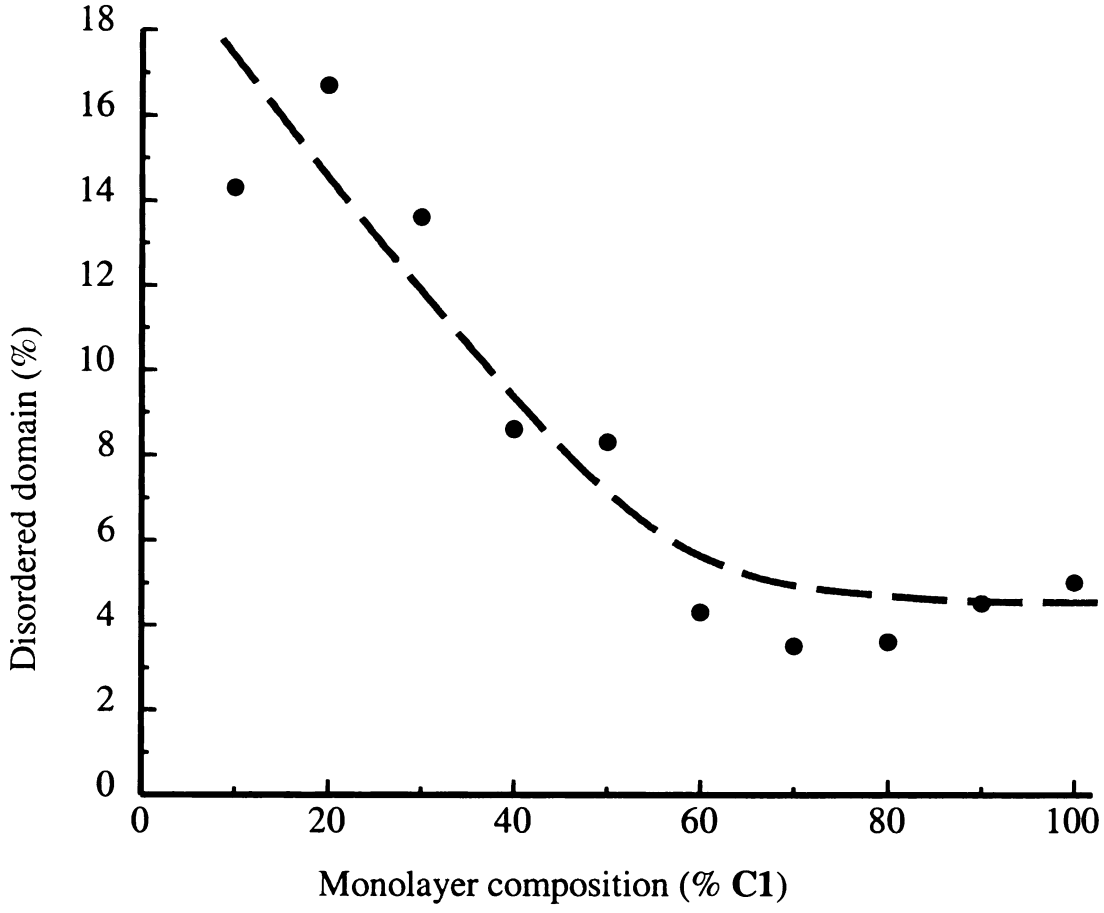

Figure 4.9. Results from calculated SHG signals for two domains. The fractional contribution of the disordered domain to the total signal is reported as a function of adlayer **C1** loading density. The dashed line is intended only as a guide to the eye.

domain. We note that, for samples with higher chromophore loading density, we do not obtain perfect agreement between model and data for high angles of incidence. We attribute this deviation to our inability to parameterize the terms Fi correctly due to elliptical polarization contributions of the fundamental and both TE and TM polarization contributions at both interfaces. The dominance of the ordered domain regardless of the fractional surface coverage indicates that intermolecular interactions are substantial for **C1**, either primarily with itself at high loading densities, or with HDPA at low loading densities. The open issue that remains is the reason for the existence of the disordered domains in the first place.

The presence of disorder in ZP layered materials has been documented previously for alkanebisphosphonates.[76] The primary reasons for disorder in these structures are the relatively limited organization intrinsic to the substrate surface and the speed with which the monolayers form. Because of the rapid formation kinetics and essentially irreversible nature of adlayer bonding, the adlayers must be considered to be kinetic products. We use SiO_x substrates in this work and previous results on this substrate material have demonstrated the existence of "island" structures with an average size of 50 – 100 Å in diameter.[53,54,77] The substrate is thus intrinsically heterogeneous, with the origin of this heterogeneity being the non-uniform distribution of surface silanol groups. A spatial variation in the density of surface silanol groups could account for the existence of the disordered domain; if adsorption occurs in a region characterized by a low initial silanol group density, intermolecular interactions that give rise to organization within the layer would not occur because of the intermolecular spacing. In this model, formation of ordered domains would occur in substrate regions characterized by a high silanol group density. The variation in relative amount of disordered domains with **C1** loading density

would be consistent with this model, where **C1**-**C1** intermolecular interactions would be more important in creating ordered domains than **C1**-HDPA interactions. The density-dependent increase in **C1**-**C1** interactions is consistent with the absorbance data for the adlayers shown in Figure 4.3. In those data, we observe a monotonic blue shift in absorption maximum with increasing **C1** loading density, with the spectral shift scaling qualitatively with the decrease in fractional contribution of the disordered domain. Unfortunately, the absorption spectrum of **C1** is sufficiently broad to preclude any useful molecular structural information from being extracted. We are thus left to argue that the spectral shift is somehow related to a monotonic variation in the local dielectric response of the medium that is related to the extent or organization within the layer.

4.4 Conclusions

We have studied the steady state linear response and second order nonlinear response of a family of monolayers comprised of two constituents, one a rigid $\chi^{(2)}$ chromophore and the other an aliphatic diluent. The absorption data for these adlayers points to a regular change in the local environment of the chromophore **C1**, and angle-dependent surface second harmonic generation intensity measurements are consistent with the presence of two chromophore domains within the adlayers. The two domains are characterized by different extents of order, with the majority domain having a chromophore orientation approximately normal to the substrate plane and the minority domain being characterized by an average tilt angle of 39°. The recovered tilt angle of the minority domain is the magic angle for second harmonic measurements, indicating substantial disorder within the domain. The fraction of **C1** that exists within the disordered domain ranges from ~15% for low **C1** surface loading densities to ~5% for high **C1** surface loading densities. These findings are consistent with the existence of a substrate characterized by a non-uniform distribution of chemically reactive sites. We believe these findings to be consistent to earlier work on excitation transport in ZP adlayers grown on SiO_x. Surface SHG intensity measurements provide a more quantitative means of evaluating the relative contribution of ordered and disordered regions of the SiO_x surface to the formation of a variety of adlayers.

4.5 Literature Cited

(1) Sullivan, D. M.; Bruening, M. L. *J. Am. Chem. Soc.* **2001**, *123*, 11805-11806.

(2) Stair, J. L.; Harris, J. J.; Bruening, M. L. *Chem. Mater.* **2001**, *13*, 2641-2648.

(3) Williams, D. J.; Editor *ACS Symposium Series, Vol. 233: Nonlinear Optical Properties of Organic and Polymeric Materials [Based on a Symposium Sponsored by the ACS Division of Polymer Chemistry at the 184th Meeting of the American Chemical Society, Kansas City, Mo., September 12-17, 1982]*, 1983.

(4) Nie, W. *Adv. Mater.* **1993**, *5*, 520-545.

(5) Marks, T. J.; Ratner, M. A. *Angew. Chem., Int. Ed. Engl.* **1995**, *34*, 155-173.

(6) Nuzzo, R. G.; Allara, D. L. *J. Am. Chem. Soc.* **1983**, *105*, 4481-4483.

(7) Nuzzo, R. G.; Dubois, L. H.; Allara, D. L. *J. Am. Chem. Soc.* **1990**, *112*, 558-569.

(8) Sagiv, J. *J. Am. Chem. Soc.* **1980**, *102*, 92-98.

(9) Ulman, A. *Chem. Rev.* **1996**, *96*, 1533-1554.

(10) Blodgett, K. B. *J. Am. Chem. Soc.* **1935**, *57*, 1007-1022.

(11) Langmuir, I. *J. Am. Chem. Soc.* **1917**, *39*, 1848-1906.

(12) Karpovich, D. S.; Blanchard, G. J. *Langmuir* **1994**, *10*, 3315-3322.

(13) Schessler, H. M.; Karpovich, D. S.; Blanchard, G. J. *J. Am. Chem. Soc.* **1996**, *118*, 9645-9651.

(14) Hong, H. G.; Sackett, D. D.; Mallouk, T. E. *Chem. Mater.* **1991**, *3*, 521-527.

(15) Lee, H.; Kepley, L. J.; Hong, H. G.; Mallouk, T. E. *J. Am. Chem. Soc.* **1988**, *110*, 618-620.

(16) Putvinski, T. M.; Schilling, M. L.; Katz, H. E.; Chidsey, C. E. D.; Mujsce, A. M.; Emerson, A. B. *Langmuir* **1990**, *6*, 1567-1571.

(17) Bakiamoh, S. B.; Blanchard, G. J. *Langmuir* **1999**, *15*, 6379-6385.

(18) Bandyopadhyay, K.; Patil, V.; Vijayamohanan, K.; Sastry, M. *Langmuir* **1997**, *13*, 5244-5248.

(19) Kohli, P.; Taylor, K. K.; Harris, J. J.; Blanchard, G. J. *J. Am. Chem. Soc.* **1998**, *120*, 11962-11968.

(20) Kohli, P.; Blanchard, G. J. *Langmuir* **2000**, *16*, 4655-4661.

(21) Kohli, P.; Blanchard, G. J. *Langmuir* **1999**, *15*, 1418-1422.

(22) Palmer, R. E.; Rous, P. J. *Rev. Mod. Phys.* **1992**, *64*, 383-440.

(23) Rous, P. J.; Palmer, R. E.; Willis, R. F. *Phys. Rev. B: Condens. Matter* **1989**, *39*, 7552-7560.

(24) Neivandt, D. J.; Gee, M. L.; Hair, M. L.; Tripp, C. P. *J. Phys. Chem. B* **1998**, *102*, 5107-5114.

(25) Hirosawa, I. *Jpn. J. Appl. Phys., Part 1* **1997**, *36*, 5192-5196.

(26) Hines, M. A.; Harris, T. D.; Harris, A. L.; Chabal, Y. J. *J. Electron Spectrosc. Relat. Phenom.* **1993**, *64-65*, 183-191.

(27) Shen, Y. R. *Nature* **1989**, *337*, 519-525.

(28) Richmond, G. L.; Robinson, J. M.; Shannon, V. L. *Prog. Surf. Sci.* **1988**, *28*, 1-70.

(29) Eisenthal, K. B. *Chem. Rev.* **1996**, *96*, 1343-1360.

(30) Corn, R. M.; Higgins, D. A. *Chem. Rev.* **1994**, *94*, 107-125.

(31) Shen, Y. R. *Annu. Rev. Phys. Chem.* **1989**, *40*, 327-350.

(32) Eisenthal, K. B. *Annu. Rev. Phys. Chem.* **1992**, *43*, 627-661.

(33) Bloembergen, N.; Pershan, P. S. *Phys. Rev.* **1962**, *128*, 606-622.

(34) Higgins, D. A.; Abrams, M. B.; Byerly, S. K.; Corn, R. M. *Langmuir* **1992**, *8*, 1994-2000.

(35) Higgins, D. A.; Byerly, S. K.; Abrams, M. B.; Corn, R. M. *J. Phys. Chem.* **1991**, *95*, 6984-6990.

(36) Campbell, D. J.; Higgins, D. A.; Corn, R. M. *J. Phys. Chem.* **1990**, *94*, 3681-3689.

(37) Kemnitz, K.; Bhattacharyya, K.; Hicks, J. M.; Pinto, G. R.; Eisenthal, K. B.; Heinz, T. F. *Chem. Phys. Lett.* **1986**, *131*, 285-290.

(38) Conboy, J. C.; Daschbach, J. L.; Richmond, G. L. *J. Phys. Chem.* **1994**, 9688-9692.

(39) Naujok, R. R.; Higgins, D. A.; Hanken, D. G.; Corn, R. M. *J. Chem. Soc., Faraday Trans.* **1995**, *91*, 1411-1420.

(40) Kott, K. L.; Higgins, D. A.; McMahon, R. J.; Corn, R. M. *J. Am. Chem. Soc.* **1993**, *115*, 5342-5343.

(41) Lynch, M. L.; Barner, B. J.; Corn, R. M. *J. Electroanal. Chem. Interfacial Electrochem.* **1991**, *300*, 447-465.

(42) Trzeciecki, M.; Dahn, A.; Hubner, W. *Phys. Rev. B: Condens. Matter Mater. Phys.* **1999**, *60*, 1144-1160.

(43) Heinz, T. F.; Tom, H. W. K.; Shen, Y. R. *Phys. Rev. A* **1983**, *28*, 1883-1885.

(44) Simpson, G. J.; Rowlen, K. L. *J. Phys. Chem. B* **1999**, *103*, 3800-3811.

(45) Simpson, G. J.; Rowlen, K. L. *J. Phys. Chem. B* **1999**, *103*, 1525-1531.

(46) Simpson, G. J.; Rowlen, K. L. *Acc. Chem. Res.* **2000**, *33*, 781-789.

(47) Simpson, G. J.; Westerbuhr, S. G.; Rowlen, K. L. *Anal. Chem.* **2000**, *72*, 887-898.

(48) Reider, G. A.; Hoefer, U.; Heinz, T. F. *J. Chem. Phys.* **1991**, *94*, 4080-4083.

(49) Rasing, T.; Stehlin, T.; Shen, Y. R.; Kim, M. W.; Valint, P., Jr. *J. Chem. Phys.* **1988**, *89*, 3386-3387.

(50) Castro, A.; Ong, S.; Eisenthal, K. B. *Chem. Phys. Lett.* **1989**, *163*, 412-416.

(51) Zhu, X. D.; Daum, W.; Xiao, X. D.; Chin, R.; Shen, Y. R. *Phys. Rev. B: Condens. Matter* **1991**, *43*, 11571-11580.

(52) Buck, M.; Eisert, F.; Grunze, M.; Traeger, F. *Appl. Phys. A: Mater. Sci. Process.* **1995**, *A60*, 1-12.

(53) Horne, J. C.; Huang, Y.; Liu, G. Y.; Blanchard, G. J. *J. Am. Chem. Soc.* **1999**, *121*, 4419-4426.

(54) Horne, J. C.; Blanchard, G. J. *J. Am. Chem. Soc.* **1996**, *118*, 12788-12795.

(55) Katz, H. E.; Wilson, W. L.; Scheller, G. *J. Am. Chem. Soc.* **1994**, *116*, 6636-6640.

(56) Bakiamoh, S. B.; Blanchard, G. J. *Langmuir* **2001**, *17*, 3438-3446.

(57) Bhattacharya, A. K.; Thyagarajan, G. *Chem. Rev.* **1981**, *81*, 415-430.

(58) Strazzolini, P.; Giumanini, A. G.; Verardo, G. *Tetrahedron* **1994**, *50*, 217-254.

(59) Horne, J. C.; Blanchard, G. J. *J. Am. Chem. Soc.* **1996**, *118*, 12788-12795.

(60) Flory, W. C.; Mehrens, S. M.; Blanchard, G. J. *J. Am. Chem. Soc.* **2000**, *122*, 7976-7985.

(61) Dong, Y.; Pappu, S. V.; Xu, Z. *Anal. Chem.* **1998**, *70*, 4730-4735.

(62) Emoto, K.; Harris, J. M.; Van Alstine, J. M. *Anal. Chem.* **1996**, *68*, 3751-3757.

(63) Wang, R.; Wunder, S. L. *Langmuir* **2000**, *16*, 5008-5016.

(64) Pedrotti, F. L.; Pedrotti, L. S. *Introduction to Optics; Prentice-Hall* **1987**, 472-487.

(65) Shen, Y. R. *in Molecular Nonlinear Optics, Edited by J. Zyss, Academic, San Diego* **1994**, 101.

(66) Guyot-Sionnest, P.; Shen, Y. R. *Phys. Rev. B: Condens. Matter* **1987**, *35*, 4420-4426.

(67) Chemla, D. S.; Zyss, J. *Nonlinear Optical Properties of Organic Molecules and Crystals; Academic Press, Orlando, Florida* **1987**.

(68) Simpson, G. J.; Rowlen, K. L. *Anal. Chem.* **2000**, *72*, 3407-3411.

(69) Simpson, G. J.; Rowlen, K. L. *Anal. Chem.* **2000**, *72*, 3399-3406.

(70) Eisenthal, K. B. *J. Phys. Chem.* **1996**, *100*, 12997-13006.

(71) Watry, M. R.; Richmond, G. L. *J. Am. Chem. Soc.* **2000**, *122*, 875-883.

(72) Paul, H. J.; Corn, R. M. *J. Phys. Chem. B* **1997**, *101*, 4494-4497.

(73) Bae, S.; Haage, K.; Wantke, K.; Motschmann, H. *J. Phys. Chem. B* **1999**, *103*, 1045-1050.

(74) Li, D.; Ratner, M. A.; Marks, T. J.; Zhang, C.; Yang, J.; Wong, G. K. *J. Am. Chem. Soc.* **1990**, *112*, 7389-7390.

(75) Simpson, G. J.; Rowlen, K. L. *J. Am. Chem. Soc.* **1999**, *121*, 2635-2636.

(76) Yang, H. C.; Aoki, K.; Hong, H. G.; Sackett, D. D.; Arendt, M. F.; Yau, S. L.; Bell, C. M.; Mallouk, T. E. *J. Am. Chem. Soc.* **1993**, *115*, 11855-11862.

(77) Horne, J. C.; Blanchard, G. J. *J. Am. Chem. Soc.* **1999**, *121*, 4427-4432.

Chapter 5

Conclusions and Future Work

5.1 Conclusions

This body of work has sought to understand molecular organization intrinsic to layered assemblies, and how that organization depends on the deposition of sequential layers. To investigate several layered systems, asymmetric layer synthesis was used in conjunction with data from linear optical techniques such as FTIR and ellipsometry, and the nonlinear optical technique of surface second harmonic generation (SHG) intensity measurement. This combined approach provides a useful means to study interface organization as well as information on changes in the structural properties of interfaces associated with layer growth.

To investigate layer organization, oriented multilayer assemblies were synthesized using asymmetric metal ion coordination chemistry with structurally simple bifunctional alkanes, where only the coordinating metal centers are $\chi^{(2)}$-active. Surfaces used for layer deposition were prepared by reacting silanol-containing surfaces directly with $POCl_3$/collidine, then $ZrOCl_2(aq)$,[1] as opposed to using conventional silane-based priming chemistry.[2] Both surface preparation techniques yield surfaces with the same properties but the former approach results in reduction of sample preparation time by about 24 hrs and has been used throughout this work. Characterization of interfaces by optical null ellipsometry, UV-visible and FTIR spectroscopy of the oriented multilayer assemblies points to moderately well organized layers that are thermally and chemically stable in a variety of solvents for up to one hour at temperatures ranging from 25 - 80 °C.

Surface second harmonic generation intensity measurements of bifunctional alkane multilayers provide insight into the magnitude of the $\chi^{(2)}$ response intrinsic to the inorganic interlayer of ionically-bound multilayer systems. Interfaces intended for use in nonlinear optics usually rely on complex conjugated chromophores with large hyperpolarizabilities for the needed nonlinear response. Where these interfaces are ionically bound, such as ZP multilayers, any nonlinear response from the inorganic interlayer is usually not considered because there exist inversion symmetries at the ionic metal centers rendering them $\chi^{(2)}$-inactive. For certain inorganic crystalline systems that do not possess inversion symmetry, large second order optical nonlinearities are seen (*e.g.* $LiIO_3$, $LiNbO_3$, KH_2PO_4), suggesting the possibility that the inorganic interlayer structures in interfacial films could potentially possess usefully large $\chi^{(2)}$ responses, if designed properly. Using oriented bifunctional alkane multilayer assemblies with $\chi^{(2)}$-active metal coordination centers, we have demonstrated for the first time that the nonlinear response from this part of the assembly is small. For interfacial assemblies, it appears that layered nonlinear optical materials containing rigid chromophores with large hyperpolarizabilities are more likely to be useful, and the $\chi^{(2)}$ response from the inorganic interlayer can be considered negligible.

The surface organization and structure of a family of monolayers comprising two constituents, a rigid $\chi^{(2)}$ chromophore and an aliphatic diluent were also investigated using angle-dependent surface second harmonic generation intensity measurements. Our SHG intensity data are consistent with presence of a complex surface structure characterized by two chromophore domains within the layers; an ordered domain where majority of the chromophores are oriented approximately normal to the surface plane and

a smaller amount of a random domain, characterized by an average chromophore tilt angle of ~ 39°. These data point to the inherent disorder present in many interfacial systems. This disorder may either be the result of a non-uniform spatial distribution of surface reactive sites on which the adlayer is grown, or significant aggregation phenomena within the adlayer structure that originates either during layer growth or subsequent to deposition.

Future Work

This dissertation has underscored the versatility, sensitivity and utility of surface second harmonic generation (SHG) intensity measurements for probing interface organization and structure. Several other research groups have used surface SHG measurements for characterizing a wide range of interfaces.[3-6] The SHG data suggest formation of domain structures within the layers, a possible consequence of substrate heterogeneity resulting from non-uniform distribution of surface silanol groups. Previous results on SiO_x substrates and single-layer interfaces containing varying concentrations of chromophore suggest the existence of "islands".[7,8] Though SHG is a surface-sensitive technique, the second harmonic signal is generated from relatively large portions of the surface in a given measurement, and the surface information (organization and structure) thus *averaged* over the dimension of the illuminated spot (~100 μm diameter here). To resolve the molecular details of surface and interface organization and structure, the nonlinear response from an illuminated spot must be interpreted in terms of *local* surface symmetry. To this end, surface second harmonic microscopy (imaging) (SHM) in

combination with SHG intensity measurements is one method that can provide more complete information on surfaces and interfaces.

The rationale for proposing SHM is that, in addition to revealing the lateral variation in nonlinearities due to local symmetry and order, it can be used to characterize mono- and multilayer morphology over μm length scales. Standard linear optical microscopic techniques are often not sensitive enough to study monolayers because of the overall number of absorptive or emissive species present in the layer and the background contributions from the substrate. The goal of SH microscopy is to map out the spatial-dependence of interfacial nonlinear susceptibility $\chi^{(2)}$, *i.e.*, to obtain an output (field) that is reflective of spatial variations in the *local* nonlinear susceptibility of the interface. The correspondence between local and mesoscopic optical response is a prerequisite for extracting morphological information from the data.[9]

SHM has been used recently to study several interfacial and layered systems including surface diffusion measurements on semiconductors,[10] photolithographically patterned SAMs,[11] domains at surface magnetic interfaces, and monitoring the lateral diffusion of adsorbates at surfaces (surface diffusion).[9] Using SHM, we will be able to observe not only the local surface structure with diffraction-limited resolution, but also layer formation and surface ordering or surface movement of the chromophores as they form ordered domains.

Though several optical configurations and image-gathering methods have been demonstrated, a non-collinear optical geometry (Figure 5.1) will provide background-free signals while maintaining independent control over the polarization of the two incident

electric fields. A surface second harmonic imaging system (Figure 5.1) is currently being installed and optimized in the Blanchard laboratories.

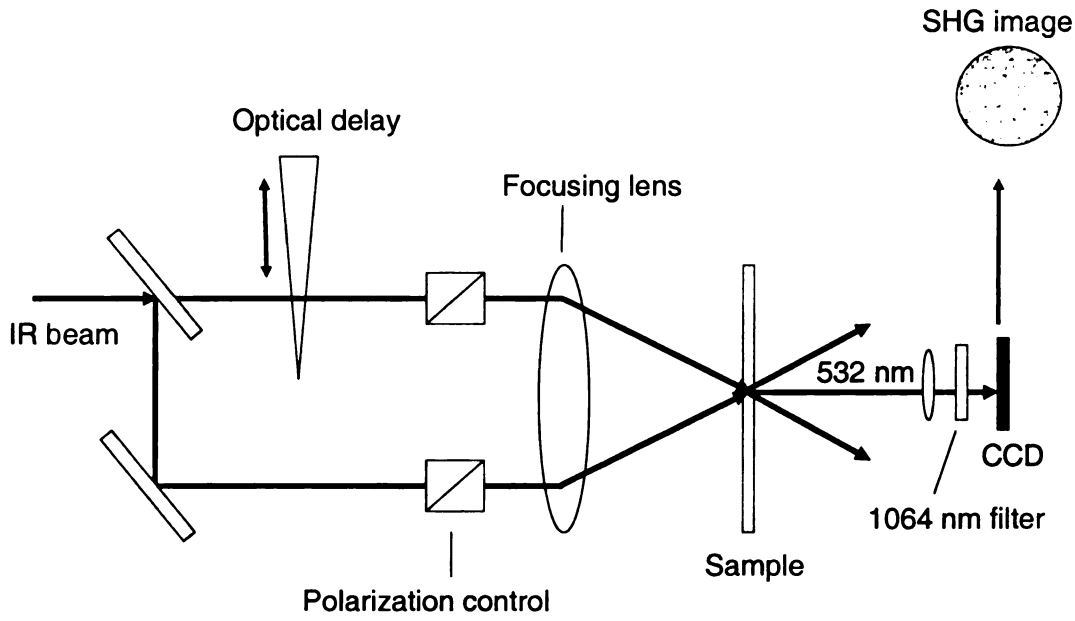

Figure 5.1. Schematic representation of surface second harmonic imaging system. This system can detect SHG images in transmission (T) or reflection (R) mode, depending on the optical properties of the substrate. Only the transmission configuration is indicated.

5.3 Literature Cited

(1) Bakiamoh, S. B.; Blanchard, G. J. *Langmuir* **1999**, *15*, 6379-6385.

(2) Horne, J. C.; Blanchard, G. J. *J. Am. Chem. Soc.* **1996**, *118*, 12788-12795.

(3) Conboy, J. C.; Richmond, G. L. *Electrochim. Acta* **1995**, *40*, 2881-2886.

(4) Katz, H. E.; Wilson, W. L.; Scheller, G. *J. Am. Chem. Soc.* **1994**, *116*, 6636-6640.

(5) Shang, X.; Liu, Y.; Yan, E.; Eisenthal, K. B. *Journal of Physical Chemistry B* **2001**, *105*, 12816-12822.

(6) Xiao, X. D.; Zhu, X. D.; Daum, W.; Shen, Y. R. *Phys. Rev. B: Condens. Matter* **1992**, *46*, 9732-9743.

(7) Horne, J. C.; Blanchard, G. J. *J. Am. Chem. Soc.* **1999**, *121*, 4427-4432.

(8) Horne, J. C.; Huang, Y.; Liu, G. Y.; Blanchard, G. J. *J. Am. Chem. Soc.* **1999**, *121*, 4419-4426.

(9) Reider, G. A.; Cernusca, M.; Hofer, M. *Appl. Phys. B: Lasers Opt.* **1999**, *B68*, 343-347.

(10) Allen, C. E.; Ditchfield, R.; Seebauer, E. G. *J. Vac. Sci. Technol., A* **1996**, *14*, 22-29.

(11) Smilowitz, L.; Jia, Q. X.; Yang, X.; Li, D. Q.; McBranch, D.; Buelow, S. J.; Robinson, J. M. *J. Appl. Phys.* **1997**, *81*, 2051-2054.